HILLE

IONIC CHANNELS OF EXCITABLE MEMBRANES

SECOND EDITION

SINAUER

Ionic Channels of Excitable Membranes

SECOND EDITION

BERTIL HILLE

Ionic Channels of Excitable Membranes

Second Edition

BERTIL HILLE

UNIVERSITY OF WASHINGTON

SINAUER ASSOCIATES INC. • *Publishers*
Sunderland, Massachusetts

IONIC CHANNELS OF EXCITABLE MEMBRANES, Second Edition

Library of Congress Cataloging-in-Publication Data

Hille, Bertil, 1940–
Ionic channels of excitable membranes / Bertil Hille.—2nd ed.
p. cm.
Includes bibliographical references and index.
ISBN 0–87893–323–9
1. Ion channels. 2. Excitable membranes. 3. Neurons. I. Title.
QH601.H55 1991
574.87'5—dc20 91-25291
CIP

Printed in U.S.A.

10 9 8 7 6 5 4 3 2 1

INTRODUCTION

Ionic channels are pores

Ionic channels are macromolecular pores in cell membranes. When they evolved and what role they may have played in the earliest forms of life we do not know, but today ionic channels are most obvious as the fundamental excitable elements in the membranes of excitable cells. These channels bear the same relation to electrical signaling in nerve, muscle, and synapse as enzymes bear to metabolism. Although their diversity is less broad than that of enzymes, there are many types of channels working in concert, opening and closing to shape the signals and responses of the nervous system. As sensitive but potent amplifiers, these ionic channels detect the sounds of chamber music, guide the artist's paintbrush, or generate the violent electric discharges of the electric eel or the electric ray. They tell the *Paramecium* to swim backward after a gentle collision, and they propagate the leaf-closing response of the *Mimosa* plant.

More than three billion years ago, primitive replicating forms became enveloped in a lipid film, a bimolecular diffusion barrier that separated the living cell from its environment. Although a lipid membrane had the advantage of retaining vital cell components, it would also prevent access to necessary ionized substrates and the loss of ionized waste products. Thus new transport mechanisms had to be developed hand in hand with the appearance of the membrane. One general solution would have been to make pores big enough to pass all small metabolites and small enough to retain macromolecules. Indeed, the *outer* membranes of gram-negative bacteria and of mitochondria are built on this plan. However, the cytoplasmic membranes of all contemporary organisms follow a more elaborate design, with many, more-selective transport devices handling different jobs, often under separate physiological control.

How do these devices work? Most of what we know about them comes from physiological flux measurements. Physiologists traditionally divided transport mechanisms into two classes, carriers and pores, largely on the basis of kinetic criteria. For example, the early literature tried to distinguish carrier from pore on the basis of molecular selectivity, saturating concentration dependence of fluxes, or stoichiometric coupling of the number of molecules transported. A carrier was viewed as a ferryboat diffusing back and forth across the membrane while carrying small molecules that could bind to stereospecific binding sites, and a pore was viewed as a narrow, water-filled tunnel, permeable to the few ions and molecules small enough to fit through the hole. The moving-ferryboat view of a

carrier is now no longer considered valid because the numerous carrier devices that have been purified from membranes are large proteins—too large to diffuse or spin around at the rate needed to account for the fluxes they catalyze. Furthermore, their amino acid sequences show that the peptide chains of the transport protein are already stably threaded back and forth in a large number of transmembrane segments. The newer view of carrier transport is that much smaller motions within the protein leave the macromolecule fixed in the membrane while exposing the transport binding site(s) alternately to the intracellular and extracellular media. It is not difficult to imagine various ways to do this, but we must develop new experimental insights before such ideas can be tested. Thus the specific mechanism of transport by such important carrier devices as the Na^+-K^+ pump, the Ca^{2+} pump, Na^+-Ca^{2+} exchange, Cl^--HCO_3^- exchange, glucose transport, the Na^+-coupled co- and countertransporters, and so on, remains unknown.

On the other hand, the water-filled pore view for the other class of transport mechanisms has now been firmly established for ionic channels of excitable membranes. In the period between 1965 and 1980, a valuable interplay between studies of excitable membrane and studies on model pores, such as the gramicidin channel in lipid bilayers, accelerated the pace of research and greatly sharpened our understanding of the transport mechanism. The biggest technical advance of this period was the development of methods to resolve the activity of single, channel molecules. As we consider much more extensively in later chapters, this led to the discovery that the rate of passage of ions through one open channel—often more than 10^6 ions per second—is far too high for any mechanism other than a pore. The criteria of selectivity, saturation, and stoichiometry are no longer the best for distinguishing pore and carrier.

Channels and ions are needed for excitation

Physiologists have long known that ions play a central role in the excitability of nerve and muscle. In an important series of papers from 1881 to 1887, Sidney Ringer showed that the solution perfusing a frog heart must contain salts of sodium, potassium, and calcium mixed in a definite proportion if the heart is to continue beating long. Nernst's (1888) work with electrical potentials arising from the diffusion of electrolytes in solution inspired numerous speculations of an ionic origin of bioelectric potentials. For example, some suggested that the cell is more negative than the surrounding medium because metabolizing tissue makes acids, and the resulting protons (positive charge) can diffuse away from the cell more easily than the larger organic anions. Soon, Julius Bernstein (1902, 1912) correctly proposed that excitable cells are surrounded by a membrane selectively permeable to K^+ ions at rest and that during excitation the membrane permeability to other ions increases. His "membrane hypothesis" explained the resting potential of nerve and muscle as a diffusion potential set up by the tendency of positively charged ions to diffuse from their high concentration in cytoplasm to their low concentration in the extracellular solution. During excita-

tion the internal negativity would be lost transiently as other ions are allowed to diffuse across the membrane, effectively short circuiting the K^+ diffusion potential. In the English-language literature, the words "membrane breakdown" were used to describe Bernstein's view of excitation.

During the twentieth century, major cellular roles have been discovered for each of the cations of Ringer's solution: Na^+, K^+, Ca^{2+}; as well as for most of the other inorganic ions of body fluids: H^+, Mg^{2+}, Cl^-, HCO_3^-, and PO_4^{2-}. The rate of discovery of new roles for ions in cell physiology has been accelerating rather than slowing, so the list of ions and their uses will continue to lengthen. Evidently, no major ion has been overlooked in evolution. Each has been assigned at least one special regulatory, transport, or metabolic task. None is purely passively distributed across the cell membrane. Each has at least one carrier-like transport device coupling its movement to the movement of another ion. Both Na^+ and H^+ ions have transport devices coupling their "downhill" movements to the "uphill" movements of organic molecules. Na^+, K^+, H^+, and Ca^{2+} ions are pumped uphill by ATP-driven pumps. Protons are pumped across some membranes by electron transport chains, and their subsequent downhill flow can drive the phosphorylation of ADP to make ATP. Proton movements, through their effects on intracellular pH, will also influence the relative rates of virtually every enzymatic reaction. All of the ionic movements listed above are considered to be mediated by the carrier class of transport devices, and although they establish the ionic gradients needed for excitation, they are not themselves part of the excitation process. Readers interested in the details of ion pumps or coupled cotransport and exchange devices can consult other books on cell physiology.

Excitation and electrical signaling in the nervous system involve the movement of ions through ionic channels. The Na^+, K^+, Ca^{2+}, and Cl^- ions seem to be responsible for almost all of the action. Each channel may be regarded as an excitable molecule, as it is specifically responsive to some stimulus: a membrane potential change, a neurotransmitter or other chemical stimulus, a mechanical deformation, and so on. The channel's response, called GATING, is apparently a simple opening or closing of the pore. The open pore has the important property of SELECTIVE PERMEABILITY, allowing some restricted class of small ions to flow passively down their electrochemical activity gradients at a rate that is very high ($>10^6$ ions per second) when considered from a molecular viewpoint. We consider the high throughput rate as a diagnostic feature distinguishing ionic channel mechanisms from those of other ion transport devices such as the Na^+-K^+ pump. An additional major feature is a restriction to downhill fluxes not coupled stoichiometrically to the immediate injection of metabolic energy.

These concepts can be illustrated using the neurotransmitter-sensitive channels of muscle fibers. At the neuromuscular junction or endplate region of vertebrate skeletal muscle, the nerve axon has the job of instructing the muscle fiber when it is time to contract. Pulse-like electrical messages called ACTION POTENTIALS are sent down the motor nerve from the central nervous system. When they reach the nerve terminal, action potentials evoke the release of a

chemical signal, the neurotransmitter acetylcholine, which in turn diffuses to the nearby muscle surface and causes acetylcholine-sensitive channels to open there. Figure 1 shows an electrical recording from a tiny patch of muscle membrane. The cell is actually an embryonic muscle in tissue culture without nerves, but it still has neurotransmitter-sensitive channels that can be opened by applying a low concentration of acetylcholine. In this experiment, ionic fluxes in the channels are detected as electric current flow in the recording circuit, and since the recording sensitivity is very high, the opening and closing of one channel appear as clear step changes in the record. Each elementary current step corresponds to over 10^7 ions flowing per second in the open channel. Gating keeps the channel open for a few milliseconds. Other experiments with substitutions of ions in the bathing medium show that this type of channel readily passes monovalent cations with diameters up to 6.5 Å (0.65 nm) but does not pass anions.

How do gated ionic fluxes through pores make a useful signal for the nervous system? For the electrophysiologist the answer is clear. Ionic fluxes are electric currents across the membrane and therefore they have an immediate effect on membrane potential. Other voltage-gated channels in the membrane detect the change in membrane potential, and they in turn become excited. In this way the electric response is made regenerative and self-propagating. This explanation does describe how most signals are propagated, but it is circular. Is the ultimate purpose of excitation to make electricity so that other channels will be excited and make electricity? Clearly not, except in the case of an electric organ. Electricity is the means to carry the signal to the point where a nonelectrical response is generated. As far as is known, this final transduction always starts through a single common pathway: A membrane potential change opens or closes a Ca^{2+}-permeable channel, either on the surface membrane or on an

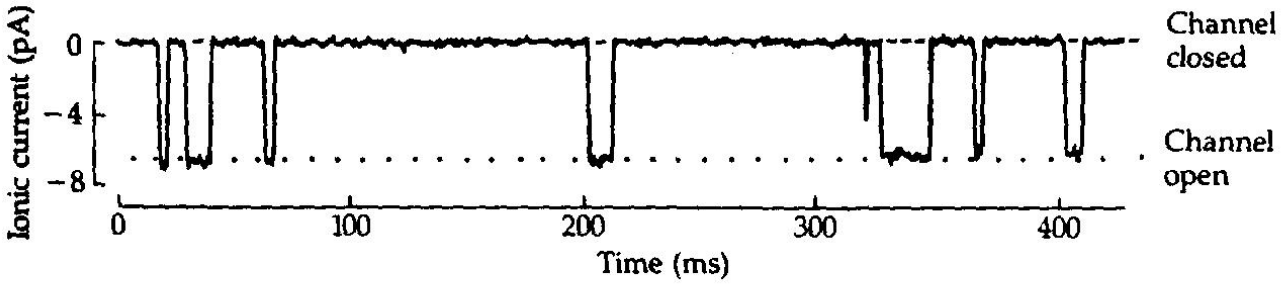

1 OPEN-SHUT GATING OF AN IONIC CHANNEL

Ionic current flowing across a tiny patch of excitable membrane showing eight brief openings (downward current deflections) of single ionic channels. The membrane patch has been excised from a cultured rat myotube and is bathed on both sides by Na salt solutions. Approximately 300 nM of the neurotransmitter, acetylcholine, applied to the extracellular membrane face is causing channels to open occasionally. At the −140 mV applied membrane potential, one open channel passes −6.6 pA, corresponding to a prodigious flow of 4.1×10^7 ions per second through a single pore. T = 23°C. [From Sánchez et al., 1986.]

internal membrane, and a Ca^{2+} flux into the cytoplasm is altered, causing a change in the internal free Ca^{2+} concentration. The ultimate response is then triggered by the internal Ca^{2+} ions. This is how the nervous system controls the contraction of a muscle fiber or the secretion of neurotransmitters, neurohormones, digestive enzymes, and so on. Internal free Ca^{2+} also controls the gating of some channels and the activities of many enzymes.

Ionic channels are undoubtedly found in the membranes of all cells. Their known functions include establishing a resting membrane potential, shaping electrical signals, gating the flow of messenger Ca^{2+} ions, controlling cell volume, and regulating the net flow of ions across epithelial cells of secretory and resorptive tissues. The emphasis in this book is on well-known channels underlying the action potentials and synaptic potentials of nerve and muscle cells. These have long been the focus of traditional membrane biophysics. As the biophysical methods eventually were applied to study fertilization of eggs, swimming of protozoa, glucose-controlled secretion of insulin by pancreatic beta cells, or acetylcholine-induced secretion of epinephrine from chromaffin cells, similar channels were found to play central roles. We must now consider that nerve, muscle, endocrine and secretory glands, white blood cells, platelets, gametes, and protists all share common membrane mechanisms in their responsiveness to stimuli. Similarly, as biophysical methods were applied to transporting epithelia, ionic channels were found. They too are ion-selective, gated pores, controlled by hormonal influences.

Nomenclature of channels

The naming of ionic channels has not been systematic. In most cases, the biophysicist first attempts to distinguish different components of membrane permeability by their kinetics, pharmacology, and response to ionic substitution. Then a kinetic model is often made expressing each of the apparent components mathematically. Finally, it is tacitly assumed that each component of the model corresponds to a type of channel, and the putative channels are given the same names as the permeability components in the original analysis. Thus in their classical analysis of ionic currents in the squid giant axon, Hodgkin and Huxley (1952d) recognized three different components of current, which they called sodium, potassium, and leakage. Today the names NA CHANNEL and K CHANNEL are universally accepted for the corresponding ionic channels in axons. The name LEAKAGE CHANNEL is also used, although there is no experimental evidence regarding the ions or transport mechanism involved.

Naming a channel after the most important permeant ion seems rational but fails when the ions involved are not adequately known, or when no ion is the *major* ion, or when numerous different kinetic components are all clearly carried by one type of ion. Such problems have led to such "names" as A, B, C, and so on, for permeability components in molluscan ganglion cells (Adams, Smith, and Thompson, 1980) or qr, si, and x_1 in cardiac Purkinje fibers (McAllister et al., 1975). Other approaches are simply descriptive: Channels have been named

after anatomical regions, as in the endplate channel; after inhibitors, as in the amiloride-sensitive Na channel; or after neurotransmitters, as in glutamate channels of crustacean muscle. Finally, a surprising number of molecular subtypes of major channels are being recognized by molecular genetic methods. These amino acid sequence differences have led to names like brain-type-I (-II or -III) Na channels. Eventually, all this loose nomenclature will be confusing, and perhaps a systematic approach analogous to that taken by the Enzyme Commission will be needed. However, such a revision ought to wait until the diversity of channels is better understood. By that time some clear structural and evolutionary relationships may form the basis for a natural classification.

Channels have families

Biophysicists long recognized that voltage-gated Na, K, and Ca channels have some functional similarities. Likewise synaptic channels gated by acetylcholine, glutamate, glycine, and γ-aminobutyric acid seemed similar. One of the great advances of the 1980s has been the sequencing by methods of molecular genetics of messenger RNAs, and even genes, that code for ionic channels. The predicted amino acid sequences reveal strong structural similarities among groups of channels that now allow us to talk about families of homologous channel proteins that would have evolved by processes of successive gene duplication, mutation, and selection from common ancestral channels. An unexpected discovery is the large size of these gene families. As has also been found for enzymes and other proteins, none of the channels we have mentioned is a single structural entity. They all come in various isoforms coded by different genes that may be selectively expressed in certain cell types and in certain periods of development and growth of the organism. Thus we suppose that there are hundreds of genes coding for channels in any individual.

Ohm's law is central

In the study of ionic channels, we see—more than in most areas of biology—how much can be learned by applying simple laws of physics. Much of what we know about ionic channels was deduced from electrical measurements. Therefore, it is essential to remember rules of electricity before discussing experiments. The remainder of this chapter is a digression on the necessary rules of physics. To do biophysical experiments well, one must often make sophisticated use of electrical ideas; however, as this book is concerned with channels and not with techniques of measurement, the essential principles are few. The most important is Ohm's law, a relation between current, voltage, and conductance, which we now review.

All matter is made up of charged particles. They are normally present in equal numbers, so most bodies are electrically neutral. A mole of hydrogen atoms contains Avogadro's number ($N = 6.02 \times 10^{23}$) of protons and the same number of electrons. Quantity of charge is measured in coulombs (abbreviated

TABLE 1. PHYSICAL CONSTANTS

Avogadro's number	$N = 6.022 \times 10^{23}\ \text{mol}^{-1}$
Elementary charge	$e = 1.602 \times 10^{-19}\ \text{C}$
Faraday's constant	$F = 9.648 \times 10^{4}\ \text{C mol}^{-1}$
Absolute temperature	$T(\text{K}) = 273.16 + T\ (^{\circ}\text{Celsius})$
Boltzmann's constant (in electrical units)	$k = 1.381 \times 10^{-23}\ \text{V C K}^{-1}$
Gas constant (in energy units)	$R = 1.987\ \text{cal K}^{-1}\ \text{mol}^{-1}$ $= 8.315\ \text{J K}^{-1}\ \text{mol}^{-1}$
Polarizability of free space	$\varepsilon_0 = 8.854 \times 10^{-12}\ \text{C V}^{-1}\ \text{m}^{-1}$
One joule	$1\ \text{J} = 1\ \text{kg m}^2\ \text{s}^{-2}$ $= 1\ \text{V C} = 1\ \text{W s}$ $= 0.2389\ \text{cal}$

C), where the charge of a proton is $e = 1.6 \times 10^{-19}$ C. Avogadro's number of elementary charges is called the FARADAY CONSTANT: $F = Ne = 6 \times 10^{23} \times 1.6 \times 10^{-19} \approx 10^5$ C/mol. This is thus the charge on a mole of protons or on a mole of Na^+, K^+, or any other monovalent cation. The charge on a mole of Ca^{2+}, Mg^{2+}, or on other divalents cations is $2F$ and the charge on a mole of Cl^- ions or other monovalent anions is $-F$.

Electrical phenomena arise whenever charges of opposite sign are separated or can move independently. Any net flow of charges is called a CURRENT. Current is measured in amperes (abbreviated A), where one ampere corresponds to a steady flow of one coulomb per second. By the convention of Benjamin Franklin, positive current flows in the direction of movement of positive charges. Hence if positive and negative electrodes are placed in Ringer's solution, Na^+, K^+, and Ca^{2+} ions will start to move toward the negative pole, Cl^- ions will move toward the positive pole, and an electric current is said to flow through the solution from positive to negative pole. Michael Faraday named the positive electrode the ANODE and the negative, the CATHODE. In his terminology, anions flow to the anode, cations to the cathode, and current from anode to cathode. The size of the current will be determined by two factors: the potential difference between the electrodes and the electrical conductance of the solution between them. POTENTIAL DIFFERENCE is measured in volts (abbreviated V) and is defined as the work needed to move a unit test charge in a frictionless manner from one point to another. To move a coulomb of charge across a 1-V difference requires a joule of work. In common usage the words "potential," "voltage," and "voltage difference" are used interchangeably to mean potential difference, especially when referring to a membrane.

ELECTRICAL CONDUCTANCE is a measure of the ease of flow of current between two points. The conductance between two electrodes in salt water can be

increased by adding more salt or by bringing the electrodes closer together, and it can be decreased by placing a nonconducting obstruction between the electrodes, by moving them farther apart, or by making the solution between them more viscous. Conductance is measured in siemens (abbreviated S and formerly called mho) and is defined by Ohm's law in simple conductors:

$$I = gE \tag{1-1a}$$

which says that current (I) equals the product of conductance (g) and voltage difference (E) across the conductor. The reciprocal of conductance is called RESISTANCE (symbolized R) and is measured in ohms (abbreviated Ω). Ohm's law may also be written in terms of resistance:

$$E = IR \tag{1-1b}$$

One can draw an analogy between Ohm's law for electric current flow and the rule for flow of liquids in narrow tubes. In tubes the flow (analog of current) is proportional to the pressure difference (analog of voltage difference) divided by the frictional resistance.

Homogeneous conducting materials may be characterized by a bulk property called the RESISTIVITY, abbreviated ρ. It is the resistance measured by two 1-cm^2 electrodes applied to opposite sides of a 1-cm cube of the material and has the dimensions ohm · centimeter (Ω · cm). Resistivity is useful for calculating resistance of arbitrary shapes of materials. For example, for a right cylindrical block of length l and cross-sectional area A with electrodes of area A on the end faces, the resistance is

$$R = \frac{\rho l}{A} \tag{1-2}$$

Later in the book we will use this formula to estimate the resistance in a cylindrical pore. Resistivity decreases as salts are added to a solution. Consider the following approximate examples at 20°C: frog Ringer's solution 80 Ω · cm, mammalian saline 60 Ω · cm, and seawater 20 Ω · cm. Indeed, in sufficiently dilute solutions each added ion gives a known increment to the overall solution conductance, and the resistivity of electrolyte solutions can be predicted by calculations from tables of single-ion equivalent conductivities, like those in Robinson and Stokes (1965). In saline solutions the resistivity of pure phospholipid bilayers is as high as 10^{15} Ω · cm, because although the physiological ions can move in lipid, they far prefer an aqueous environment over a hydrophobic one. The electrical conductivity of biological membranes comes not from the lipid, but from the ionic channels embedded in the lipid.

To summarize what we have said so far, when one volt is applied across a 1 Ω resistor or 1-S conductor, a current of one ampere flows; every second, $1/F$ moles of charge (10.4 μmol) move and one joule of heat is produced. Ohm's law plays a central role in membrane biophysics because each ionic channel is an elementary conductor spanning the insulating lipid membrane. The total electrical conductance of a membrane is the sum of all these elementary conductances in parallel.

It is a measure of how many ionic channels are open, how many ions are available to go through them, and how easily the ions pass.

The membrane as a capacitor

In addition to containing many conducting channels, the lipid bilayer of biological membranes separates internal and external conducting solutions by an extremely thin insulating layer. Such a narrow gap between two conductors forms, of necessity, a significant electrical capacitor.

To create a potential difference between objects requires only a separation of charge. CAPACITANCE (symbolized C) is a measure of how much charge (Q) needs to be transferred from one conductor to another to set up a given potential and is defined by

$$C = \frac{Q}{E} \tag{1-3}$$

The unit of capacitance is the farad (abbreviated F). A 1-F capacitor will be charged to 1 V when +1.0 C of charge is on one conductor and −1.0 C on the other. In an ideal capacitor the passage of current simply removes charge from one conductor and stores it on another in a fully reversible manner and without evolving heat. The rate of change of the potential under a current I_C is obtained by differentiating Equation 1-3.

$$\frac{dE}{dt} = \frac{I_C}{C} \tag{1-4}$$

The capacity to store charges arises from their mutual attraction across the gap and by the polarization they develop in the insulating medium. The capacitance depends on the dielectric constant of that medium and on the geometry of the conductors. In a simple capacitor formed by two parallel plates of area A and separated by an insulator of dielectric constant ϵ and thickness d, the capacitance is

$$C = \frac{\varepsilon \varepsilon_0 A}{d} \tag{1-5}$$

where ε_0, called the polarizability of free space, is $8.85 \times 10^{-12}\ CV^{-1}m^{-1}$. Cell membranes are parallel-plate capacitors with specific capacitances[1] near 1.0 $\mu F/cm^2$, just slightly higher than that of a pure lipid bilayer, 0.8 $\mu F/cm^2$ (see Cole, 1968; Almers, 1978). According to Equation 1-5, this means that the thickness d of the insulating bilayer is only 23 Å (2.3 nm), assuming that the dielectric constant of hydrocarbon chains is 2.1. Hence the high electrical capacitance of biological membranes is a direct consequence of their molecular dimensions.

The high capacitance gives a lower limit to how many ions (charges) must move (Equation 1-3) and how rapidly they must move (Equation 1-4) to make a

[1] In describing cell membranes, the phrases "specific capacitance," "specific resistance," and "specific conductance" refer to electrical properties of a 1-cm^2 area of membrane. They are useful for comparing the properties of different membranes.

a given electrical signal. In general, capacitance slows down the voltage response to any current by a characteristic time τ that depends on the product RC of the capacitance and any effective parallel resistance. For example, suppose that a capacitor is charged up to 1.0 V and then allowed to discharge through a resistor R as in Figure 2. From Ohm's law the current in the resistor is $I = E/R$, which discharges the capacitor at a rate (Equation 1-4)

$$\frac{dE}{dt} = \frac{I_C}{C} = -\frac{E}{RC} \tag{1-4a}$$

The solution of this first-order differential equation has an exponentially decaying time course

$$E = E_0 \exp\left(-\frac{t}{RC}\right) = E_0 \exp\left(-\frac{t}{\tau}\right) \tag{1-6}$$

where E_0 is the starting voltage, t is time in seconds, and exp is the exponential function (power of e, the base of natural logarithms).

For biological membranes the product, $R_M C_M$, of membrane resistance and capacitance is often called the membrane time constant, τ_M. It can be determined, using equations like Equation 1-6, from measurements of the time course of membrane potential changes as small steps of current are applied across the membrane. For example, in Figure 3 steps of current are applied from an intracellular microelectrode across the cell membrane of a *Paramecium*. The time course of the membrane potential changes corresponds to a membrane time constant of 60 ms. Since C_M is approximately 1 $\mu F/cm^2$ in all biological membranes, the measured τ_M gives a convenient first estimate of specific membrane resistance. For the *Paramecium* in the figure, R_M is τ_M/C_M or 60,000 $\Omega \cdot cm^2$. In

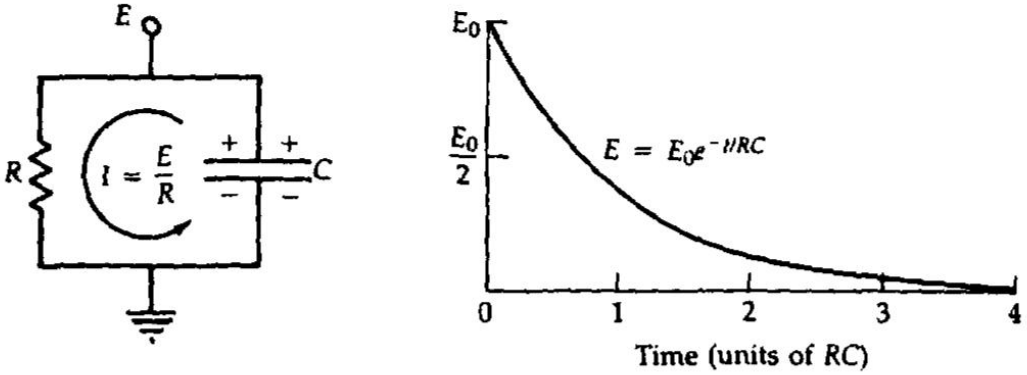

(A) CIRCUIT (B) TIME COURSE OF DISCHARGE

2 DISCHARGE OF AN *RC* CIRCUIT

The circuit has a resistor and a capacitor connected in parallel, and the voltage across the capacitor is measured from the two terminals. At zero time the capacitor has been charged up to a voltage of E_0 and begins to discharge through the resistor. Charge and voltage decay exponentially so that in every RC seconds they fall to $1/e$ or 0.367... of their previous value.

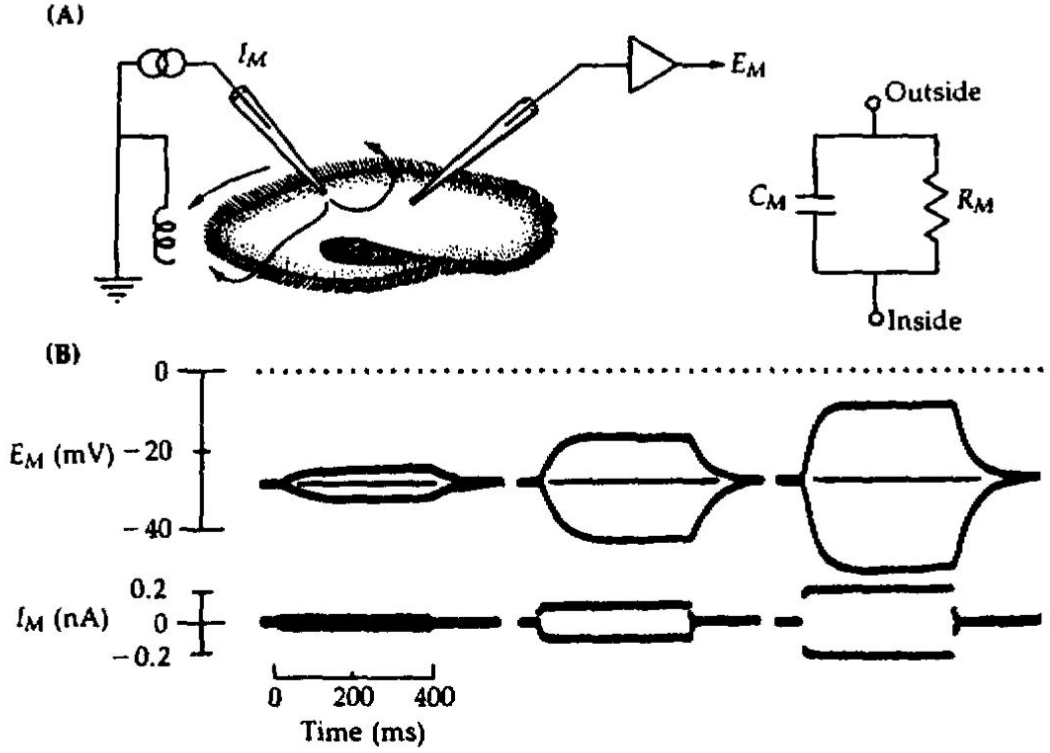

3 THE CELL MEMBRANE AS AN *RC* CIRCUIT

An experiment to study membrane electrical properties of a *Paramecium*. The cell is impaled with two intracellular electrodes. One of them passes steps of current I_M across the membrane to an electrode in the bath. The other records the changes of membrane potential E_M with an amplifier, symbolized as a triangle. On the right, a current of 0.23 nA makes a voltage deflection of 23 mV, corresponding from Ohm's law to a membrane resistance of 100 MΩ (10^8 Ω). The exponential time constant τ_M of the rise and fall of the voltage response is approximately 60 ms. This *Paramecium* contains a genetic mutation of the normal excitability mechanism, so its responses to current steps are simpler than for the genetic wild-type *Paramecium*. [From Hille, 1989a; after Kung and Eckert, 1972.]

different resting cell membranes, τ_M ranges from 10 μs to 1 s, corresponding to resting R_M values of 10 to 10^6 Ω · cm^2. This broad range of specific resistances shows that the number of ionic channels open at rest differs vastly from cell to cell.

Equilibrium potentials and the Nernst equation

The final physical topic concerns equilibrium. All systems are moving toward EQUILIBRIUM, a state where the tendency for further change vanishes. At equilibrium, thermal forces balance the other existing forces and forward and backward fluxes in every microscopic transport mechanism and chemical reaction are equal. We want to consider the problem illustrated in Figure 4. Two compartments of a bath are separated by a membrane containing pores permeable only to K^+ ions. A high concentration of a salt KA (A for anion) is introduced into the

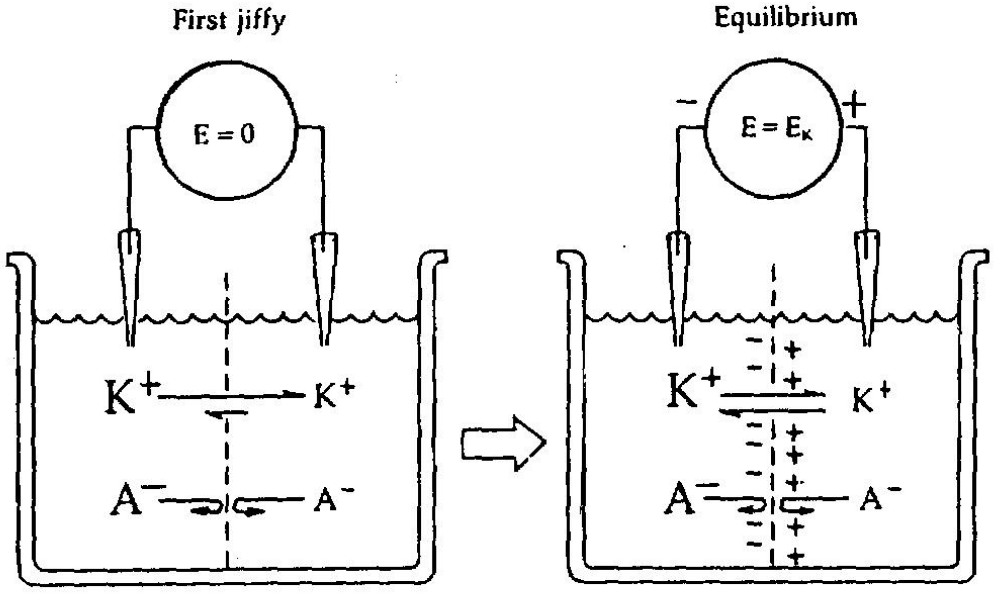

4 DIFFUSION POTENTIALS IN PORES

A membrane with perfectly K^+-selective pores separates solutions with different concentrations of a potassium salt, KA. A voltmeter records the potential across the porous membrane. At the moment when the salt solutions are poured in, there is no membrane potential, $E = 0$. However, as a few K^+ ions diffuse from side 1 to side 2, a potential develops with side 2 becoming positive. Eventually the membrane potential reaches the Nernst potential for K^+ ions, $E = E_K$.

left side and a low concentration into the right side. A voltmeter measures the membrane potential. In the first jiffy, the voltmeter reads 0 mV, as both sides are neutral. However, K^+ ions immediately start diffusing down their concentration gradient into the right-hand side, giving that side an excess positive charge and building up an electrical potential difference across the membrane. The anion cannot cross the membrane, so the charge separation persists. However, the thermal "forces" causing net diffusion of K^+ to the right are now countered by a growing electrical force tending to oppose the flow of K^+. The potential builds up until it finally reaches an equilibrium value, E_K, where the electrical force balances the diffusional force and the system no longer changes. The problem is to find a formula for E_K, the "equilibrium potential for K^+ ions." This is called an equilibrium problem even though parts of the system, such as the anions A^- and the water molecules (osmotic pressure), are not allowed to equilibrate. We may focus on K^+ ions alone and discuss their equilibrium. As we shall see, equilibrium potentials are the starting point in any description of biological membrane potentials.

A physicist would begin the problem with the BOLTZMANN EQUATION of statistical mechanics, which gives the relative probabilities at equilibrium of finding a particle in state 1 or in state 2 if the energy difference between these states is $u_2 - u_1$:

$$\frac{p_2}{p_1} = \exp\left(-\frac{u_2 - u_1}{kT}\right) \tag{1-7}$$

Here k is Boltzmann's constant and T is absolute temperature on the Kelvin scale. This equation conveniently describes the equilibrium distribution of particles in force fields. Qualitatively it says that a particle spends less time in states of higher energy than in states of lower energy. For example, the molecules in the Earth's atmosphere are attracted by the Earth's gravitational field, and Equation 1-7 correctly predicts that the probability of finding O_2 molecules at the top of Mt. Everest is only ⅓ of that of finding them at sea level.

For our purposes, Equation 1-7 can be recast into in a slightly more chemical form by changing from probabilities p to concentrations c and from single-particle energies u to molar energies U

$$\frac{c_2}{c_1} = \exp\left(-\frac{U_2 - U_1}{RT}\right) \tag{1-8}$$

where R is the gas constant ($R = kN$). Finally, taking natural logarithms of both sides and rearranging gives

$$U_1 - U_2 = RT \ln \frac{c_2}{c_1} \tag{1-9}$$

Now we have a useful equilibrium relation between concentration ratios and energy differences. In our problem $U_1 - U_2$ is the molar electrical energy difference of the permeable ion due to the membrane potential difference $E_1 - E_2$. If we consider a mole of an arbitrary ion S with charge z_S, then $U_1 - U_2$ becomes $z_S F(E_1 - E_2)$. Substituting into Equation 1-9 gives the equilibrium potential E_S as a function of the concentration ratio and the valence:

$$E_S = E_1 - E_2 = \frac{RT}{z_S F} \ln \frac{[S]_2}{[S]_1} \tag{1-10}$$

This well-known relationship is called the NERNST EQUATION (Nernst, 1888).

Before discussing the meaning of the equation, let us note as an aside that the equilibrium potential E_S can be derived in other, equivalent ways. A chemist would probably think in terms of the thermodynamics, using the principle of J.W. Gibbs that the electrochemical potential of ion S is the same on both sides at equilibrium, or equivalently that the work of transfer of a tiny quantity of S from side 2 to side 1 has to be zero. This work comprises two terms: the work of concentrating the ions as they cross, $-RT \ln (c_2/c_1)$, plus all other energy changes, $U_1 - U_2$, which in this case is only the electrical term. These considerations lead at once to Equations 1-9 and 1-10. Thermodynamics would also point out that because all solutions are at least slightly nonideal (unlike ideal gases), one should use activities rather than concentrations (see, e.g., Moore, 1972). This book refers to the symbol [S] as the concentration of S while recognizing that careful quantitative work requires consideration of activities instead.

According to the Nernst equation, ionic equilibrium potentials vary linearly with the absolute temperature and logarithmically with the ionic concentration ratio. As would be expected from our discussion of Figure 4, equilibrium potentials change sign if the charge of the ion is reversed or if the direction of the

gradient is reversed, and they fall to zero when there is no gradient. To correspond to the physiological convention, we now define side 1 as inside (intracellular), 2 as outside (extracellular), and all membrane potentials to be measured inside minus outside. Then we can write the equilibrium potentials for K^+ ions and for the other biologically relevant ions.

$$E_K = \frac{RT}{F} \ln \frac{[K]_o}{[K]_i} \tag{1-11a}$$

$$E_{Na} = \frac{RT}{F} \ln \frac{[Na]_o}{[Na]_i} \tag{1-11b}$$

$$E_{Ca} = \frac{RT}{2F} \ln \frac{[Ca]_o}{[Ca]_i} \tag{1-11c}$$

$$E_{Cl} = \frac{RT}{F} \ln \frac{[Cl]_i}{[Cl]_o} \tag{1-11d}$$

The subscripts o and i stand for outside and inside, respectively. The meaning of the numbers E_K, E_{Na}, and so on, can be stated in two ways. Using E_K as an example: (1) If the pores in a membrane are permeable only to K^+ ions, the membrane potential will change to E_K; (2) If the membrane potential is held somehow at E_K, there will be no net flux of K^+ ions through K^+-selective pores.

How large are the equilibrium potentials for living cells? Table 2 lists values of the factor RT/F in the Nernst equation; also given are values of $2.303(RT/F)$ for calculations with $\log_{10}$ instead of ln as follows:

$$E_K = \frac{RT}{F} \ln \frac{[K]_o}{[K]_i} = 2.303 \frac{RT}{F} \log_{10} \frac{[K]_o}{[K]_i} \tag{1-11e}$$

From Table 2 at 20°C an e-fold ($e \approx 2.72$) K^+ concentration ratio corresponds to

TABLE 2. VALUES OF *RT/F* (OR *kT/e*)

Temperature (°C)	*RT/F* (mV)	2.303 *RT/F* (mV)
0	23.54	54.20
5	23.97	55.19
10	24.40	56.18
15	24.83	57.17
20	25.26	58.17
25	25.69	59.16
30	26.12	60.15
35	26.55	61.14
37	26.73	61.54

TABLE 3. FREE IONIC CONCENTRATIONS AND EQUILIBRIUM POTENTIALS FOR MAMMALIAN SKELETAL MUSCLE

Ion	Extracellular concentration (mM)	Intracellular concentration (mM)	$\frac{[Ion]_o}{[Ion]_i}$	Equilibrium potential[a] (mV)
Na^+	145	12	12	+67
K^+	4	155	0.026	−98
Ca^{2+}	1.5	10^{-7} M	15,000	+129
Cl^-	123	4.2[b]	29[b]	−90[b]

[a] Calculated from Equation 1-11 at 37°C.
[b] Calculated assuming a −90-mV resting potential for the muscle membrane and that Cl^- ions are at equilibrium at rest.

$E_K = -25.3$ mV, a 10-fold ratio corresponds to $E_K = -58.2$ mV, and a 100-fold ratio corresponds to $E_K = -58.2 \times 2 = -116.4$ mV. Table 3 lists the actual concentrations of some ions in mammalian skeletal muscle and their calculated equilibrium potentials ranging from −98 to +128 mV. E_K and E_{Cl} are negative, and E_{Na} and E_{Ca} are positive numbers. E_K sets the negative limit and E_{Ca} the positive limit of membrane potentials that can be achieved by opening ion-selective pores in the muscle membrane. All excitable cells have negative resting potentials because at rest they have far more open K-selective channels (and in muscle, Cl-selective channels, too) than Na-selective or Ca-selective ones.

Current–voltage relations of channels

Biophysicists like to represent the properties of membranes and channels by simple electrical circuit diagrams that have equivalent electrical properties to the membrane. We have discussed the membrane as a capacitor and the channel as a conductor. But if we try to test Ohm's law on the membrane of Figure 4, we would immediately recognize a deviation: Current in the pores goes to zero at E_K and not at 0 mV. The physical chemist would say, "Yes, you have a concentration gradient, so Ohm's law doesn't work." The biophysicist would then suggest that a gradient is like a battery with an electromotive force (emf) in series with the resistor (see Figure 5) and the modified current–voltage law becomes

$$I_K = g_K(E - E_K) \tag{1-12}$$

The electromotive force is E_K and the net driving force on K^+ ions is now $E - E_K$ and not E. This modification is, like Ohm's law itself, empirical and requires experimental test in each situation. To a first approximation this linear law is often excellent, but many pores are known to have nonlinear current–voltage relations when open. Some curvature is predicted, as we shall see later, by explicit calculations of the electrodiffusion of ions in pores, particularly when there is a higher concentration of permeant ion on one side of the membrane than on the other or when the structure of the channel is asymmetrical.

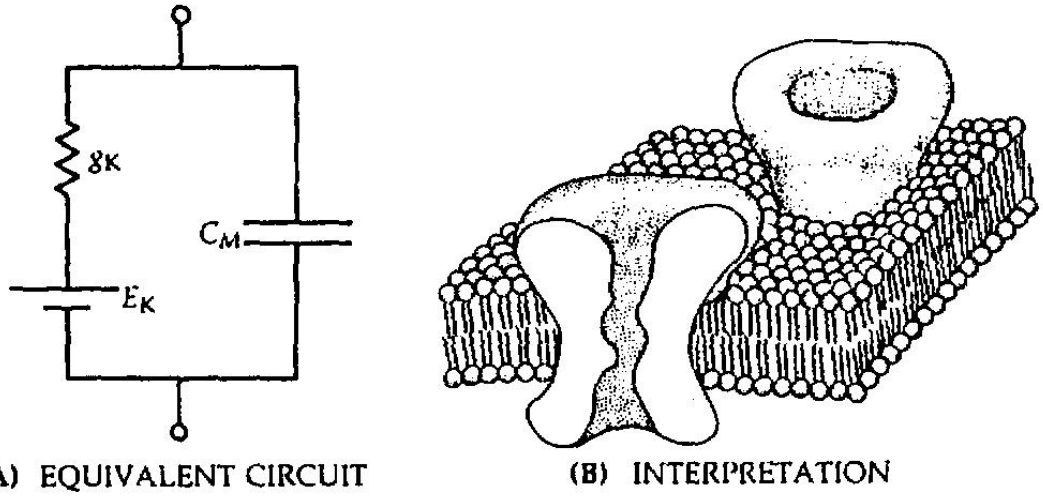

(A) EQUIVALENT CIRCUIT (B) INTERPRETATION

5 TWO VIEWS OF A K^+-SELECTIVE MEMBRANE

In electrical experiments the membrane acts like an equivalent circuit with two branches. The conductive branch with an EMF of E_K suggests a K^+-selective aqueous diffusion path, a pore. The capacitive branch suggests a thin insulator, the lipid bilayer.

Consider now how simple current–voltage measurements can be used to gain information on ionic channels. Figure 6 gives examples of hypothetical observations and their interpretation in terms of electrical equivalent circuits. Figure 6A shows three linear *I–E* curves. They pass through the origin, so no battery is required in the equivalent circuit, meaning either that the channels are nonselective or that there is no effective ionic gradient. The slopes of the successive *I–E* relations decrease twofold, so the equivalent conductance, and hence the number of open channels, differs correspondingly. Thus conductances give a useful measure of how many channels are open in an area of membrane.

6 CURRENT–VOLTAGE RELATIONS OF MEMBRANES ►

Measured *I–E* relations can be interpreted in terms of electrical equivalent circuits and the modified form of Ohm's law (Equation 1-12) that takes into account the electromotive force in the pores. Four hypothetical conditions are shown. (A) Membranes with 1, 2, and 3 pores open give *I–E* relations with relative slopes of 1, 2, and 3. (B) Pores with negative or positive electromotive forces give *I–E* relations with negative or positive zero-current potentials. (C) Pores that step from a low-conductance state to a high-conductance state (see inset graph of g versus E) give *I–E* relations consisting of two line segments. (D) Pores with smoothly voltage-dependent probability of being open (see inset graph of average g versus E) give curved *I–E* relations. The dashed lines, corresponding to a constant high conductance, are the same *I–E* relations as in part B. However, when the pores close at negative potentials, lowering g, the current decreases correspondingly from its maximal value.

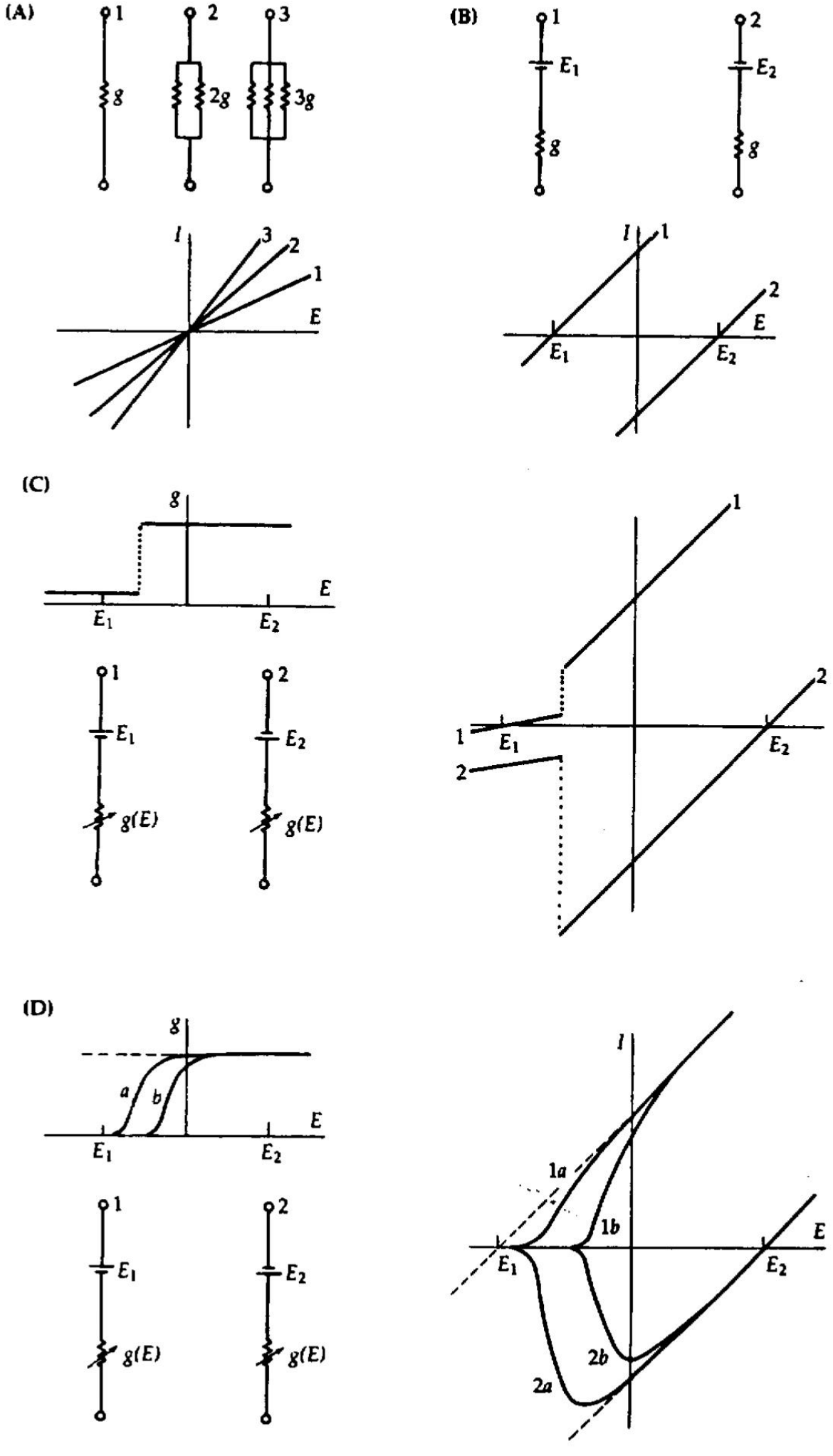
(A)
1
2
3
g
2g
3g
I
E
(B)
E1
E2
(C)
g(E)
(D)
a
b
1a
1b
2a
2b

Figure 6B shows two *I–E* relations of equal slope but with different zero-current potentials. The corresponding equivalent circuits have equal conductances but different electromotive forces in their batteries. This could arise from different channels with different ionic selectivities or from the same channel bathed on the two sides by different concentrations of its permeant ions. Hence zero-current potentials are useful in studies of selectivity.

Figure 6C shows the effect of a CONDUCTANCE CHANGE. This is a little harder and needs to be analyzed in several steps. Since the *I–E* relations do not pass through the origin, we know again that there is an electromotive force in these channels. Both a negative emf, E_1, and a positive emf, E_2, are illustrated, as in Figure 6B. Unlike Figure 6B, however, here the *I–E* relations are not single straight lines. This tells us that the membrane conductance changes with voltage, a property called RECTIFICATION in electric circuit theory. In biological membranes, strong rectification usually means that the ionic channels carrying current are open at some membrane potentials and shut at others. We can imagine a voltage-gated switch that opens and closes the channels. In this example, the conductance is low at very negative membrane potentials and suddenly steps up to a higher level as the potential is made less negative. The low- and high-conductance segments of the *I–E* relation are each linear and extrapolate back to a zero-current point corresponding to the emf of the channels when open.

Figure 6C corresponds to measurements on a system with a sharp voltage threshold for opening of ionic channels. Real voltage-gated channels cannot measure the membrane potential this precisely and the voltage dependence of their opening is less abrupt, as in Figure 6D. The case illustrated in Figure 6D may seem difficult, but because it corresponds closely to practical observations, it is worth working through. First note that there is no ionic current at membrane potentials more negative than E_1. Hence the conductance is zero there, and the channels must be closed. Positive to 0 mV, the *I–E* relations are steep, straight lines like those in Figure 6B. Here the conductance is high, and the channels must be open. In the intermediate voltage range, between E_1 and 0 mV, the current is smaller than expected from the maximal conductance (dashed lines). Hence only some of the channels are open.

To determine how many channels are open at each voltage, we should calculate the ionic conductance at each potential. When this is done using the modified form of Ohm's law (Equation 1-12) and the appropriate channel electromotive force, E_1 or E_2, one derives the conductance–voltage (g–E) relations shown in the inset. The conductance changes from fully off to fully on over a narrow voltage range. As a first approximation, this continuous conductance–voltage relation reflects the steep voltage dependence of the open probability of the channel.[2] We can think of this channel as being electrically excitable, a voltage-gated pore.

The *I–E* relations in Figure 6 are representative of observations made daily in biophysical studies of ionic channels. Examples will appear in Chapter 2. Inter-

[2] Some nonlinearities may be due to other factors, including an intrinsic nonlinearity of the *I–E* curve for a single open channel, discussed above.

ested readers will want to work out for themselves how voltage-dependent channel opening accounts for the results by resketching each *I–E* relation and calculating the corresponding conductance–voltage relation point-by-point from Equation 1-12.

Ionic selectivity

It is essential for electrical excitability that different ionic channels be selective for different ions. However, no channel is perfectly selective. Thus the Na channel of axons is fairly permeable to NH_4^+ ions and even slightly permeable to K^+ ions. How can we determine ionic selectivity from electrical measurements? The simplest way is to measure the electromotive force or zero-current potential for the channel with, say, ion A^+ on the outside and B^+ on the inside. This is called a BIIONIC POTENTIAL. Suppose that A^+ and B^+ have the same valence. If no other permeant[3] ion is present, the permeability ration P_A/P_B is defined by the equation

$$E_{rev} = \frac{RT}{zF} \ln \frac{P_A [A]_o}{P_B [B]_i} \tag{1-13}$$

where the zero-current potential is often called the REVERSAL POTENTIAL (E_{rev}) since that is the potential around which the current reverses sign.

Equation 1-13 resembles the Nernst equation, but now with two ions. It expresses an important, simple idea: The permeability of a channel for A^+ is said to be half that for B^+ when you need two concentration units of A on one side and one concentration unit of B on the other to get zero electromotive force. Equation 1-13 is the simplest form of an expression derived from diffusion theory by Goldman (1943) and Hodgkin and Katz (1949). Unlike the Nernst equation, such expressions describe a steady-state interdiffusion of ions away from equilibrium. Therefore, the simplifying rules of equilibrium cannot be applied, and the derivation must make assumptions about the structure of the channel.

Signaling requires only small ionic fluxes

To close this chapter we can exercise our electrical knowledge by reconsidering the experiment in Figure 4 using biologically realistic numbers and the electrical equivalent circuit in Figure 5. Suppose that the membrane contains K-selective pores that contribute 20 pS (20×10^{-12} siemens) of electrical conductance apiece.[4] If an average of 0.5 pore is open per square micrometer, the specific membrane conductance is

$$g_M = \frac{0.5 \times 20 \times 10^{-12}\ \text{S}/\mu\text{m}^2}{10^{-8}\ \text{cm}^2/\mu\text{m}^2} = 1\ \text{mS/cm}^2$$

[3] The words "permeable" and "permeant" are sometimes confused. A channel is *permeable*: capable of being permeated. An ion is *permeant*: capable of permeating. In French a raincoat is *un imperméable*.

[4] Most biological ionic channels have an electrical conductance in the range of 1 to 150 pS.

Then the specific membrane resistance is $R_M = 1/g_M = 1000\ \Omega \cdot \text{cm}^2$, and the membrane time constant for $C_M = 1\ \mu\text{F/cm}^2$ is $\tau_M = R_M C_M = 1$ ms. Suppose that the concentration ratio of KA salt across the membrane is 52:1 so that E_K is $58.2 \log_{10} (\frac{1}{52}) = -100$ mV. Now what happens immediately after the salt solutions are introduced and K^+ ions start to diffuse? The voltmeter reports a membrane potential changing from 0 mV to −100 mV along an exponential time course with a time constant of 1 ms.

$$E = [1 - \exp(-t/1\ \text{ms})] \cdot 100\ \text{mV}$$

After a few milliseconds the system has reached equilibrium and an excess charge of $Q = EC_M = 10^{-7}\ \text{C/cm}^2$, all carried by K^+ ions, has been separated across the membrane. This amounts to a movement of $Q/F = 10^{-12}$ mol of K^+ ions per cm^2 of membrane, a tiny amount that would alter the original 52-fold gradient very little. Hence our calculation shows that full-sized electrical signals can be generated rapidly even with relatively few pores per unit area and with only minute ionic fluxes.

Notice that the size of the needed ionic flux depends on the *surface area* of the cell, whereas the effect of the flux on internal ionic concentrations depends on the *volume* of the cell. In a giant cell (a 1000-μm-diameter squid axon) the surface-to-volume ratio is the lowest, and electrical signaling with a 110-mV action potential changes the available ionic concentration gradient by only 1 part in 10^5. On the other hand, the smallest cells (a 0.1-μm axon or dendrite), the surface-to-volume ratio is 10^4 times higher and a single action potential might move as much as 10% of the stored-up ions.

Having reviewed some essential rules of physics, we may now turn to the experimental study of ionic channels.

PART I

CLASSICAL DESCRIPTION OF CHANNELS

The electrical excitability of nerve and muscle has attracted physically minded scientists for several centuries. A variety of formal, quantitative descriptions of excitation prevailed long before there was knowledge of the molecular constituents of biological membranes. This tradition culminated in the Hodgkin–Huxley model for action potentials of the squid giant axon. Theirs was the first model to recognize separate, voltage-dependent permeability changes for different ions. It was the first to describe the ionic basis of excitation correctly. It revolutionized electrophysiology.

The Hodgkin–Huxley model became the focus as subsequent work sought to explore two questions: Is excitation in all cells and in all organisms explained by the same sodium and potassium permeability changes that work so well for the squid giant axon? And what are the molecular and physicochemical mechanisms underlying these permeabilities? Naturally, such questions are strongly interrelated. Nevertheless, this book is divided broadly along these lines. Part I concerns the original work with the squid giant axon and the subsequent discovery of many kinds of ionic channels using classical electrical methods. Part I is phenomenological and touches on biological questions of diversity and function. It shows that excitation and signaling can be accounted for by the opening and closing of channels with different reversal potentials. Part II concerns the underlying mechanisms. It is more analytical, physical, and chemical.

CLASSICAL BIOPHYSICS OF THE SQUID GIANT AXON

What does a biophysicist think about?

Scientific work proceeds at many levels of complexity. Scientists assume that all observable phenomena could ultimately be accounted for by a small number of unifying physical laws. Science, then, is the attempt to find ever more fundamental laws and to reconstruct the long chains of causes from these foundations up to the full range of natural events.

In adding its link to the chain, each scientific discipline adopts a set of phenomena to work on and develops rules that are considered a satisfactory "explanation" of what is seen. What a higher discipline may view as its fundamental rules might be considered by a lower discipline as complex phenomena needing explanation. So it is also in the study of excitable cells. Neurophysiologists seek to explain patterns of animal behavior in terms of anatomical connections of nerve cells and rules of cellular response such as excitation, inhibition, facilitation, summation, or threshold. Membrane biophysicists seek to explain these rules of cellular response in terms of physical chemistry and electricity. For the neurophysiologist, the fine units of signaling are membrane potentials and cell connections. For the biophysicist the coarse observables are ionic movements and permeability changes of the membrane and the fundamental rules are at the level of electrostatics, kinetic theory, and molecular mechanics.

Membrane biophysicists delight in electronics and simplified preparations consisting of parts of single cells. They like to represent dynamic processes as equations of chemical kinetics and diffusion, membranes as electric circuits, and molecules as charges, dipoles, and dielectrics. They often conclude their investigations with a kinetic model describing hypothetical interconversions of states and objects that have not yet been seen. A good model should obey rules of thermodynamics and electrostatics, give responses like those observed, and suggest some structural features of the processes described. The biophysical method fosters sensitive and extensive electrical measurements and leads to detailed kinetic descriptions. It is austere on the chemical side, however, as it cares less about the chemistry of the structures involved than about the dynamic and equilibrium properties they exhibit. Biophysics has been highly successful, but it is only one of several disciplines needed in order to develop a well-rounded picture of how excitability works and what it is good for.

This chapter concerns an early period in membrane biophysics when a sophisticated kinetic description of membrane permeability changes was achieved without definite knowledge of the membrane molecules involved, indeed without knowledge of ionic channels at all. The major players were Kenneth Cole and Howard Curtis in the United States and Alan Hodgkin, Andrew Huxley, and Bernard Katz in Great Britain. They studied the passive membrane properties and the propagated action potential of the squid giant axon. In this heroic time of what can be called classical biophysics (1935–1952) the membrane ionic theory of excitation was transformed from untested hypothesis to established fact. As a result, electrophysiologists became convinced that all the known electrical signals, action potentials, synaptic potentials, and receptor potentials had a basis in ionic permeability changes. Using the new techniques, they set out to find the relevant ions for signals in the variety of cells and organisms that could be studied. This program of description still continues.

The focus here is on biophysical ideas relevant to the discussion of ionic channels in later chapters rather than on the physiology of signaling. The story illustrates the tremendous power of purely electrical measurements in testing Bernstein's membrane hypothesis. Most readers will already have studied an outline of nervous signaling in courses of biology. Those wanting to know more neurobiology or neurophysiology can consult recent texts (Junge, 1991; Kandel et al., 1991; Kuffler et al., 1984; Levitan and Kaczmarek, 1991; Patton et al., 1989; Shepherd, 1988).

The action potential is a regenerative wave of Na^+ permeability increase

ACTION POTENTIALS are the rapidly propagated electrical messages that speed along the axons of the nervous system and over the surface of some muscle and glandular cells. In axons they are brief, travel at constant velocity, and maintain a constant amplitude. Like all electrical messages of the nervous system, the action potential is a membrane potential change caused by the flow of ions through ionic channels in the membrane.

As a first approximation an axon may be regarded as a cylinder of axoplasm surrounded by a continuous surface membrane. The membrane potential, E_M, is defined as the inside potential minus the outside, or if, as is usually done, the outside medium is considered to be at ground potential (0 mV), the membrane potential is simply the intracellular potential. Membrane potentials can be measured with glass micropipette electrodes, which are made from capillary tubing pulled to a fine point and filled with a concentrated salt solution. A silver chloride wire inside the capillary leads to an amplifier. The combination of pipette, wire electrode, and amplifier is a sensitive tool for measuring potentials in the region just outside the tip of the electrode. In practice, the amplifier is zeroed with the pipette outside the cell, and then the pipette is advanced until it suddenly pops through the cell membrane. Just as suddenly, the amplifier reports a negative change of the recorded potential. This is the resting membrane potential. Values between -40 and -100 mV are typical.

Figure 1A shows the time course of membrane potential changes recorded with microelectrodes at two points in a squid giant axon stimulated by an electric shock. At rest the membrane potential is negative, as would be expected from a membrane primarily permeable to K^+ ions. The stimulus initiates an action potential that propagates to the end of the axon. When the action potential

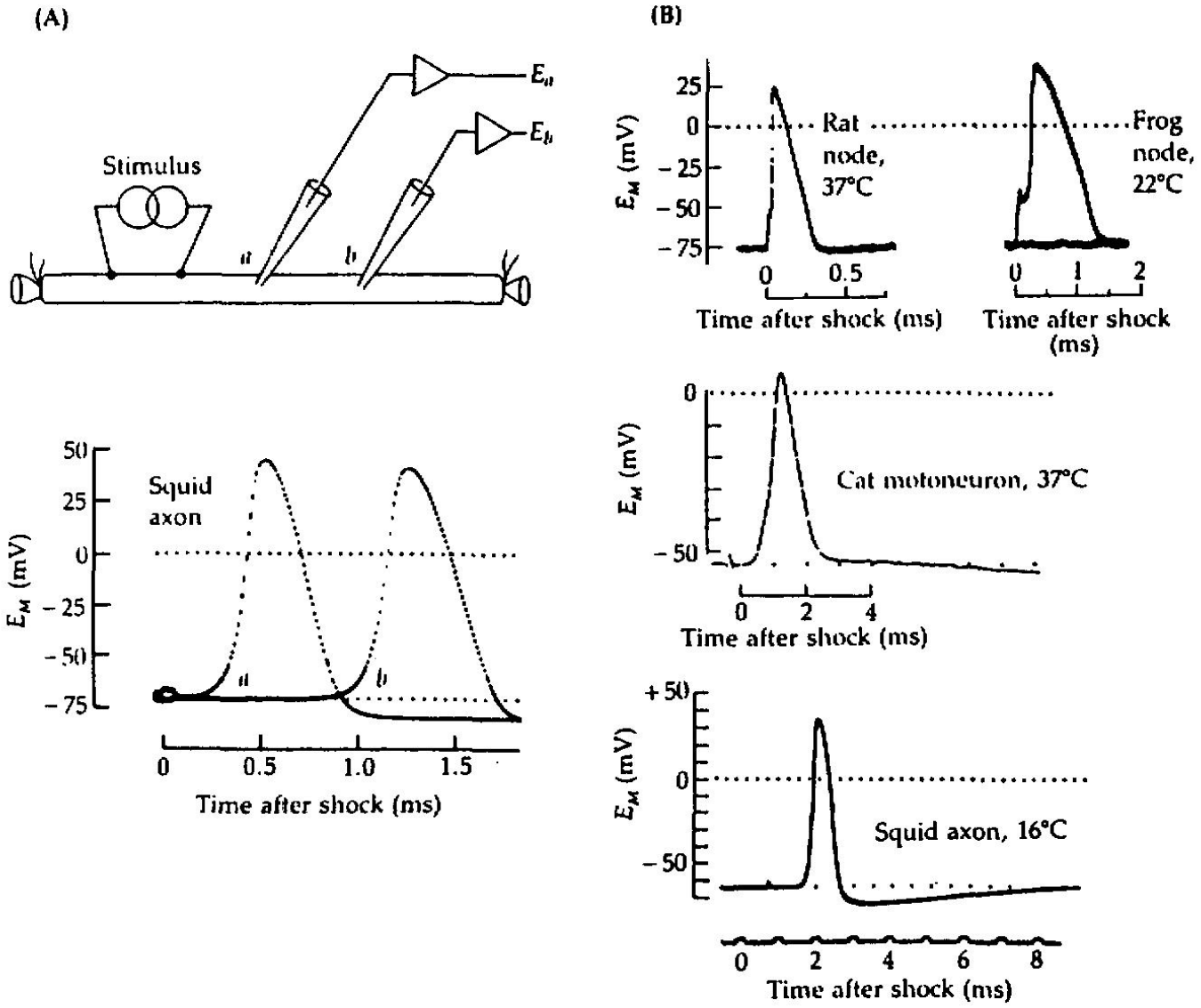

1 ACTION POTENTIALS IN NERVE MEMBRANES

(A) Propagated action potential recorded intracellularly from two points along a squid giant axon. The recording micropipettes *a* and *b* are separated by 16 mm, and a stimulator applies a shock to the axon. The two potential traces show the action potential sweeping by the two electrodes with a 0.75-ms propagation time between a and b, corresponding to a conduction velocity of 21.3 m/s. [After del Castillo and Moore, 1959.] (B) Comparison of action potentials from different cells. The recordings from nodes of Ranvier show the brief depolarization caused by the stimulating shock applied to the same node and followed by the regenerative action potential. [From Dodge, 1963; and W. Nonner, M. Horáckova, and R. Stämpfli, unpublished.] In the other two recordings, the stimulus (marked as a slight deflection) is delivered some distance away and the action potential has propagated to the recording site. [From W.E. Crill, unpublished; and Baker et al., 1962.]

sweeps by the recording electrodes, the membrane is seen to depolarize (become more positive), overshoot the zero line, and then repolarize (return to rest). Figure 1B shows action potentials from other cells. Cells that can make action potentials can always be stimulated by an electric shock. The stimulus must make a suprathreshold membrane depolarization. The response is a further sharp, all-or-none depolarization, the stereotyped action potential. Such cells are called ELECTRICALLY EXCITABLE.

Even as late as 1930, textbooks of physiology presented vague and widely diverging views of the mechanism underlying action potentials. To a few physiologists the very existence of a membrane was dubious and Bernstein's membrane hypothesis (1902, 1912) was wrong. To others, propagation of the nervous impulse was a chemical reaction confined to axoplasm and the action potential was only an epiphenomenon—the membrane reporting secondarily on interesting disturbances propagating chemically within the cell. To still others, the membrane was central and itself electrically excitable, propagation then being an electrical stimulation of unexcited membrane by the already active regions (Hermann, 1872, 1905a). This view finally prevailed. Hermann (1872) recognized that the potential changes associated with the excited region of an axon would send small currents (*Strömchen*) in a circuit down the axis cylinder, out through what we now call the membrane, and back in the extracellular space to the excited region (Figure 2A). These local circuit currents flow in the correct direction to stimulate the axon. He suggested thus that propagation is an electrical self-stimulation.

Following the lead of Höber, Osterhout, Fricke, and others, K.S. Cole began in 1923 to study membrane properties by measuring the electric impedance of cell suspensions and (with H.J. Curtis) of single cells. The cells were placed between two electrodes in a Wheatstone bridge and the measured impedances were translated into an electrical equivalent circuit made up of resistors and capacitors, representing the membrane, cytoplasm, and extracellular medium. The membrane was represented as an *RC* circuit. Careful experiments with vertebrate and invertebrate eggs, giant algae, frog muscle, and squid giant axons all gave essentially the same result. Each cell has a high-conductance cytoplasm, with an electrical conductivity 30 to 60% that of the bathing saline, surrounded by a membrane of low conductance and an electrical capacitance of about 1 $\mu F/cm^2$. Such measurements were important for Bernstein's theory. They showed that all cells have a thin plasma membrane of molecular dimensions and low ionic permeability, and that ions in the cytoplasm can move about within the intracellular space almost as freely as in free solution. The background and results of Cole's extensive studies are well summarized in his book (Cole, 1968).

These properties also confirmed the essential assumptions of Hermann's (1905a,b) core-conductor or cable-theory model for the passive[1] spread of poten-

[1] The early literature adopted the word "passive" to describe properties and responses that could be understood by simple electrical cable theory where, as we have already done, the cytoplasm is described as a fixed resistor and the membrane as a fixed resistor and capacitor. Potentials spreading this way were said to spread "electrotonically," a term coined by du Bois Reymond to

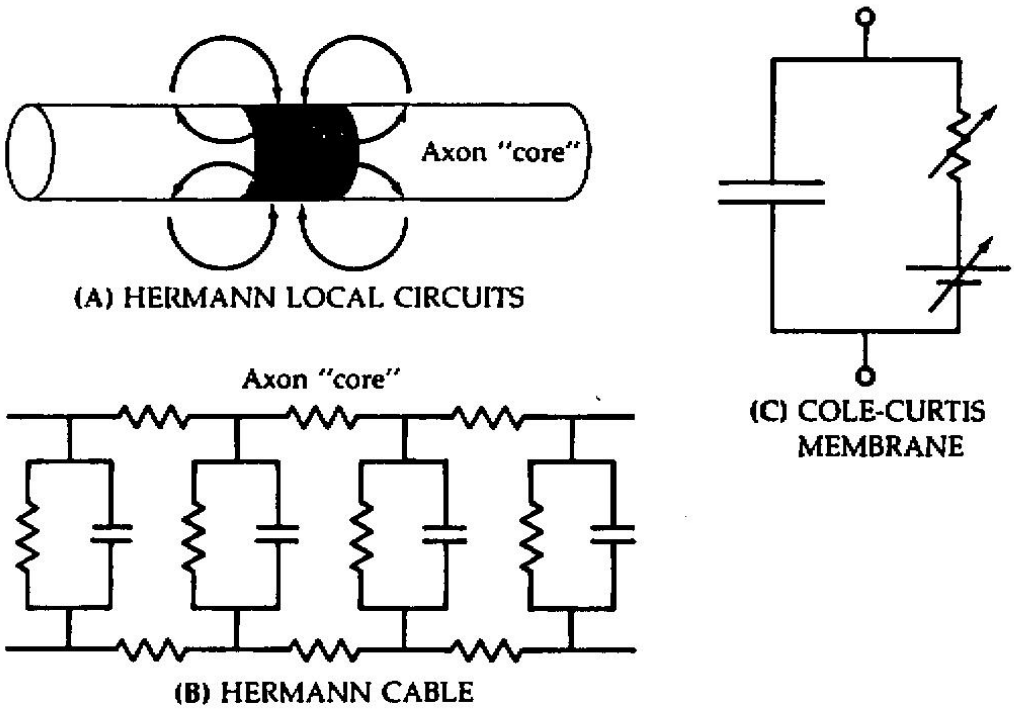

2 EARLY DESCRIPTIONS OF EXCITATION

Biophysicists sought to represent excitation and propagation of action potentials in terms of simple electrical circuits. (A) Hermann (1872) suggested that the potential difference between excited and unexcited regions of an axon would cause small currents (later named local circuit currents by Hodgkin) to flow between them in the correct direction to stimulate the previously unexcited region. [Drawing after Hermann, 1905a.] (B) Hermann (1905b) described the passive spread of potentials in axons and muscle by the theory for a "leaky" telegraph cable. Here the protoplasmic core and extracellular region are represented as chains of resistors and the region between them (now called the membrane), as parallel capacitors and resistors. (C) Cole and Curtis (1938) used this equivalent circuit to interpret their measurements of membrane impedance during the propagated action potential. They concluded that during excitation the membrane conductance increases and the emf decreases *pari passu*, but the membrane capacitance stays constant. The diagonal arrows signify circuit components that change with time.

tials in excitable cells. In that model the axon was correctly assumed to have a cylindrical conducting core, which, like a submarine cable, is insulated by material with finite electrical capacity and resistance (Figure 2B). An electrical disturbance at one point of the "cable" would spread passively to neighboring regions by flow of current in a local circuit down the axis cylinder, out through the membrane, and back in the extracellular medium (Figure 2A). The cable theory is still an important tool in any study where the membrane potential of a cell is not uniform at all points (Hodgkin and Rushton, 1946; Jack et al., 1983; Rall, 1989).

---

denote the distribution of potentials in a nerve or muscle polarized by weak currents from externally applied electrodes. Responses not explained by passive properties were often termed "active" responses because they reflected a special membrane "activity," local changes in membrane properties. Excitation required active responses.

Impressed by the skepticism among leading axonologists about Hermann's local-circuit theory of propagation, A.L. Hodgkin began in 1935 to look for electrical spread of excitation beyond a region of frog sciatic nerve blocked locally by cold. He had already found that an action potential arrested at the cold block transiently elevated the excitability of a short stretch of nerve beyond the block. He then showed that this hyperexcitability was paralleled by a transient depolarization spreading beyond the blocked region (Hodgkin, 1937a,b). The depolarization and the lowering of threshold spread with the same time course and decayed exponentially with distance in the same way as electrotonic depolarizations produced by externally applied currents. These experiments showed that depolarization spreading passively from an excited region of membrane to a neighboring unexcited region is the stimulus for propagation. Action potentials propagate electrically.

After the rediscovery of the squid giant axon (Young, 1936), Cole and Curtis (1939) turned their Wheatstone bridge to the question of a membrane permeability increase during activity. During the fall and winter when squid were not available they refined the method with the slow, propagating action potential of the giant alga *Nitella* (Cole and Curtis, 1938). Despite the vast differences between an axon and a plant cell[2] and the 1000-fold difference in time scale, the electrical results were nearly the same in the two tissues. Each action potential was accompanied by a dramatic impedance decrease (Figure 3), which was shown in squid axon to be a 40-fold increase in membrane conductance with less than a 2% change in membrane capacity. The membrane conductance rose transiently from less than 1 mS/cm^2 to about 40 mS/cm^2. Bernstein's proposal of a permeability increase was thus confirmed. However, the prevalent idea of an extensive membrane "breakdown" had to be modified. Even at the peak of the action potential, the conductance of the active membrane turned out to be less than one millionth of that of an equivalent thickness of seawater (as can be verified with Equation 1-2). Cole and Curtis (1939) correctly deduced that if conductance is "a measure of the ion permeable aspect of the membrane" and capacitance, of the "ion impermeable" aspect, then the change on excitation must be very "delicate" if it occurs uniformly throughout the membrane or, alternatively, if the change is drastic it "must be confined to a very small membrane area."

Cole and Curtis drew additional conclusions on the mechanism of the action potential. They observed that the membrane conductance increase begins only after the membrane potential has risen many millivolts from the resting potential. They argued, from cable theory applied to the temporal and spatial derivatives of the action potential, that the initial, exponentially rising foot of the action potential represents the expected discharging of the membrane by local circuits from elsewhere, but that, at the inflection point on the rise, the membrane itself suddenly generates its own net inward current. Here, they said, the electromo-

[2] Even the ionic basis of the action potentials is different (Gaffey and Mullins, 1958; Kishimoto, 1965; Lunevsky et al., 1983).

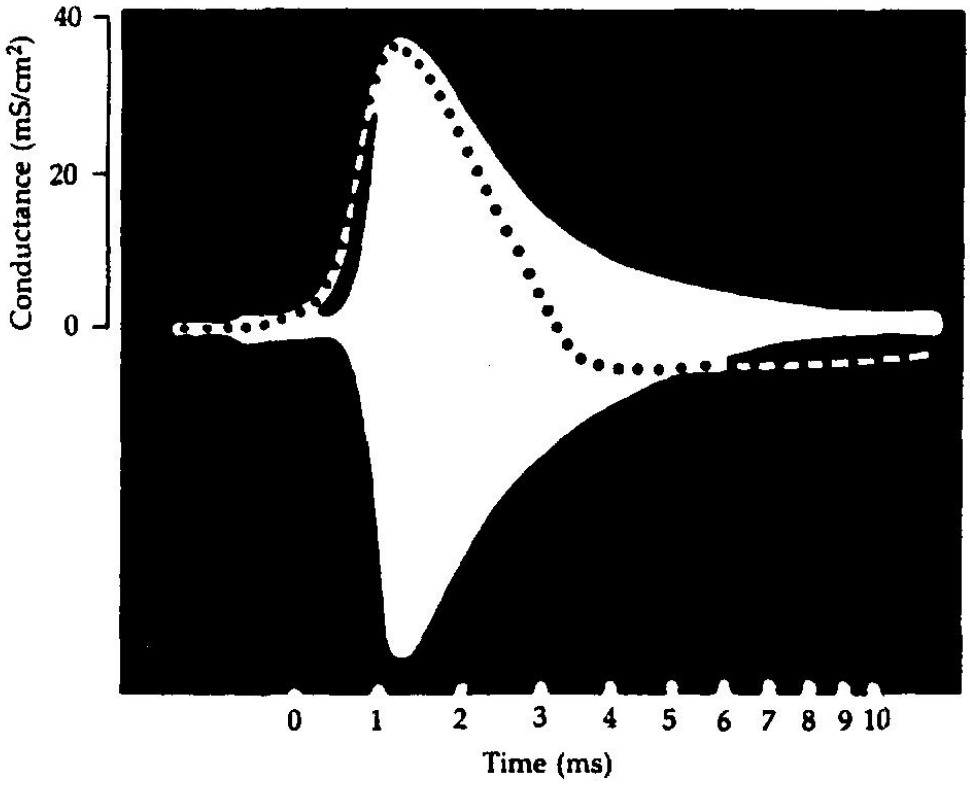

3 CONDUCTANCE INCREASE IN EXCITATION

This classical picture is the first direct demonstration of an ionic permeability increase during the propagated action potential. The time course of membrane conductance increase in a squid giant axon is measured by the width of the white band photographed from the face of an oscilloscope during the action potential (dotted line). The band is drawn by the imbalance signal of a high-frequency Wheatstone bridge applied across the axon to measure membrane impedance. [From Cole and Curtis, 1939.]

tive force (emf) of the membrane changes, and, they found, the impedance decreases exactly in parallel (Cole and Curtis, 1938):

> For these reasons, we shall assume that the membrane resistance and E.M.F. are so intimately related that they should be considered as series elements in the hypothetical equivalent membrane circuit [as shown in Figure 2C]. These two elements may be just different aspects of the same membrane mechanism.

Cole and Curtis attempted primarily to describe the membrane as a linear circuit element and were cautious in offering any interpretation. Their observations and their words boosted the case for Bernstein's membrane theory.

Just as most features of Bernstein's theory seemed confirmed, another important discrepancy with the idea of membrane breakdown was found. For the first time ever, Hodgkin and Huxley (1939, 1945) and Curtis and Cole (1940, 1942)

measured the full action potential of an axon with an intracellular micropipette. They had expected to observe a transient drop of membrane potential to near 0 mV as the membrane became transiently permeable to all ions, but instead E_M overshot zero and reversed sign by tens of millivolts, more than could be explained by any artifact (Figure 1).

The puzzle of the unexpected positive overshoot was interrupted by World War II and only in 1946 was the correct idea finally considered in Cambridge that the membrane might become selectively permeable to Na^+ ions. In that case, the new membrane electromotive force would be the sodium equilibrium potential (near +60 mV; Table 3 in Chapter 1); inward-rushing Na^+ ions would carry the inward current of the active membrane, depolarizing it from rest to near E_{Na} and eventually bringing the next patch of membrane to threshold as well. Hodgkin and Katz (1949) tested their sodium hypothesis by replacing a fraction of the NaCl in seawater with choline chloride, glucose, or sucrose. In close agreement with the theory, the action potential rose less steeply, propagated less rapidly, and overshot less in low-Na external solutions (Figure 4). Soon experiments using ^{24}Na as a tracer showed that excitation is accompanied by an extra Na^+ influx of several picomoles per centimeter square per impulse (Keynes, 1951). The sodium theory was confirmed.

Let us summarize the classical viewpoint so far. Entirely electrical arguments showed that there is an exceedingly thin cell membrane whose ion permeability is low at rest and much higher in activity. At the same moment as the permeability increases, the membrane changes its electromotive force and generates an inward current to depolarize the cell. Sodium ions are the current carrier and E_{Na} is the electromotive force. The currents generated by the active membrane are sufficient to excite neighboring patches of membrane so that propagation, like excitation, is an electrical process. For completeness we should also consider the ionic basis of the negative resting potential. Before and after Bernstein, experiments had shown that added extracellular K^+ ions depolarize nerve and muscle, as would be expected for a membrane permeable to K^+. The first measurements with intracellular electrodes showed that at high $[K]_o$, the membrane potential followed E_K closely, but at the normal, very low $[K]_o$, E_M was less negative than E_K (Curtis and Cole, 1942; Hodgkin and Katz, 1949). The deviation from E_K was correctly interpreted to mean that the resting membrane in axons is primarily K-selective but also slightly permeable to some other ions (Goldman, 1943; Hodgkin and Katz, 1949).

The voltage clamp measures current directly

Studies of the action potential established the important concepts of the ionic hypothesis. These ideas were proven and given a strong quantitative basis by a new type of experimental procedure developed by Marmont (1949), Cole (1949), and Hodgkin, Huxley, and Katz (1949, 1952). The method, known as the VOLTAGE CLAMP, has been the best biophysical technique for the study of ionic channels for over 40 years. To "voltage clamp" means to control the potential across the cell membrane.

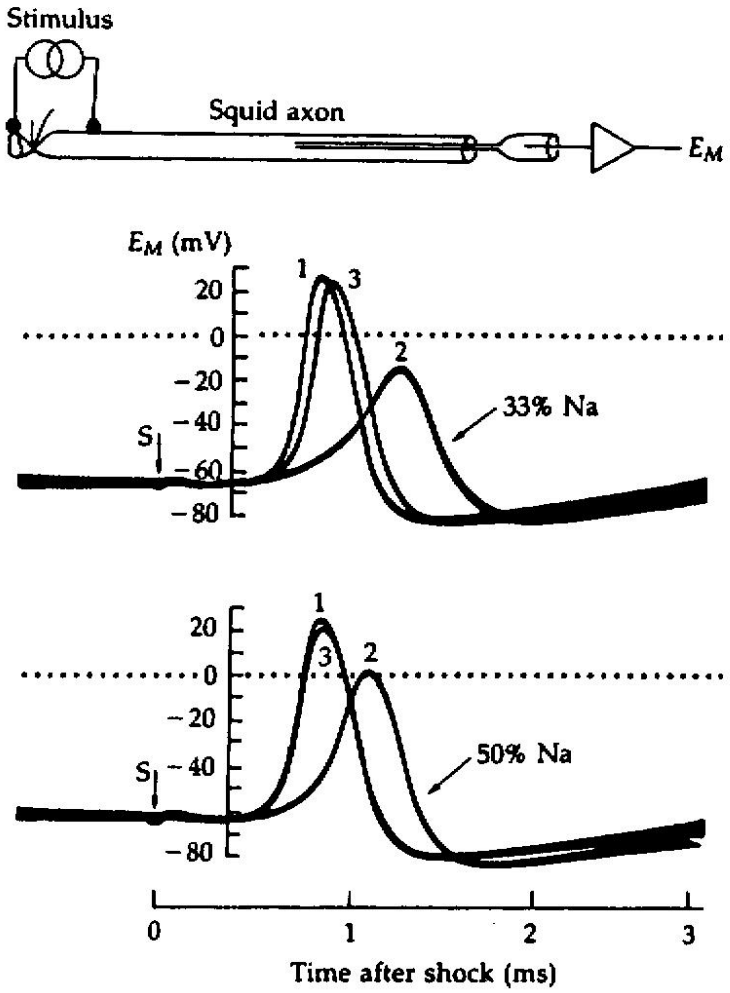

4 Na^+-DEPENDENCE OF THE ACTION POTENTIAL

This is the first experiment to demonstrate that external Na^+ ions are needed for propagated action potentials. Intracellular potential is recorded with an axial microelectrode inside a squid giant axon. The action potential is smaller and rises more slowly in solutions containing less than the normal amount of Na^+. External bathing solutions are Records 1 and 3 in normal sea water; Record 2 in low-sodium solution containing 1:2 or 1:1 mixtures of sea water with isotonic glucose. An assumed 15 mV junction potential has been subtracted from the voltage scale. [From Hodgkin and Katz, 1949.]

In much electrophysiological work, current is applied as a stimulus and the ensuing changes in potential are measured. Typically, the applied current flows locally across the membrane both as ionic current and as capacity current, and also spreads laterally to distant patches of membrane. The voltage clamp reverses the process: The experimenter applies a voltage and measures the current. In addition, simplifying conditions are used to minimize capacity currents and the spread of local circuit currents so that the observed current can be a direct measure of ionic movements across a known membrane area at a known, uniform membrane potential.

If one wanted only to keep the membrane potential constant, one might expect that some kind of ideal battery could be connected across the cell mem-

brane. Current would flow from the battery to counter exactly any current flowing across the membrane, and the membrane potential would remain constant. Unfortunately, the circuit has to be a bit more complicated because current flow out of the electrodes produces unpredictable local voltage drops at the electrode and in the neighboring solutions, and therefore only the electrodes and not the membrane would remain at constant potential. Instead, most practical voltage clamps measure the potential near the membrane and, often through other electrodes, supply whatever current is needed to keep the potential constant even when the membrane permeability is changing. As ionic permeability changes can be rapid, a feedback amplifier with a good high-frequency response is used to readjust the current continually rather than a slower device such as the human hand.

Some simplified arrangements for voltage clamping cell membranes are shown in Figure 5. Most comprise an intracellular electrode and follower circuit to measure the membrane potential, a feedback amplifier to amplify any difference (error signal) between the recorded voltage and the desired value of the membrane potential, and a second intracellular electrode for injecting current from the output of the feedback amplifier. The circuits are examples of negative feedback since the injected current has the sign required to reduce any error signal. To eliminate spread of local circuit currents, these methods measure the membrane currents in a patch of membrane with no spatial variation of membrane potential. In giant axons and giant muscle fibers, spatial uniformity of potential, called the SPACE-CLAMP condition, can be achieved by inserting a highly conductive axial wire inside the fiber. In other cells, uniformity is achieved by using a small membrane area delimited either by the natural anatomy of the cell or by gaps, partitions, and barriers applied by the experimenter. Details of classical voltage-clamp methods are found in the original literature (Hodgkin et al., 1952; Dodge and Frankenhaeuser, 1958; Deck et al., 1964; Chandler and Meves, 1965; Nonner, 1969; Adrian et al., 1970a; Connor and Stevens, 1971a; Shrager, 1974; Hille and Campbell, 1976; Lee et al., 1980; Bezanilla et al., 1982; Byerly and Hagiwara, 1982). Today, by far the most popular methods use the gigaseal patch and whole-cell techniques developed in Göttingen by Erwin Neher and Bert Sakmann (Hamill et al., 1981; Sakmann and Neher, 1983; Wonderlin et al., 1990).

In a standard voltage-clamp experiment, the membrane potential might be stepped from a holding value near the resting potential to a depolarized level, say -10 mV, for a few milliseconds, and then it is stepped back to the holding potential. If the membrane were as simple as the electrical equivalent circuit in Figure 2, the total membrane current would be the sum of two terms: current I_i carried by ions crossing the conductive pathway through the membrane and current I_C carried by ions moving up to the membrane to charge or discharge its electrical capacity.

$$I_M = I_i + I_c = I_i + C_M \frac{dE}{dt} \tag{2-1}$$

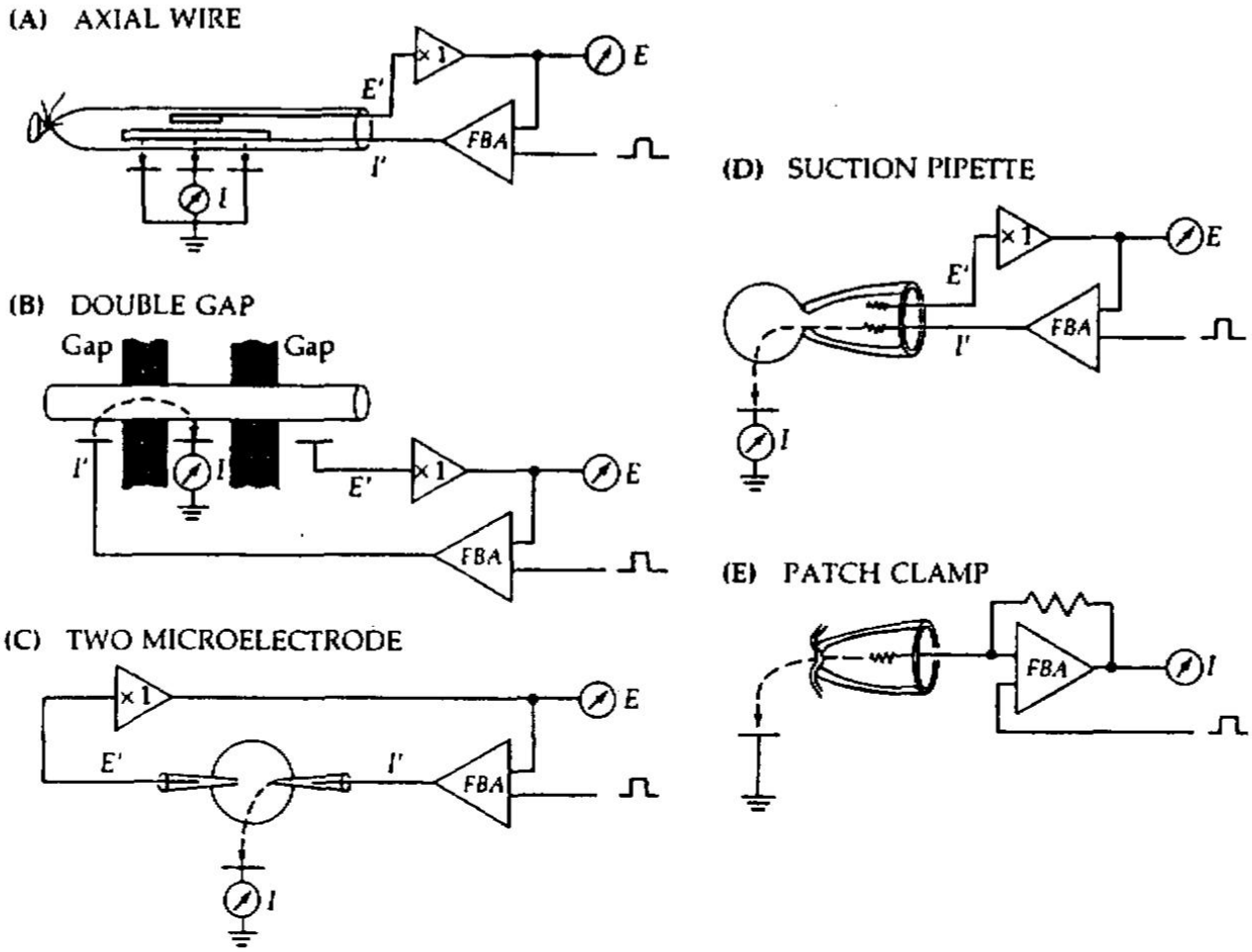

5 VOLTAGE-CLAMP METHODS

Most methods have two intracellular electrodes, a voltage-recording electrode E' and a current-delivering electrode I'. The voltage electrode connects to a high impedance follower circuit ($\times 1$). The output of the follower is recorded at E and also compared with the voltage-clamp command pulses by a feedback amplifier (*FBA*). The highly amplified difference of these signals is applied as a current (dashed arrows) through I', across the membrane, and to the bath-grounding electrode, where it can be recorded (I). In the gap method, the extracellular compartment is divided into pools by gaps of Vaseline, sucrose, or air and the end pools contain a depolarizing "intracellular" solution. The patch-clamp method can study a minute patch of membrane sealed to the end of a glass pipette, as explained in Figure 3 of Chapter 4.

Step potential changes have a distinct advantage for measuring ionic current I_i since, except at the moment of transition from one level to another, the change of membrane potential, dE/dt, is zero. Thus with a step from one potential to another, capacity current I_C stops flowing as soon as the change of membrane potential has been completed and from then on the recorded current is only the ionic component I_i. Much of what we know today about ionic channels comes from studies of I_i.

The ionic current of axons has two major components: I_{Na} and I_K

Figure 6 shows membrane current records measured from a squid giant axon cooled to 3.8°C to slow down the membrane permeability changes. The axon is voltage clamped with the axial wire method and the membrane potential is changed in steps. By convention, outward membrane currents are considered positive and are shown as upward deflections, while inward currents are considered negative and are shown as downward deflections. The hyperpolarizing voltage step to −130 mV produces a tiny, steady inward ionic current. This 65-

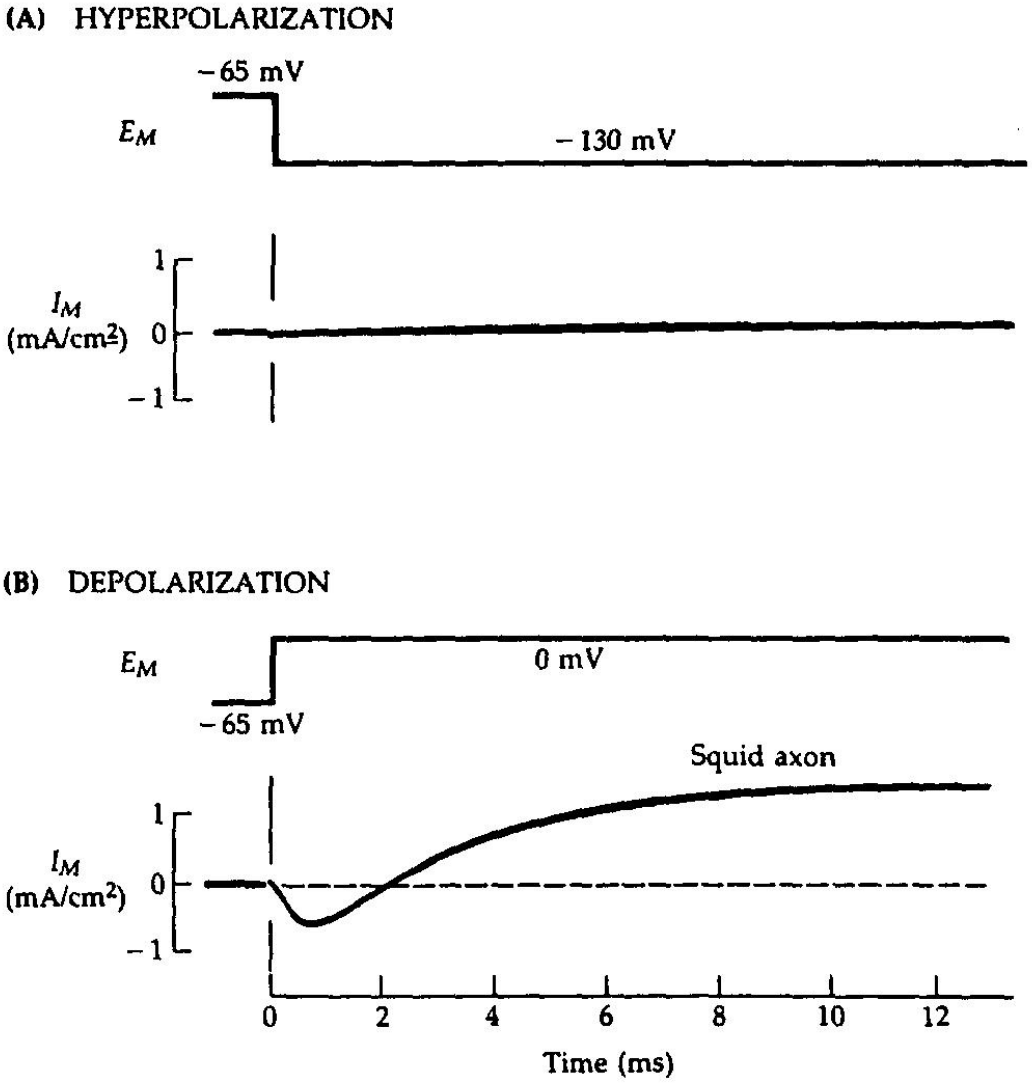

6 VOLTAGE-CLAMP CURRENTS IN SQUID AXON

An axon is bathed in sea water and voltage-clamped by the axial wire method (Figure 5). The membrane potential is held at −65 mV and then hyperpolarized in a step to −130 mV or depolarized in a step to 0 mV. Outward ionic current is shown as an upward deflection. The membrane permeability mechanisms are clearly asymmetrical. Hyperpolarization produces only a small inward current, while depolarization elicits a larger and biphasic current. T = 3.8°C [Adapted from Hodgkin et al., 1952.]

mV hyperpolarization from rest gives an ionic current density of only $-30\ \mu A/cm^2$, corresponding to a low resting membrane conductance of $0.46\ mS/cm^2$. A brief surge of inwardly directed capacity current occurs in the first 10 μs of the hyperpolarization but is too fast to be photographed here. When, on the other hand, the axon is depolarized to 0 mV, the currents are quite different. A brief, outward capacity current (not seen) is followed by a small outward ionic current that reverses quickly to give a large inward current, only to reverse again, giving way to a large maintained outward ionic current. The ionic permeability of the membrane must be changed in a dramatic manner by the step depolarization. The transient inward and sustained outward ionic currents produced are large enough to account for the rapid rate of rise and fall of the action potential that this membrane can generate.

The voltage clamp offered for the first time a quantitative measure of the ionic currents flowing across an excitable membrane. Hodgkin and Huxley set out to determine which ions carry the current and how the underlying membrane permeability mechanisms work. As this was new ground, they had to formulate new approaches. First, they reasoned that each ion seemed to move passively down its electrochemical gradient, so basic thermodynamic arguments could be used to predict whether the net movement of an ion would be inward or outward at a given membrane potential. For example, currents carried by Na^+ ions should be inward at potentials negative to the equilibrium potential, E_{Na}, and outward at potentials positive to E_{Na}. If the membrane were clamped to E_{Na}, Na^+ ions should make no contribution to the observed membrane current, and if the current reverses sign around E_{Na}, it is probably carried by Na^+ ions. The same argument could be applied to K^+, Ca^{2+}, Cl^-, and so on. Second, ions could be added to or removed from the external solutions. (Ten years later practical methods were found for changing the internal ions as well: Baker et al., 1962; Oikawa et al., 1961.) In the extreme, if a permeant ion were totally replaced by an impermeant ion, one component of current would be abolished. Hodgkin and Huxley (1952a) also formulated a quantitative relation, called the INDEPENDENCE RELATION, to predict how current would change as the concentration of permeant ions was varied. The independence relation was a test for the independent movement of individual ions, derived from the assumption that the probability that a given ion crosses the membrane does not depend on the presence of other ions (Chapters 13 and 14).

Using these approaches, Hodgkin and Huxley (1952a) identified two major components, I_{Na} and I_K, in the ionic current. As Figure 7 shows, the early transient currents reverse their sign from inward to outward at around +60 mV as would be expected if they are carried by Na^+ ions. The late currents, however, are outward at all test potentials, as would be expected for a current carried by K^+ ions with a reversal potential more negative than −60 mV. The identification of I_{Na} was then confirmed by replacing most of the NaCl of the external medium by choline chloride (Figure 8). The early inward transient current seen in the control ("100% Na") disappears in low Na ("10% Na"), while the late outward current remains. Subtracting the low-Na record from the

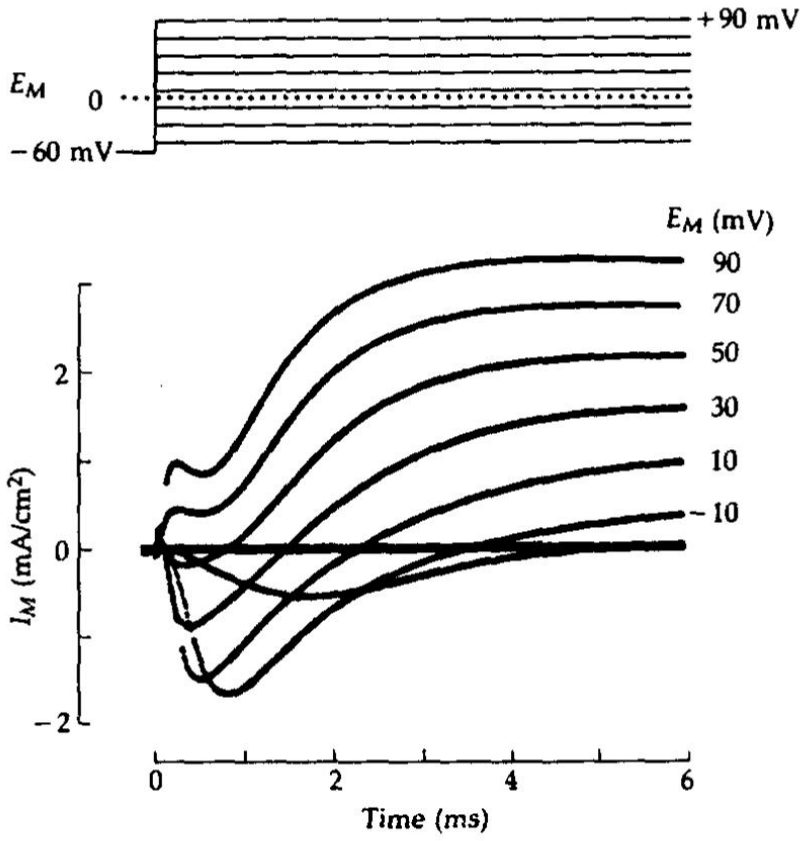

7 FAMILY OF VOLTAGE-CLAMP CURRENTS

A squid giant axon membrane is stepped under voltage clamp from a holding potential of −60 mV to test pulse potentials ranging in 20-mV steps from −40 mV to +100 mV. Successive current traces on the oscilloscope screen have been superimposed photographically. The time course and direction of ionic currents varies with the potential of the test pulse. T = 6.6°C. [From Armstrong, 1969.]

control record reconstructs the transient time course of the sodium current, I_{Na}, shown below. Although Hodgkin and Huxley did not attempt to alter the internal or external K^+ concentrations, subsequent investigators have done so many times, and confirm the identification of the late current with I_K. Thus the trace, recorded in low-Na solutions, is almost entirely I_K. Hodgkin and Huxley also recognized a minor component of current, dubbed LEAKAGE CURRENT, I_L. It was a small, relatively voltage-independent background conductance of undetermined ionic basis.

The properties of I_{Na} and I_K are frequently summarized in terms of current–voltage relations. Figure 9 shows the peak I_{Na} and the late I_K plotted as a function of the voltage-clamp potential. A resemblance to the hypothetical I–E relations considered earlier in Figure 6 of Chapter 1 is striking. Indeed, the interpretation used there applies here as well. Using a terminology developed only some years after Hodgkin and Huxley's work, we would say that the axon membrane has two major types of ionic channels: Na channels with a positive reversal potential, E_{Na}, and K channels with a negative reversal potential, E_K.

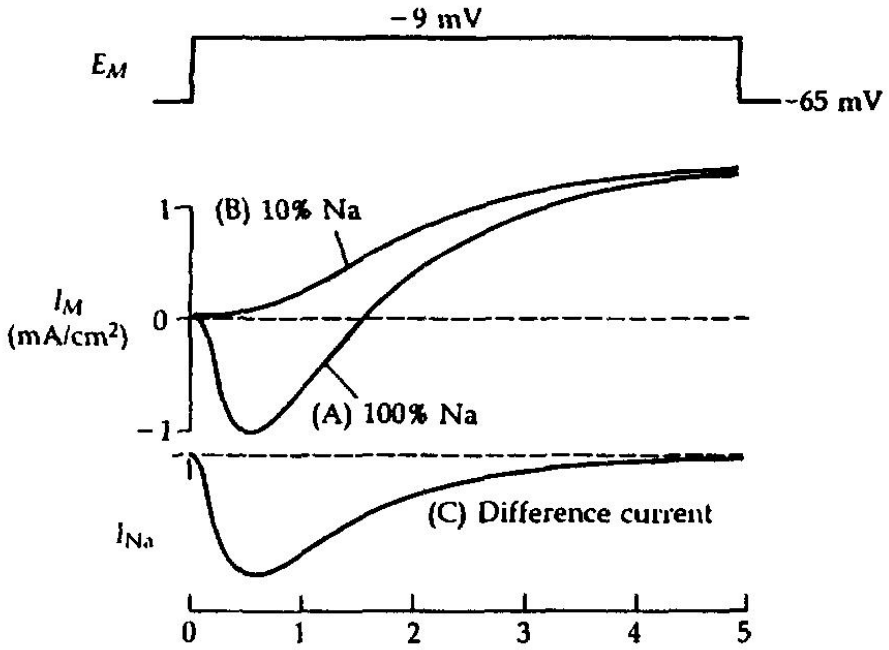

8 SEPARATION OF Na AND K CURRENTS

An illustration of the classical ionic substitution method for analyzing the ionic basis of voltage-clamp currents. Ionic currents are measured in a squid axon membrane stepped from a holding potential of −65 mV to −9 mV. The component carried by Na^+ ions is dissected out by substituting impermeant choline ions for most of the external sodium. (A) Axon in seawater, showing inward and outward ionic currents. (B) Axon in low-sodium solution with 90% of the NaCl substituted by choline chloride, showing only outward ionic current. (C) Algebraic difference between experimental records A and B, showing the transient inward component of current due to the inward movement of *external* Na^+ *ions.* T = 8.5°C. [*From* Hodgkin, 1958; adapted from Hodgkin and Huxley, 1952a.]

Both channels are largely closed at rest and they open with depolarization at different rates. We now consider the experimental evidence for this picture.

Ionic conductances describe the permeability changes

Having separated the currents into components I_{Na} and I_K, Hodgkin and Huxley's next step was to find an appropriate quantitative measure of the membrane ionic permeabilities. In Chapter 1 we used conductance as a measure of how many pores are open. This is, however, not a fundamental law of nature, so its appropriateness is an experimental question. The experiment must determine if the relation between ionic current and the membrane potential at constant permeability is linear, as Ohm's law implies.

To study this question, Hodgkin and Huxley (1952b) measured what they called the "instantaneous current–voltage relation" by first depolarizing the axon long enough to raise the permeability, then stepping the voltage to other levels to measure the current within 10 to 30 μs after the step, before further

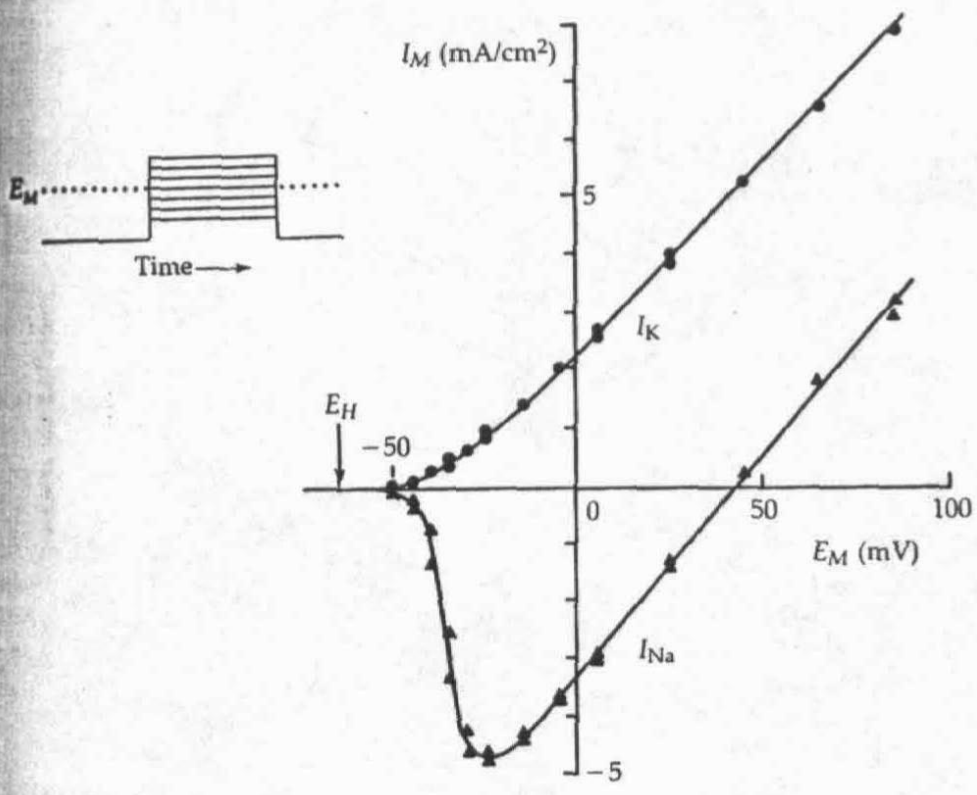

9 CURRENT-VOLTAGE RELATIONS OF SQUID AXON

The axon membrane potential is stepped under voltage clamp from the negative holding potential (E_H) to various test potentials as in Figure 7. Peak transient sodium current (triangles) and steady-state potassium current (circles) from each trace are plotted against the test potential. The curvature of the two *I–E* relations between −50 to −20 mV reflects the voltage-dependent opening of Na and K channels as is explained in Figure 6 of Chapter 1. [From Cole and Moore, 1960.]

permeability change occurred. One experiment was done at a time when Na permeability was high and another, when K permeability was high. Both gave approximately linear current-voltage relations as in Ohm's law. Therefore, Hodgkin and Huxley introduced ionic conductances defined by

$$g_{Na} = \frac{I_{Na}}{E - E_{Na}} \tag{2-2}$$

$$g_K = \frac{I_K}{E - E_K} \tag{2-3}$$

as measures of membrane ionic permeability, and they refined the equivalent circuit representation of an axon membrane to include, for the first time, *several* ion-conducting branches (Figure 10). In the newer terminology we would say that the current–voltage relation of an open Na channel or K channel was found to be linear and that g_{Na} and g_K are therefore useful measures of how many channels are open. However, the linearity is actually only approximate and

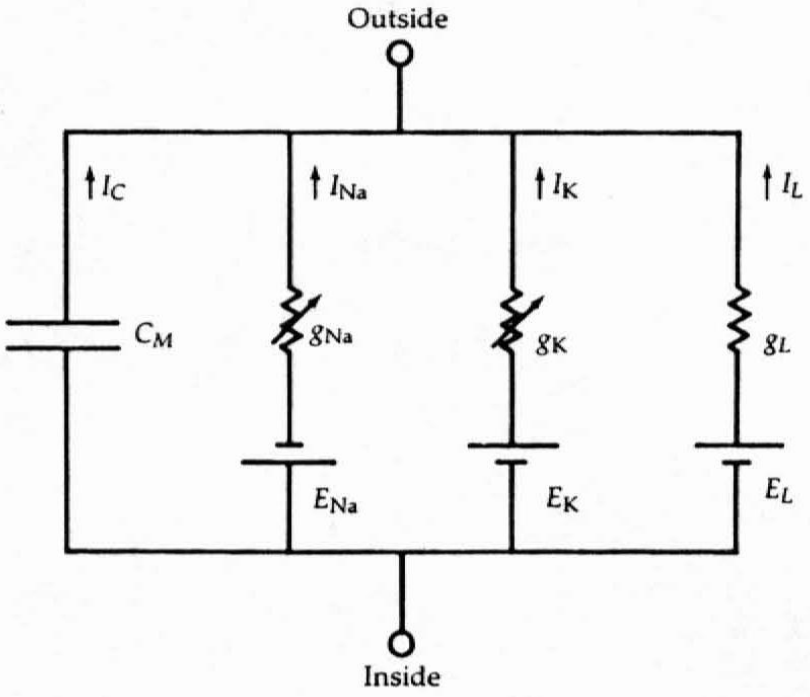

10 EQUIVALENT CIRCUIT OF AXON MEMBRANE

Hodgkin and Huxley described the axon membrane as an electrical circuit with four parallel branches. The capacitative branch represents the thin dielectric properties of the membrane. The three conductive branches represent sodium, potassium, and leak conductances with their different electromotive forces. The resistors with arrows through them denote time- and voltage-varying conductances arising from the opening and closing of ionic channels. [From Hodgkin and Huxley, 1952d.]

holds neither under all ionic conditions nor in Na and K channels of all organisms. As we show in Chapters 4 and 13, factors such as asymmetry of ionic concentrations and asymmetry of channels can contribute to nonlinear *I–E* relations in open channels.

Changes in the conductances g_{Na} and g_K during a voltage-clamp step are now readily calculated by applying Equations 2-2 and 2-3 to the separated currents. Like the currents, g_{Na} and g_K are voltage and time dependent (Figure 11). Both g_{Na} and g_K are low at rest. During a step depolarization, g_{Na} rises rapidly with a short delay, reaches a peak, and falls again to a low value: fast "activation" and slow "inactivation." If the membrane potential is returned to rest during the period of high conductance, g_{Na} falls exponentially and very rapidly (dashed lines). Potassium conductance activates almost 10 times more slowly than g_{Na}, reaching a steady level without inactivation during the 10-ms depolarization. When the potential is returned to rest, g_K falls exponentially and relatively slowly.

The same calculation, applied to a whole family of voltage-clamp records at different potentials, gives the time courses of g_{Na} and g_K shown in Figure 12. Two new features are evident. The larger the depolarization, the larger and

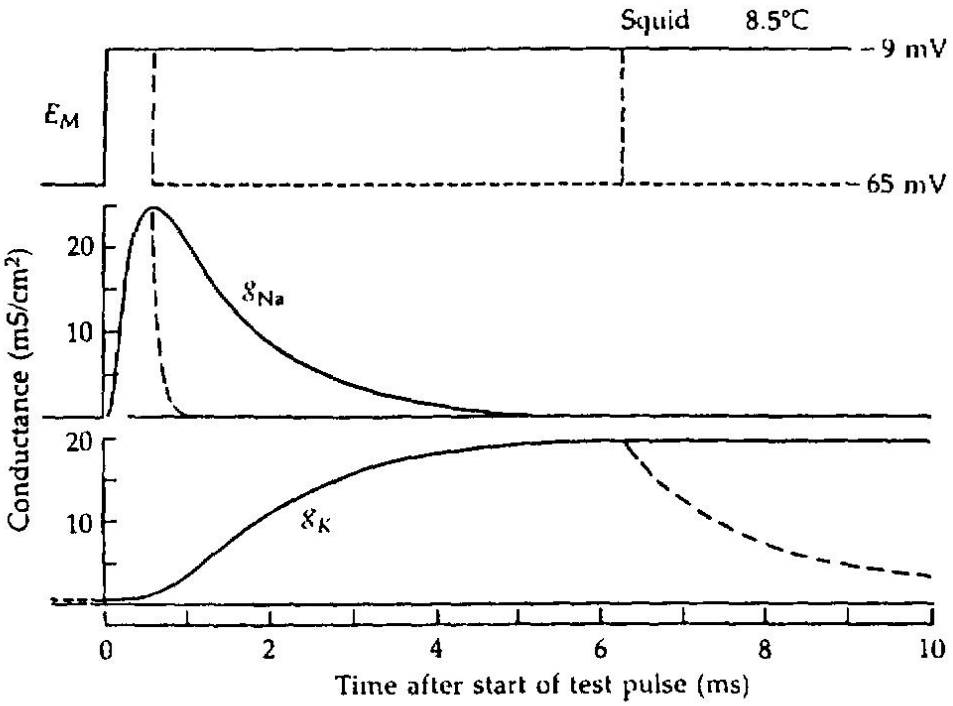

11 IONIC CONDUCTANCE CHANGES IN SQUID AXON

Time courses of sodium and potassium conductance changes during a depolarizing voltage step to −9 mV. Conductances calculated by Equations 2-2 and 2-3 from the separated current traces in Figure 8. Dashed lines show how g_{Na} decreases rapidly to resting levels if the membrane is repolarized to −65 mV at 0.63 ms, when g_{Na} is high, and how g_K decreases more slowly if the membrane is repolarized at 6.3 ms, when g_K is high. T = 8.5°C. [From Hodgkin, 1958; adapted from Hodgkin and Huxley, 1952a,b,d.]

faster are the changes of g_{Na} and g_K, but for very large depolarizations both conductances reach a maximal value. A saturation at high depolarizations is even more evident in Figure 13, which shows on semilogarithmic scales the voltage dependence of peak g_{Na} and steady-state g_K. In squid giant axons the peak values of the ionic conductances are 20 to 50 mS/cm², like the peak membrane conductance found by Cole and Curtis (1939) during the action potential. The limiting conductances differ markedly from one excitable cell to another, but even after another 40 years of research no one has succeeded in finding electrical, chemical, or pharmacological treatments that make g_{Na} or g_K rise much above the peak values found in simple, large depolarizations. Hence the observed limits may represent a nearly maximal activation of the available ionic channels.

Two kinetic processes control g_{Na}

The sodium permeability of the axon membrane rises rapidly and then decays during a step depolarization (Figures 11 and 12). Hodgkin and Huxley (1952b,c) said that g_{Na} activates and then inactivates. In newer terminology we would say

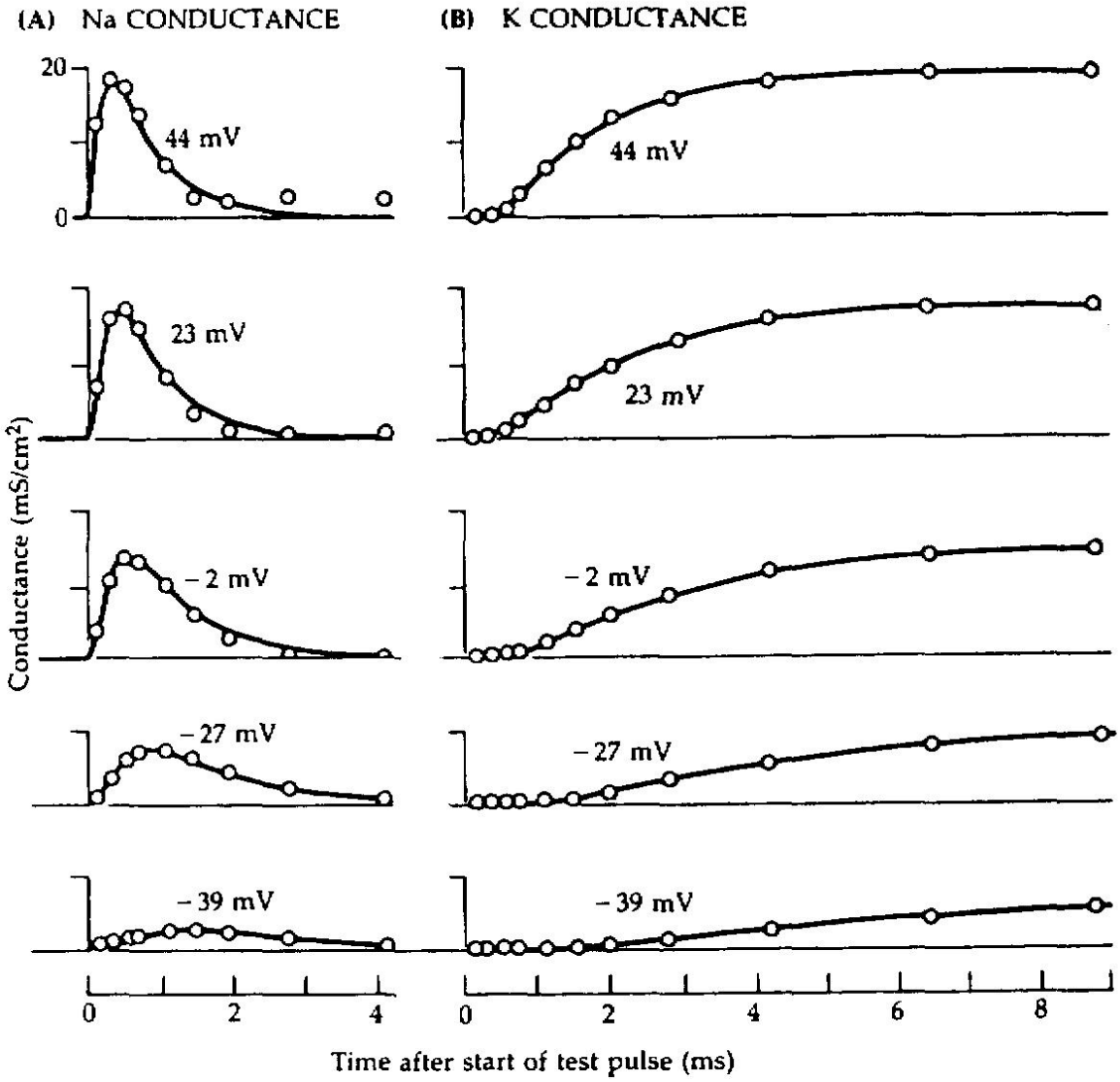

12 CONDUCTANCE CHANGES AT MANY VOLTAGES

Time courses of g_{Na} (A) and g_K (B) during depolarizing steps to the indicated voltages. Circles are the ionic conductances measured in a squid giant axon at 6.3°C. Smooth curves are the conductance changes calculated from the Hodgkin–Huxley model. [From Hodgkin, 1958; adapted from Hodgkin and Huxley, 1952d.]

that Na channels activate and then inactivate. Many major research papers have been devoted to untangling the distinguishable, yet tantalizingly intertwined, processes of activation and inactivation.

In the Hodgkin–Huxley analysis, ACTIVATION is the rapid process that opens Na channels during a depolarization. A quick reversal of activation during a repolarization accounts for the rapid closing of channels after a brief depolarizing pulse is terminated (dashed line in Figure 11). The very steep voltage dependence of the peak g_{Na} (Figure 13) arises from a correspondingly steep voltage dependence of activation. According to the Hodgkin–Huxley view, if there were no inactivation process, g_{Na} would increase to a new steady level in a fraction of a millisecond with any voltage step in the depolarizing direction, and

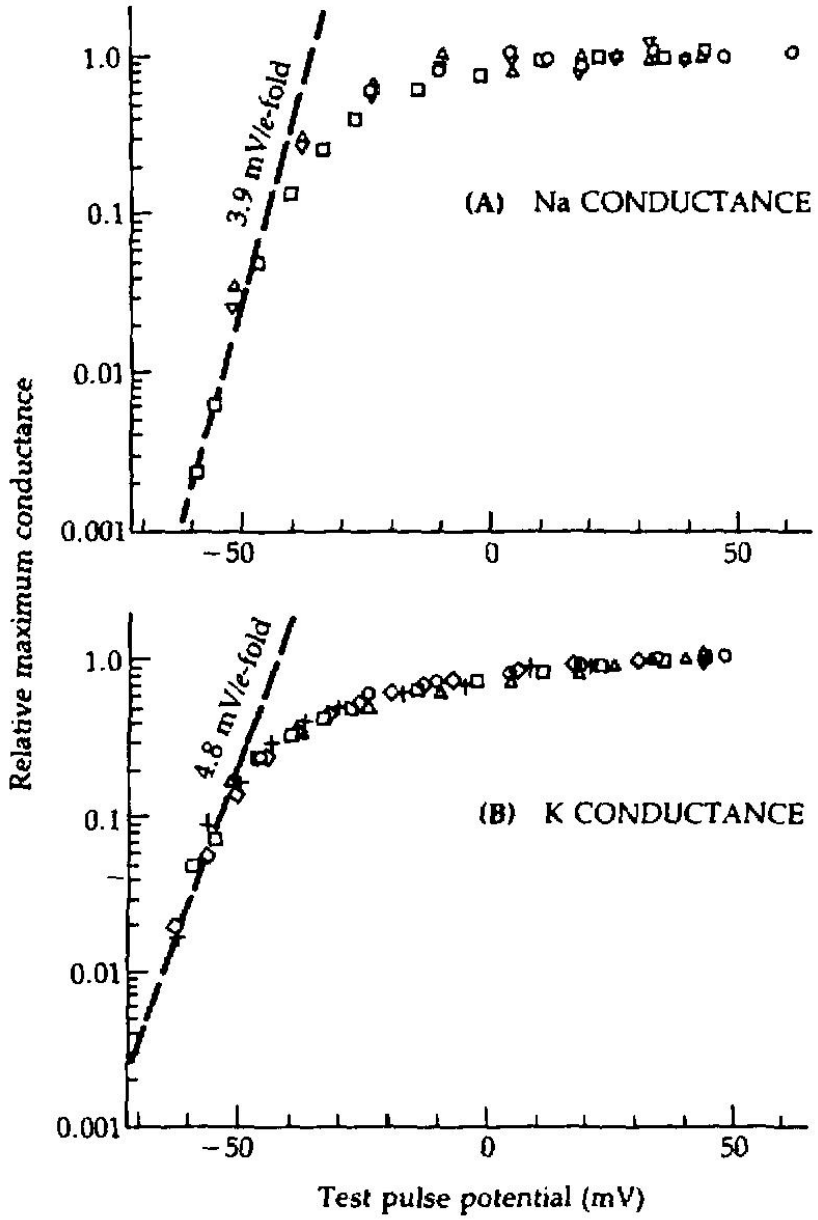

13 VOLTAGE DEPENDENCE OF IONIC CONDUCTANCES

Peak g_{Na} (A) and steady-state g_K (B) are measured during depolarizing voltage steps under voltage clamp. Symbols are measurements from several squid giant axons, normalized to 1.0 at large depolarizations, and plotted on a logarithmic scale aginst the potential of the test pulse. Dashed lines show limiting equivalent voltage sensitivities of 3.9 mV per *e*-fold increase of g_{Na} and 4.8 mV per *e*-fold increase of g_K for small depolorizations. [Adapted from Hodgkin and Huxley, 1952a.]

would decrease to a new steady level, again in a fraction of a millisecond, with any step in the hyperpolarizing direction. Without inactivation, such rapid opening and closing of channels could be repeated as often as desired. As we shall see later, Na channels do behave exactly this way if they are modified by certain chemical treatments or natural toxins (Chapter 17).

INACTIVATION is a slower process that closes Na channels during a depolarization. Once Na channels have been inactivated, the membrane must be repolarized or hyperpolarized, often for many milliseconds, to remove the inac-

tivation. Inactivated channels cannot be activated to the conducting state until their inactivation is removed. The inactivation process overrides the tendency of the activation process to open channels. Thus inactivation is distinguished from activation in its kinetics, which are slower, and in its effect, which is to close rather than to open during a depolarization. Inactivation of Na channels accounts for the loss of excitability that occurs if the resting potential of a cell falls by as little as 10 or 15 mV—for example, when there is an elevated extracellular concentration of K^+ ions, or after prolonged anoxia or metabolic block.

Figure 14 shows a typical experiment to measure the steady-state voltage dependence of Na inactivation. This is an example of a two-pulse voltage-clamp protocol, illustrated with a frog myelinated nerve fiber. The first 50-ms voltage step, the variable PREPULSE or CONDITIONING PULSE, is intended to be long enough to permit the inactivation process to reach its steady-state level at the prepulse potential. The second voltage step to a fixed level, the TEST PULSE, elicits the usual transient I_{Na} whose relative amplitude is used to determine what fraction of the channels were not inactivated by the preceding prepulse. The experiment consists of different trials with different prepulse potentials. After a

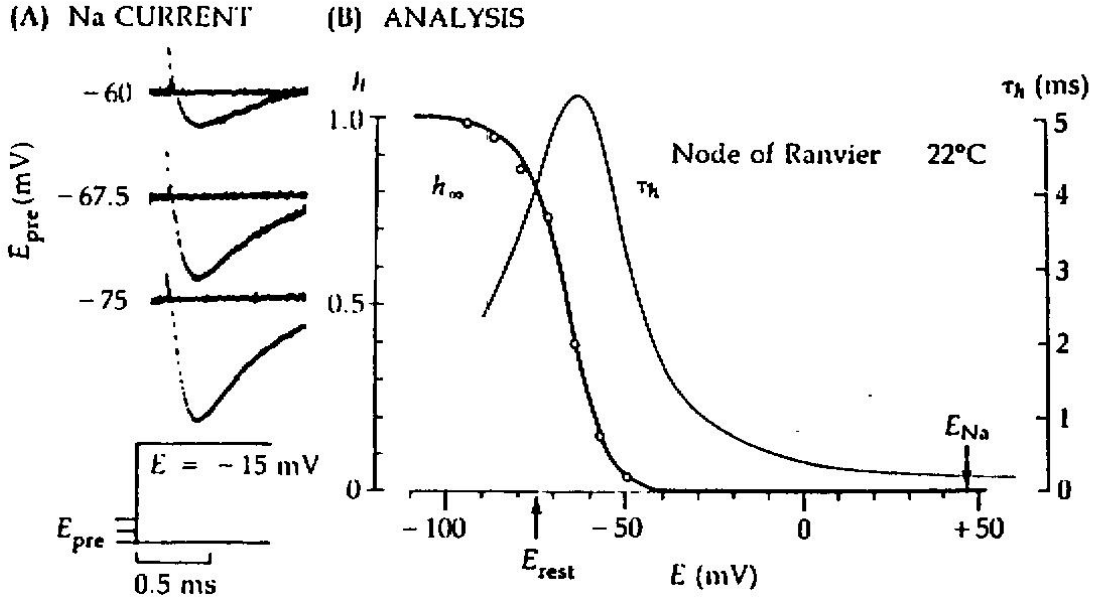

14 INACTIVATION OF SODIUM CURRENT

A voltage-clamp experiment to measure the steady-state voltage dependence of inactivation. A node of Ranvier of frog myelinated nerve fiber is bathed in frog Ringer's solution and voltage-clamped by the Vaseline gap method (Figure 5). (A) Sodium currents elicited by test pulses to −10 mV after 50 ms prepulses to three different levels (E_{pre}). I_{Na} is decreased by a depolarizing prepulses. (B) Symbols plot the relative peak size of I_{Na} versus the potential of the prepulse, forming the "steady-state inactivation curve" or the "h_∞ curve" of the HH model. Bell-shaped τ_h curve shows the voltage dependence of the exponential time constant of development or recovery from inactivation measured as in Figure 15. T = 22°C. [From Dodge, 1961, copyright by the American Association for the Advancement of Science.]

hyperpolarizing prepulse, I_{Na} becomes larger than at rest, and after a depolarizing prepulse, smaller. As the experiment shows, even at rest (−75 mV in this axon), there is about 30% inactivation, and the voltage dependence is relatively steep, so that a 20-mV depolarization from rest will inactivate Na channels almost completely, and a 20-mV hyperpolarization will remove almost all of the resting inactivation.

Two-pulse experiments are a valuable tool for probing the kinetics of gating in channels. A different style of two-pulse experiment, shown in Figure 15, can be used to determine the rate of recovery from inactivation. Here a pair of identical depolarizing pulses separated by a variable time, t, elicits Na currents. The first control pulse elicits a large I_{Na} appropriate for a rested axon. The pulse is long enough to inactivate Na channels completely. Then the membrane is repolarized to the holding potential for a few milliseconds to initiate the removal of inactivation and finally tested with the second test pulse to see how far the recovery has proceeded after different times. As the interval between pulses is lengthened, the test I_{Na} gradually recovers toward the control size. The recovery is approximately described by an exponential function $[1 - \exp(t/\tau_h)]$, where τ_h is called the TIME CONSTANT for Na inactivation (and has a value close to 5 ms in this experiment). When this experiment is repeated with other recovery potentials, the time constant τ_h is found to be quite voltage dependent, with a maximum near the normal resting potential. The voltage dependence of τ_h is shown as a smooth curve in Figure 14.

The Hodgkin–Huxley model describes permeability changes

Hodgkin and Huxley's goal was to account for ionic fluxes and permeability changes of the excitable membrane in terms of molecular mechanisms. After an intensive consideration of different mechanisms, they reluctantly concluded that still more needed to be known before a unique mechanism could be proven. Indeed, this conclusion is unfortunately still valid. They determined instead to develop an *empirical* kinetic description that would be simple enough to make practical calculations of electrical responses, yet sufficiently good as to predict correctly the major features of excitability such as the action potential shape and conduction velocity. In this goal they succeeded admirably. Their model not only comprises mathematical equations but also suggests major features of the gating mechanisms. Their ideas have been a strong stimulus for all subsequent work. We will call their model (Hodgkin and Huxley, 1952d) the HH MODEL. Although we now know of many specific imperfections, it is essential to review the HH model at length in order to understand most subsequent work on voltage-sensitive channels.

The HH model has separate equations for g_{Na} and g_K. In each case there is an upper limit to the possible conductance, so g_{Na} and g_K are expressed as maximum conductances $\bar{g}_{Na}$ and $\bar{g}_K$ multiplied by coefficients representing the fraction of the maximum conductances actually expressed. The multiplying coeffi-

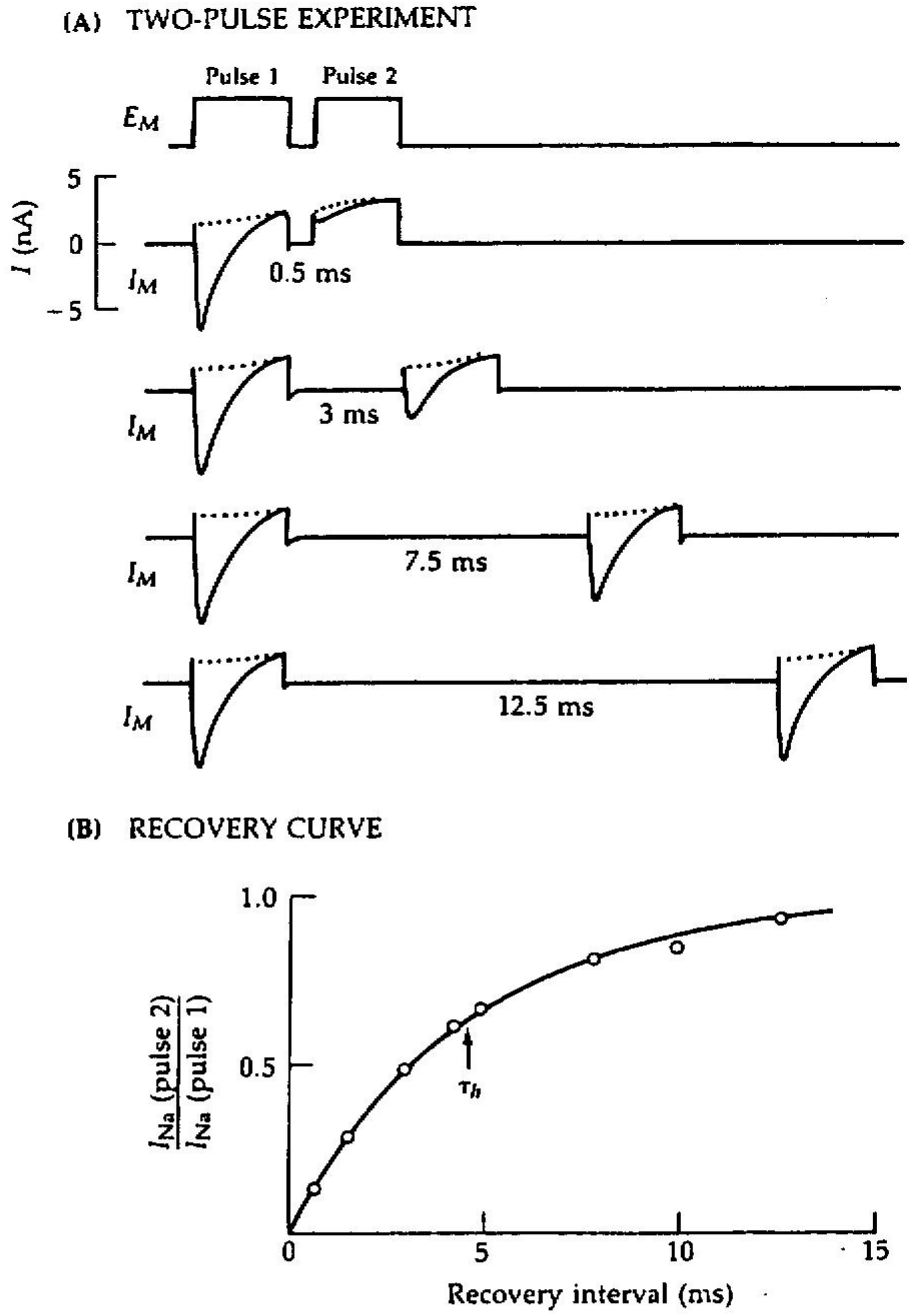

15 RECOVERY FROM SODIUM INACTIVATION

A two-pulse experiment measuring the time course of recovery from sodium inactivation in a frog node of Ranvier. (A) The first pulse to −15 mV activates and inactivates Na channels. During the interpulse interval some channels recover from inactivation. The second pulse determines what fraction have recovered in that time. Dotted lines show the estimated contribution of potassium and leak currents to the total current. (B) Relative peak I_{Na} recovers with an approximately exponential time course (τ_h = 4.6 ms) during the interpulse interval at −75 mV. T = 19°C. [From Dodge, 1963.]

cients are numbers varying between zero and 1. All the kinetic properties of the model enter as time dependence of the multiplying coefficients. In the model the conductance changes depend only on voltage and time and not on the concen-

trations of Na^+ or K^+ ions or on the direction or magnitude of current flow. All experiments show that g_{Na} and g_K change gradually with time with no large jumps, even when the voltage is stepped to a new level, so the multiplying coefficients must be continuous functions in time.

The time dependence of g_K is easiest to describe. On depolarization the increase of g_K follows an S-shaped time course, whereas on repolarization the decrease is exponential (Figures 11 and 12). As Hodgkin and Huxley noted, such kinetics would be obtained if the opening of a K channel were controlled by several independent membrane-bound "particles." Suppose that there are four identical particles, each with a probability n of being in the correct position to set up an open channel. The probability that all four particles are correctly placed is n^4. Because opening of K channels depends on membrane potential, the hypothetical particles are assumed to bear an electrical charge which makes their distribution in the membrane voltage dependent. Suppose further that each particle moves between its permissive and nonpermissive position with first-order kinetics so that when the membrane potential is changed, the distribution of particles described by the probability n relaxes exponentially toward a new value. Figure 16 shows that if n rises exponentially from zero, n^4 rises along an S-shaped curve, imitating the delayed increase of g_K on depolarization; and if n falls exponentially to zero, n^4 also falls exponentially, imitating the decrease of g_K on repolarization.

To put this in mathematical form, I_K is represented in the HH model by

$$I_K = n^4 \bar{g}_K (E - E_K) \tag{2-4}$$

and the voltage- and time-dependent changes of n are given by a first-order reaction

$$\text{"1 - } n\text{"} \underset{\beta_n}{\overset{\alpha_n}{\rightleftharpoons}} n \tag{2-5}$$

where the gating particles make transitions between the permissive and nonpermissive forms with voltage-dependent rate constants α_n and β_n. If the initial value of the probability n is known, subsequent values can be calculated by solving the simple differential equation

$$\frac{dn}{dt} = \alpha_n(1 - n) - \beta_n n \tag{2-6}$$

An alternative to using rate constants, α_n and β_n, is to use the voltage-dependent time constant τ_n and steady-state value n_∞, which are defined by

$$\tau_n = \frac{1}{\alpha_n + \beta_n} \tag{2-7}$$

$$n_\infty = \frac{\alpha_n}{\alpha_n + \beta_n} \tag{2-8}$$

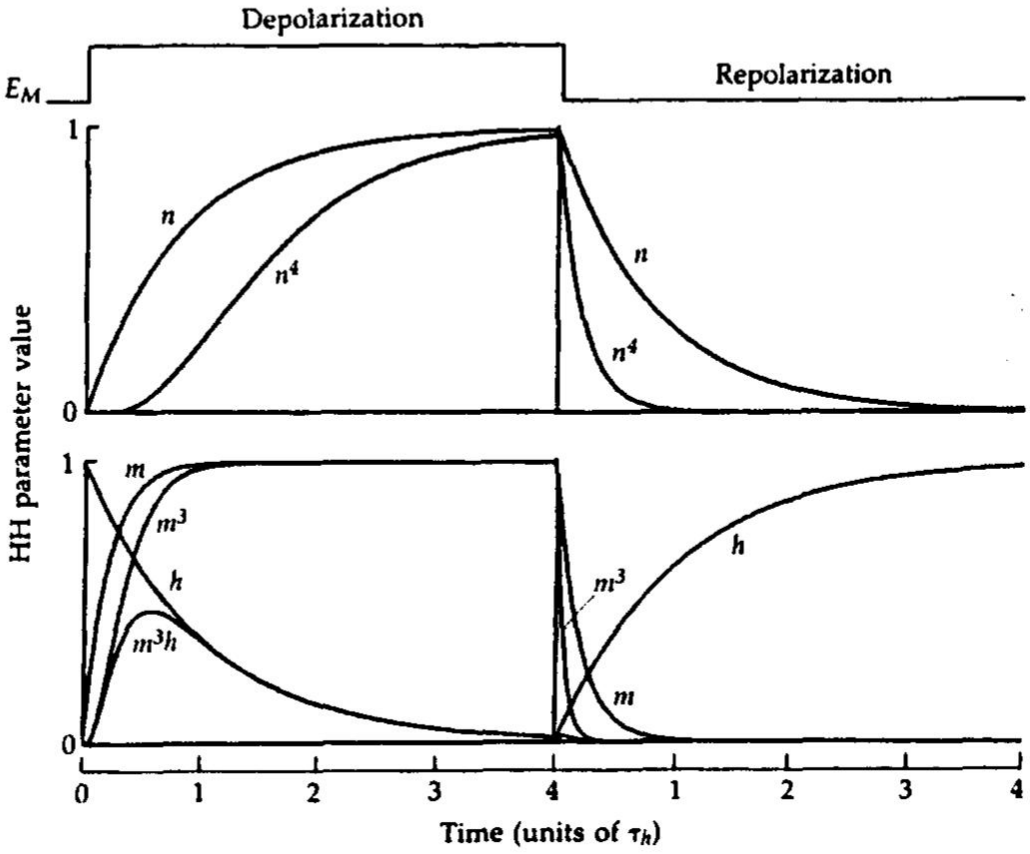

16 TIME COURSE OF HH-MODEL PARAMETERS

A purely hypothetical example representing a depolarizing step followed by a repolarization. The time constants τ_m, τ_h, and τ_n are assumed to be in the ratio 1:5:4 and the duration of the depolarization (to the middle vertical line) is assumed to be $4\tau_h$. Unlike a real case, the time constants are taken to be the same at both potentials. Curves for n and m on left and h on the right are $1 - \exp(-t/\tau)$, i.e., an exponential rise toward a value of 1.0. Curves for n and m on the right and h on the left are $\exp(-t/\tau)$, i.e., an exponential fall toward a value of zero. Other curves are the indicated powers and products of m, n, and h, showing how n^4 and m^3h imitate the time course of g_K and g_{Na} in the HH model. [From Hille, 1977c.]

Curves showing the voltage dependence of τ_n and n_∞ for a squid giant axon at 6.3°C are shown in Figure 17. At very negative potentials (e.g., −75 mV) n_∞ is small, meaning that K channels would tend to close. At positive potentials (e.g., +50 mV) n_∞ is nearly 1, meaning that channels tend to open. The changes of n with time can be calculated by solving the differential equation

$$\frac{dn}{dt} = \frac{n_\infty - n}{\tau_n} \tag{2-9}$$

This is just Equation 2-6 written in a different form. According to the τ_n curve of Figure 17, the parameter n relaxes slowly to new values at −75 mV and much more rapidly at +50 mV.

The HH model uses a similar formalism to describe I_{Na}, with four hypothetical gating particles making independent first-order transitions between permis-

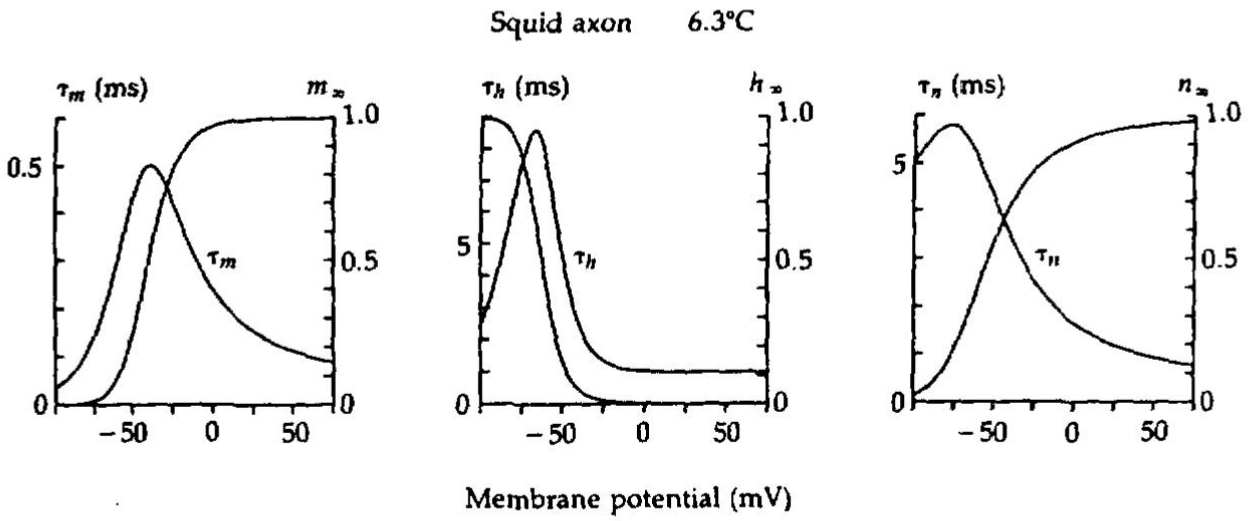

17 VOLTAGE-DEPENDENT PARAMETERS OF HH MODEL

Time constants τ_m, τ_h, and τ_n and steady-state values m_∞, h_∞, and n_∞ calculated from the empirical equations of the Hodgkin–Huxley model for squid giant axon membrane at 6.3°C. Depolarizations increase m_∞ and n_∞ and decrease h_∞. The time constants of relaxation are maximal near the resting potential and become shorter on either side. [From Hille, 1970.]

sive and nonpermissive positions to control the channel. However, because there are two opposing gating processes, activation and inactivation, there have to be two kinds of gating particles. Hodgkin and Huxley called them m and h. Three m particles control activation and one h particle, inactivation. Therefore, the probability that they are all in the permissive position is m^3h, and I_{Na} is represented by

$$I_{Na} = m^3h\bar{g}_{Na}(E - E_{Na}) \tag{2-10}$$

Figure 16 illustrates how the changes of m^3h imitate the time course of g_{Na} during and after a depolarizing testpulse. At rest m is low and h is high. During the depolarization m rises rapidly and h falls slowly. Taking the cube of m sets up a small delay in the rise, and multiplying by the slowly falling h makes m^3h eventually fall to a low value again. After the depolarization, m recovers rapidly and h slowly to the original values. As for the n parameter of K channels, m and h are assumed to undergo first-order transitions between permissive and nonpermissive forms:

$$\text{“}1 - m\text{”} \underset{\beta_m}{\overset{\alpha_m}{\rightleftharpoons}} m \tag{2-11}$$

$$\text{“}1 - h\text{”} \underset{\beta_h}{\overset{\alpha_h}{\rightleftharpoons}} h \tag{2-12}$$

with rates satisfying the differential equations

$$\frac{dm}{dt} = \alpha_m (1 - m) - \beta_m m = \frac{m_\infty - m}{\tau_m} \tag{2-13}$$

$$\frac{dh}{dt} = \alpha_h (1 - h) - \beta_h h = \frac{h_\infty - h}{\tau_h} \tag{2-14}$$

where

$$\tau_m = \frac{1}{\alpha_m + \beta_m} \tag{2-15}$$

$$\tau_h = \frac{1}{\alpha_h + \beta_h} \tag{2-16}$$

$$m_\infty = \frac{\alpha_m}{\alpha_m + \beta_m} \tag{2-17}$$

$$h_\infty = \frac{\alpha_h}{\alpha_h + \beta_h} \tag{2-18}$$

When the membrane potential is stepped to a new value and held there, the equations predict that h, m, and n relax exponentially to their new values. For example,

$$m(t) = m_\infty - (m_\infty - m_0) \exp\left(-\frac{t}{\tau_m}\right) \tag{2-19}$$

where m_0 is the value of m at $t = 0$.

The HH model treats activation and inactivation as entirely independent of each other. Both depend on membrane potential; either can prevent a channel from being open; but one does not know what the other is doing. Figure 17 summarizes experimental values of m_∞, τ_m, h_∞, and τ_h for squid giant axons at 6.3°C. Within the assumptions of the model, these values give an excellent description (Figure 12, smooth curves) of the conductance changes measured under voltage clamp.

Recall that h is the probability that a Na channel is *not* inactivated. The experiments in Figures 14 and 15, which measured the steady-state voltage dependence and the rate of recovery from Na inactivation in a frog axon, are therefore also experiments to measure h_∞ and τ_h as defined by the HH model. Comparing Figure 14 with Figure 17 shows strong similarities in gating properties between axons of squid and frog.

To summarize, the HH model for the squid giant axon describes ionic current across the membrane in terms of three components.

$$I_i = m^3 h \bar{g}_{Na} (E - E_{Na}) + n^4 \bar{g}_K (E - E_K) + \bar{g}_L (E - E_L) \tag{2-20}$$

where $\bar{g}_L$ is a fixed background leakage conductance. All of the electrical excitability of the membrane is embodied in the time and voltage dependence of the

three coefficients h, m, and n. These coefficients vary so as to imitate the membrane permeability changes measured in voltage clamp experiments.

One difference between Figures 14 and 17 is the temperature of the experiments. Warming an axon by 10°C speeds the rates of gating two- to fourfold (Q_{10} = 2 to 4; Hodgkin et al., 1952; Frankenhaeuser and Moore, 1963; Beam and Donaldson, 1983). As we know now, gating involves conformational changes of channel proteins, and the rates of these conformational changes are temperature sensitive. Therefore, we should try to state the temperature whenever we give a rate. Unlike gating, the conductance of an open channel can be relatively temperature insensitive with a Q_{10} of only 1.2 to 1.5, which is like that for aqueous diffusion of ions.

The Hodgkin–Huxley model predicts action potentials

The physiological motivation for Hodgkin and Huxley's quantitative analysis of voltage-clamp currents was to explain the classical phenomena of electrical excitability. Therefore, they concluded their work with calculations, done on a hand calculator, of membrane potential changes predicted by their equations. They demonstrated the considerable power of the model to predict appropriate subthreshold responses, a sharp threshold for firing, propagated action potentials, ionic fluxes, membrane impedance changes, and other axonal properties.

Figure 18 shows a more recent calculation of an action potential propagating away from an intracellular stimulating electrode. The time course of the membrane potential changes is calculated entirely from Equation 2-1, the cable equation for a cylinder, and the HH model with no adjustable constants. Recall that the model was developed from experiments under voltage-clamp and space-clamp conditions. Since the calculations involve neither voltage clamp nor space clamp, they are a sensitive test of the predictive value of the model. In this example, solved with a digital computer, a stimulus current is applied at $x = 0$ for 200 μs and the time course of the predicted voltage changes is drawn for $x = 0$ and for $x = 1$, 2, and 3 cm down the "axon." The membrane depolarizes to −35 mV during the stimulus and then begins to repolarize. However, the depolarization soon increases the Na permeability and Na^+ ions rush in, initiating a regenerative spread of excitation down the model axon. All of these features imitate excellently the responses of a real axon. Figure 19 shows the calculated time course of the opening of Na and K channels during the propagated action potential. After local circuit currents begin to depolarize the membrane, Na channels activate rapidly and the depolarization becomes regenerative, but even before the peak of the action potential, inactivation takes over and the Na permeability falls. In the meantime the strong depolarization slowly activates K channels, which, together with leak channels, produce the outward current needed to repolarize the membrane. The time course of repolarization depends on the rate of Na channel inactivation and the rate of K channel activation, for if either is slowed in the model, the action potential is prolonged.

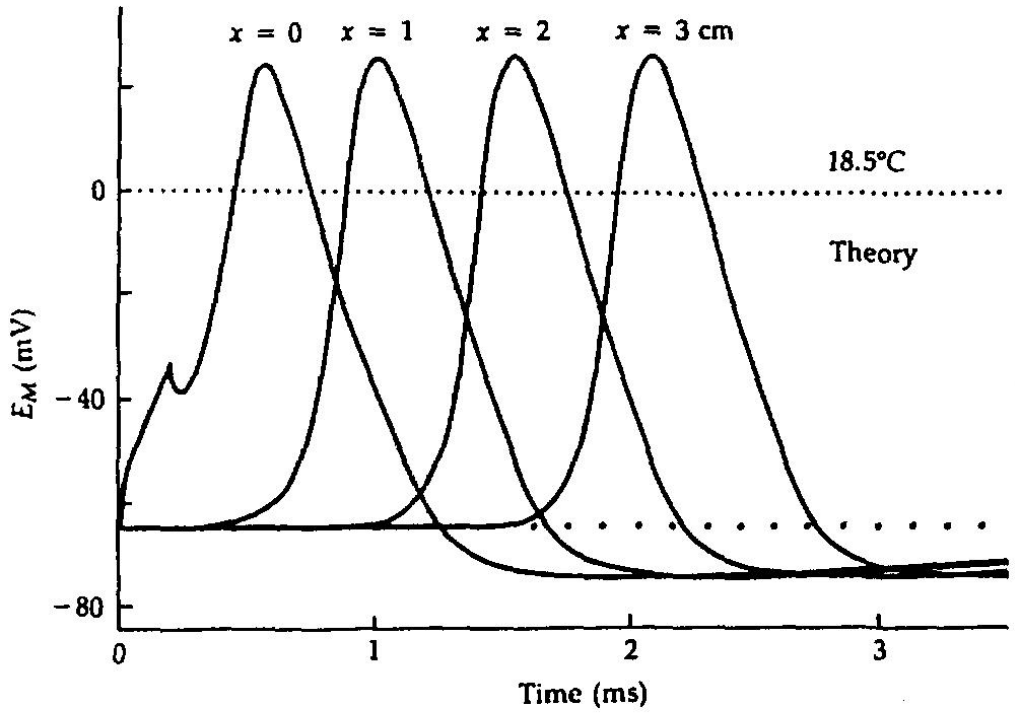

18 CALCULATED PROPAGATING ACTION POTENTIAL

Computer-calculated responses of a simulated axon of 476 μm diameter and 35.4 Ω · cm axoplasmic resistivity assumed to have a membrane described by the HH model adjusted to 18.5°C. In the simulation a stimulus current is applied at $x = 0$ for 200 μs. It depolarizes the membrane locally but not as far away as $x = 1$ cm. However, the stimulus is above threshold for excitation of an action potential, which appears successively at $x = 0$, 1, 2, and 3 cm, propagating at a calculated steady velocity of 18.7 m/s. [From Cooley and Dodge, 1966.]

For a brief period after the action potential the model membrane remains refractory to restimulation as Na channels recover from their inactivation and K channels close.

Hundreds of papers have now been written with calculations for new stimuli, for new geometries of axonal tapering, branching, and so on, and even for nerve networks using the HH model. These studies contribute to our understanding of the physiology of nerve axons and of the nervous system. However, as they usually elucidate membrane responses rather than mechanisms of ionic channels, we shall not discuss them in this book. Readers interested in these questions can consult the literature and reviews (Cooley and Dodge, 1966; Hodgkin and Huxley, 1952a; Jack et al., 1983; Khodorov, 1974; Khodorov and Timin, 1975; Koch and Segev, 1989; Noble, 1966).

The success of the HH model is a triumph of the classical biophysical method in answering a fundamental biological question. Sodium and potassium ion fluxes account for excitation and conduction in the squid giant axon. Voltage-dependent permeability mechanisms and ionic gradients suffice to explain electrical excitability. The membrane hypothesis is correct. A new era began in which an ionic basis was sought for every electrical response of every cell.

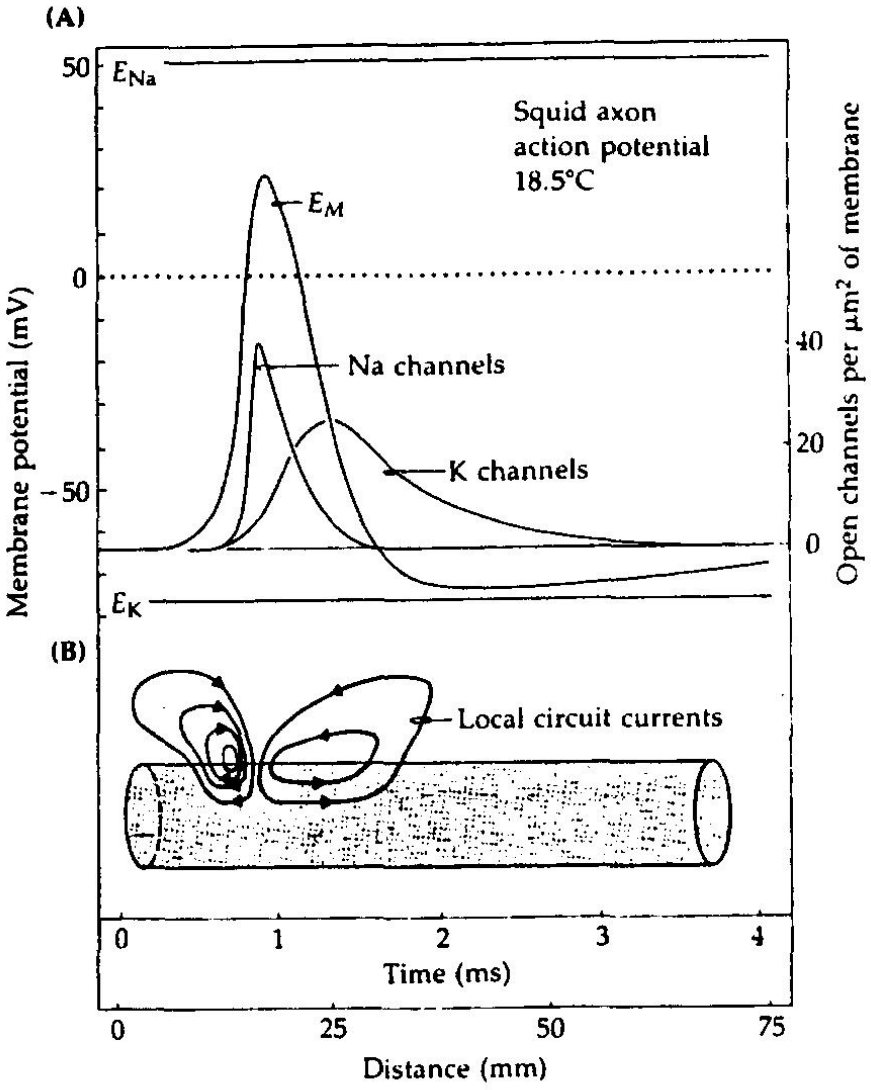

19 CHANNEL OPENINGS AND LOCAL CIRCUITS

Events during the propagated action potential. These diagrams describe the time course of events at one point in an axon, but since the action potential is a wave moving at uniform velocity, the diagrams may equally well be thought of as an instantaneous "snapshot" of the spatial extent of an action potential. Hence both time and distance axes are given below. (A) Action potential and underlying opening of Na and K channels calculated from the HH model at 18.5°C. (B) Diagram of the local circuit current flows associated with propagation; inward current at the excited region spreads forward inside the axon to bring unexcited regions above firing threshold. The diameter of the axon is greatly exaggerated in the drawing and should be only 0.5 mm. [Adapted from Hodgkin and Huxley, 1952d.]

Do models have mechanistic implications?

The HH model certainly demonstrates the importance of Na and K permeability changes for excitability and describes their time course in detail. But does it say *how* they work? In one extreme view, the model is mere curve fitting of arbitrary equations to summarize experimental observations. Then it could say nothing about molecular mechanism. According to a view at the opposite extreme, the

model demonstrates that there are certain numbers of independent h, m, and n particles moving in the electric field of the membrane and controlling independent Na and K permeabilities. In addition, there are intermediate views. How does one decide?

The scientific method says to reject hypotheses when they are contradicted, but it does not offer a clear prescription of when propositions are to be promoted from the status of hypothesis to one of general acceptance. Claude Bernard (1865) insisted that experimentalists maintain constant philosophic doubt, questioning all assumptions and regarding theories as partial and provisional truths whose only certainty is that they are literally false and will be changed. He cautioned against giving greater weight to theories than to the original observations. Yet theory and hypothesis are essential as guides to new experiments and eventually may be supported by so many observations that their contradiction in the future is hardly conceivable. Certainly, by that time, the theory should be regarded as established and should be used as a touchstone in pursuing other hypotheses. At some point, for example, Watson and Crick's bold hypothesis of the DNA double helix and its role in genetics became fundamental fact rather than mere speculation. Some of the challenge of science then lies in the art of choosing a strong, yet incompletely tested framework for thinking. The sooner one can recognize "correct" hypotheses and reject false ones, the faster the field can be advanced into new territory. However, the benefits must be balanced against the risks of undue speed: superficiality, weak science, and frank error.

Consider then whether the HH model could be regarded as "true." In their extensive experience with kinetic modeling of chemical reactions, chemical kineticists have come to the general conclusion that fitting of models can disprove a suggested mechanism but cannot prove one. There always are other models that fit. These models may be more complicated, but the products of biological evolution are not required to seem simplest to the human mind or to make "optimal" use of physical laws and materials. Kineticists usually require other direct evidence of postulated steps before a mechanism is accepted. Therefore, the strictly kinetic aspects of the HH model, such as control by a certain number of independent h, m, and n particles making first-order transitions between two positions, cannot be proven by curve fitting. Indeed, Hodgkin and Huxley (1952d) stated that better fits could be obtained by assuming more n particles and they explicitly cautioned: "Certain features of our equations [are] capable of physical interpretation, but the success of our equations is no evidence in favor of the mechanism of permeability change that we tentatively had in mind when formulating them." The lesson is easier to accept now that, after 40 more years of work, new kinetic phenomena have finally been observed that disagree significantly with some specific predictions of their model (Chapter 18).

Even if its kinetic details cannot be taken literally, the HH model has important general properties with mechanistic implications that must be included in future models. For example, I_{Na} reverses at E_{Na} and I_K reverses at E_K. (Even these simple statements need to be qualified as we shall see later.) These

properties mean that the ions are moving passively with thermal and electrical forces down their electrochemical gradients rather than being driven by metabolic energy or being coupled stoichiometrically to other fluxes. K channels and Na channels activate along an S-shaped time course, implying that several components, or several steps in series, control the opening event, as is expressed in the model by the movement of several m or n particles. At least one more step is required in Na channels to account for inactivation. All communication from channel to channel is via the membrane potential, as is expressed in the voltage dependence of the α's and β's or τ's and the steady-state values, m_∞, h_∞, and n_∞, of the controlling reactions; hence the energy source for gating is the electric field and not chemical reactions. Finally, activation depends very steeply on membrane potential as is seen in the steep, peak g_{Na}–E curve in Figure 13 and expressed in the n_∞–E and m_∞–E curves in Figure 17. The implications of steep voltage dependence are discussed in the next section.

Voltage-dependent gates have gating charge and gating current

In order for a process like gating to be controlled and powered by the electric field, the field has to do work on the system by moving some charges. Three possibilities come quickly to mind: (1) the field moves an important soluble ion such as Na^+, K^+, Ca^{2+}, or Cl^- across the membrane or up to the membrane, and the gates are responding to the accumulation or depletion of this ion; (2) the field squeezes the membrane and the gates are responding to this mechanical force; and (3) the field moves charged and dipolar components of the channel macromolecule or its environment and this rearrangement is, or induces, the gating event. Although the first two mechanisms are seriously considered for other channels, they seem now to be ruled out for the voltage-gated Na and K channels of axons. If their gating were normally driven by a local ionic concentration change, they would respond sensitively to experimentally imposed concentration changes of the appropriate ion. In modern work, several good methods exist to change ions on the extracellular and on the axoplasmic side of the membrane. The interesting effects of H^+ and divalent ions are described in Chapter 15, and the insensitivity to total replacement of Na^+ and K^+ ions is described in Chapter 13. Suffice it to say here, however, that the ionic accumulation or depletion hypothesis has not explained gating in Na and K channels of axons. The second hypothesis runs into difficulty because electrostriction (the mechanical squeezing effect) should depend on the magnitude (actually the square) of the field but not on the sign. Thus electrostriction and effects dependent on it would be symmetrical about 0 mV. Gating does not have such a symmetry property. More strictly, because the membrane is asymmetrical and bears asymmetrical surface charge, the point of symmetry could be somewhat offset from 0 mV.

These arguments leave only a direct action of the field on charges that are part of or associated with the channel, a viewpoint that Hodgkin and Huxley

(1952d) endorsed with their idea of charged h, m, and n particles moved by the field. The relevant charges, acting as a molecular voltmeter, are now often called the GATING CHARGE or the VOLTAGE SENSOR. Since opening is favored by depolarization, the opening event must consist of an inward movement of negative gating charge, an outward movement of positive gating charge, or both. Hodgkin and Huxley pointed out that the necessary movement of charged gating particles within the membrane should also be detectable in a voltage clamp as a small electric current that would precede the ionic currents. At first the term "carrier current" was used for the proposed charge movement, but as we no longer think of channels as carriers, the term GATING CURRENT is now universally used. Gating current was not actually detected until the 1970s (Schneider and Chandler, 1973; Armstrong and Bezanilla, 1973, 1974; Keynes and Rojas, 1974) and then quickly became an important tool in studying channels.

A lower limit for the magnitude of the gating charge can be calculated from the steepness of the voltage dependence of gating. We follow Hodgkin and Huxley's (1952d) treatment here, using a slightly more modern language. Suppose that a channel has only two states, closed (C) and open (O).

$$\text{(closed) C} \rightleftharpoons \text{O (open)}$$

The transition from C to O is a conformational change that moves a gating charge of valence z_g from the inner membrane surface to the outer, across the full membrane potential drop E. There will be two terms in the energy change of the transition. Let the conformational energy increase upon opening the channel in the absence of a membrane potential ($E = 0$) be w. The other term is the more interesting voltage-dependent one due to movement of the gating charge z_g when there is a membrane potential. This electrical energy increase is $-z_g eE$, where e is the elementary charge, and the total energy change becomes $(w - z_g eE)$. The Boltzmann equation (Equation 1-7) dictates the ratio of open to closed channels at equilibrium in terms of the energy change,

$$\frac{\text{O}}{\text{C}} = \exp\left(-\frac{w - z_g E}{kT}\right) \tag{2-21}$$

and explicitly gives the voltage dependence of gating in the system. Finally, rearranging gives the fraction of open channels:

$$\frac{\text{O}}{\text{O} + \text{C}} = \frac{1}{1 + \exp\left[(w - z_g eE)/kT\right]} \tag{2-22}$$

Figure 20 is a semilogarithmic plot of the predicted fraction of open channels for different charge valences z_g. The higher the charge, the steeper the rising part of the curve. These curves can be compared with the actual voltage dependence of peak g_{Na} and g_K in Figure 13. In this simple model the best fit requires that $z_g \approx 4.5$ for g_K. A quick estimate of the charge can be obtained by noting that the theoretical curves reach a limiting slope of an e-fold ($e \approx 2.72$) increase per kT/ze millivolts at negative potentials. Peak g_{Na} has a limiting slope of e-fold per 4

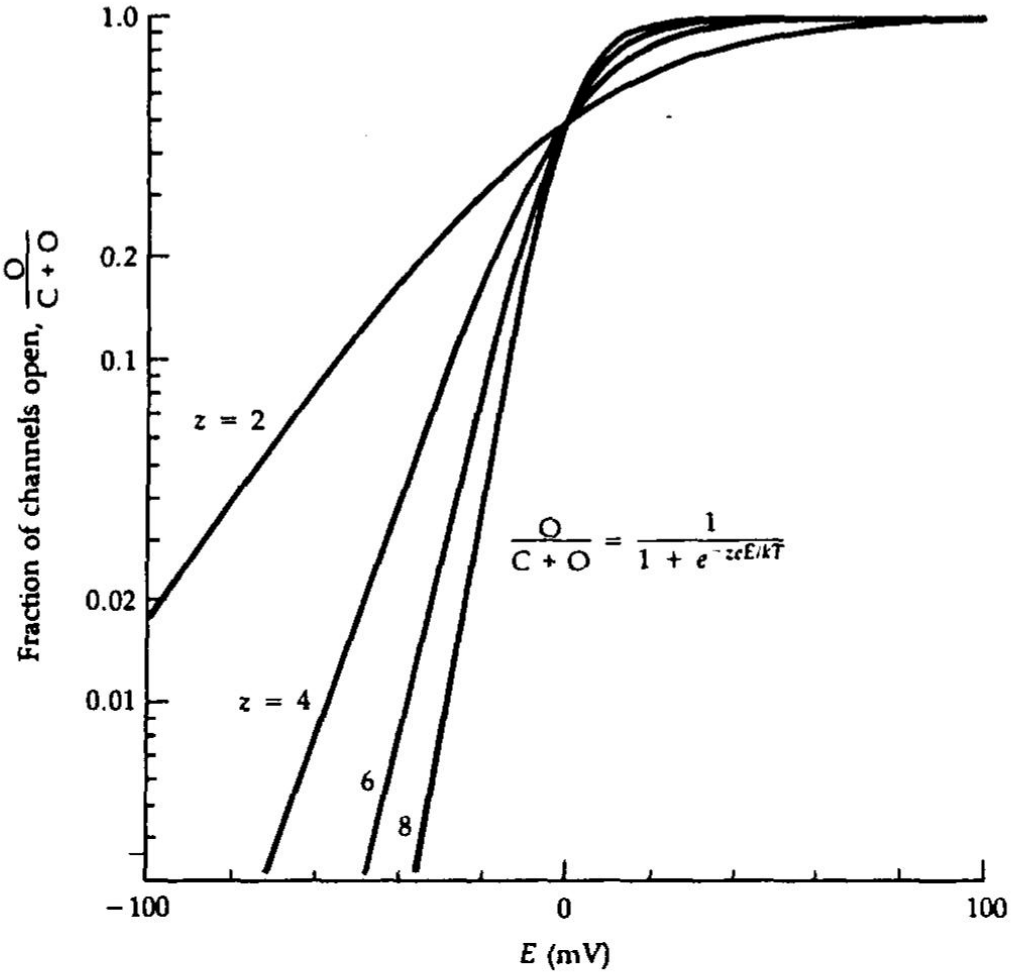

20 BOLTZMANN THEORY FOR VOLTAGE DEPENDENCE

In this simple, two-state theory of equilibrium voltage dependence, channel opening is controlled by the movement of a polyvalent charged particle of charge, z_g, between positions on opposite sides of the membrane. The equilibrium fraction of open channels then must obey the Boltzmann equation, Equation 2-22. As the assumed charge is increased from 2 to 8, the predicted voltage dependence is steeper and steeper. The calculations assume $w = 0$ in the equation, i.e., 50% of the channels are open in the absence of a membrane potential.

mV. Since kT/e is about 24 mV (Table 2 in Chapter 1), z_g is 24/4 = 6. Therefore, the gating charge for opening a Na channel is equivalent to six elementary charges.

The model considered is oversimplified in several respects. Charged groups on the channel might move only partway through the membrane potential drop. In that case more charge would be required to get the same net effect. For example, 18 charges would be needed if they could move only a third of the way. Second, we have already noted that gating kinetics require more than two kinetic states of the channel. Each of the transitions among the states might have a partial charge movement. If all states but one are closed, the limiting steepness reflects the total charge movement needed to get to the open state from which-

ever closed state is most favored by strong hyperpolarizations (Almers, 1978). Because of these complications, we will consider the limiting steepness, called the LIMITING LOGARITHMIC POTENTIAL SENSITIVITY by Almers (1978), as a measure of an *equivalent* gating charge. This equivalent charge is less than the actual number of charges that may move. Some or all of the equivalent charge movement could even be movements of the hundreds of partial charges, often thought of as dipoles, of the polar bonds of the channel. We consider gating charge and gating current in more detail in Chapters 8 and 18.

Note that thermodynamics does not permit channels to have a sharp voltage threshold for opening. Every step in gating must follow a Boltzmann equilibrium law, which is a continuous, even if steep, function of voltage. The absence of a threshold is suggested empirically by the many voltage-clamp experiments that show that a few Na channels are open at rest, and that even depolarization by a couple of millivolts increases the probability of opening Na channels in a manner well described by the limiting steepness of the Boltzmann equation. Nevertheless, for all practical purposes, a healthy axon does show a sharp threshold for firing an action potential. This, however, is not a threshold for channel opening at all but a threshold for the reversal of net membrane current. At any potential there are several types of channel open. A depolarizing stimulus to the firing threshold opens *just enough* Na channels to make an inward current that exactly counterbalances the sum of the outward currents carried by K^+, Cl^-, and any other ion in other channels and the local circuit currents drawn off by neighboring patches of membrane. The resulting *net* accumulation of positive charge inside makes the upstroke of the action potential. A much more sophisticated discussion of threshold may be found in *Electric Current Flow in Excitable Cells* by Jack, Noble, and Tsien (1983). The important point to be made here is that channels have no threshold for opening.

Recapitulation of the classical discoveries

Two of the central concepts for understanding electrical excitation had been stated clearly early in this century but remained unsupported for decades. Bernstein (1902, 1912) had proposed that potentials arise across a membrane that is selectively permeable and separates solutions of different ionic concentrations. He believed that excitation involves a permeability increase. Hermann (1872, 1905a,b) had proposed that propagation is an electrical self-stimulation of the axon by inward action currents spreading passively from an excited region to neighboring unexcited regions. Only in the heroic period 1935–1952 were these hypotheses shown to be correct. Local circuit currents were shown to depolarize and bring resting membrane into action (Hodgkin, 1937a,b). The membrane permeability was found to increase dramatically (Cole and Curtis, 1938, 1939). The inward ionic current was attributed to a selective permeability increase to Na^+ ions (Hodgkin and Katz, 1949). Finally, the kinetics of the ionic permeability changes were described with the help of the voltage clamp (Hodgkin et al., 1952; Hodgkin and Huxley, 1952a,b,c,d).

The voltage clamp revealed two major permeability mechanisms, distinguished by their ionic selectivities and their clearly separable kinetics. One is Na selective and the other is K selective. Both have voltage-dependent kinetics. Together they account for the action potential. These were the first two ionic channels to be recognized and described in detail.

Na AND K CHANNELS OF AXONS

Until the mid-1960s, there were few clues as to how ions actually move across the membranes of excitable cells. A variety of mechanisms were considered possible. They included permeation in a homogeneous membrane, binding and migration along charged sites, passage on carriers, and flow through pores. The pathways for different ions could be the same (only one kind of channel) with time-varying affinities or pore radii, or they could be different. The pathways for different ions could be preformed in specialized molecules or they might just be created spontaneously by thermal agitation as defects or vacancies in molecular packing. The pathways might be formed by phospholipid or by protein or even nucleic acid. Each of these ideas was seriously advanced and rationalized in published articles.

This chapter begins with a diversion into pharmacology because pharmacological experiments helped to clarify the concept of ionic channels as distinct molecules. Then we formulate a hypothesis about what channels look like. Finally we return to biophysical experiments that start to ask if we can generalize the ideas gained by studying the squid axon.

Drugs and toxins help separate currents and identify channels

Pharmacological experiments with the molecules shown in Figure 1 provided the evidence needed to define channels as discrete entities. The magic bullet was tetrodotoxin (dubbed TTX by K.S. Cole), a paralytic poison of some puffer fish and of other fishes of the order Tetraodontiformes (Halstead, 1978). In Japan this potent toxin had attracted medical attention because puffer fish is prized there as a delicacy—with occasional fatal effects. Tetrodotoxin blocks action potential conduction in nerve and muscle. Toshio Narahashi brought a sample of TTX to John Moore's laboratory in the United States. Their first voltage-clamp study with lobster giant axons revealed that TTX blocks I_{Na} selectively, leaving I_K and I_L untouched (Narahashi et al., 1964). Only nanomolar concentrations were needed. This highly selective block was soon verified in squid giant axons, eel electric organ, and frog myelinated axons (Nakamura et al., 1965a,b; Hille 1966, 1967a, 1968a). For example, Figure 2A shows a typical voltage-clamp experiment with the frog node of Ranvier. The control measurement in normal Ringer's shows the transient I_{Na} and delayed outward I_K of a healthy axon. Ohmic leakage currents, I_L, have already been subtracted mathematically by the computer that recorded and then drew out the family of currents. In the presence of

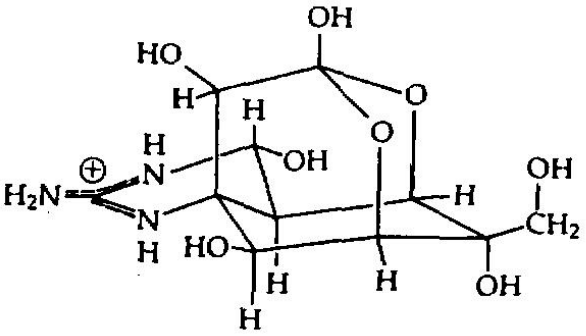

TTX

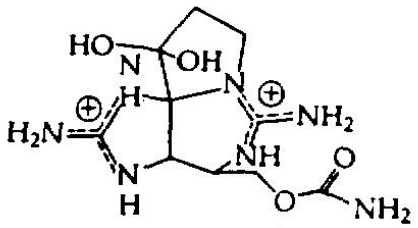

STX

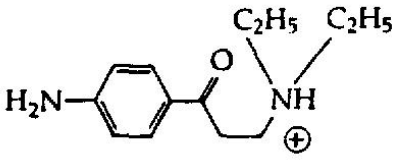

Procaine

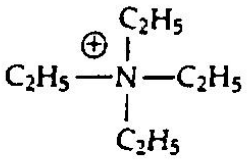

TEA

1 CHEMICAL STRUCTURES OF CHANNEL BLOCKERS

Tetrodotoxin (TTX) and saxitoxin (STX) are paralytic natural toxins which are exceptionally specific blockers of Na channels. The local anesthetic, procaine, is a synthetic agent used clinically to block Na channels. Tetraethylammonium ion (TEA) is a simple quaternary ammonium compound used experimentally to block K channels. All of these agents act reversibly.

300 nM TTX, the delayed I_K is quite unchanged, but no trace of I_{Na} remains. The drug cleanly separates ionic currents into the same two major components that are more laboriously obtained by Hodgkin and Huxley's (1952a) ionic substitution method.

Around the same time another natural toxin, saxitoxin (STX), was shown to have pharmacological properties almost identical to TTX. Like TTX, STX is a small water-soluble molecule that blocks I_{Na} in nanomolar concentrations when applied outside the cell. Early voltage-clamp experiments were done with the electric organ of the electric eel (Nakamura et al., 1965b), lobster giant axon (Narahashi et al., 1967), and frog node of Ranvier (Hille, 1967b, 1968a). STX is one of several related paralytic toxins in marine dinoflagellates of the genus *Gonyaulax* and others (Taylor and Seliger, 1979).[1] In some seasons, the population of microscopic dinoflagellates "blooms," even discoloring the water with their reddish color ("red tide"), and filter-feeding shellfish become contaminated with accumulated toxin. The name "saxitoxin" and its alternate, "paralytic

[1] It has been puzzling that molecules of such complex and unusual structure as STX and TTX appear in several evolutionarily distant organisms. For example, TTX is found in certain Pacific puffer fish, a Californian salamander, a South American frog, an Australian octopus and some Japanese platyhelminth, nematode, and nemertean worms. An explanation is that the toxins are synthesized by bacteria that may be symbiotic with these various hosts. Indeed STX occurs in a freshwater cyanobacterium, *Aphanizomenon flos-aquae*, and TTX in a bacterium, *Vibrio alginolyticus*.

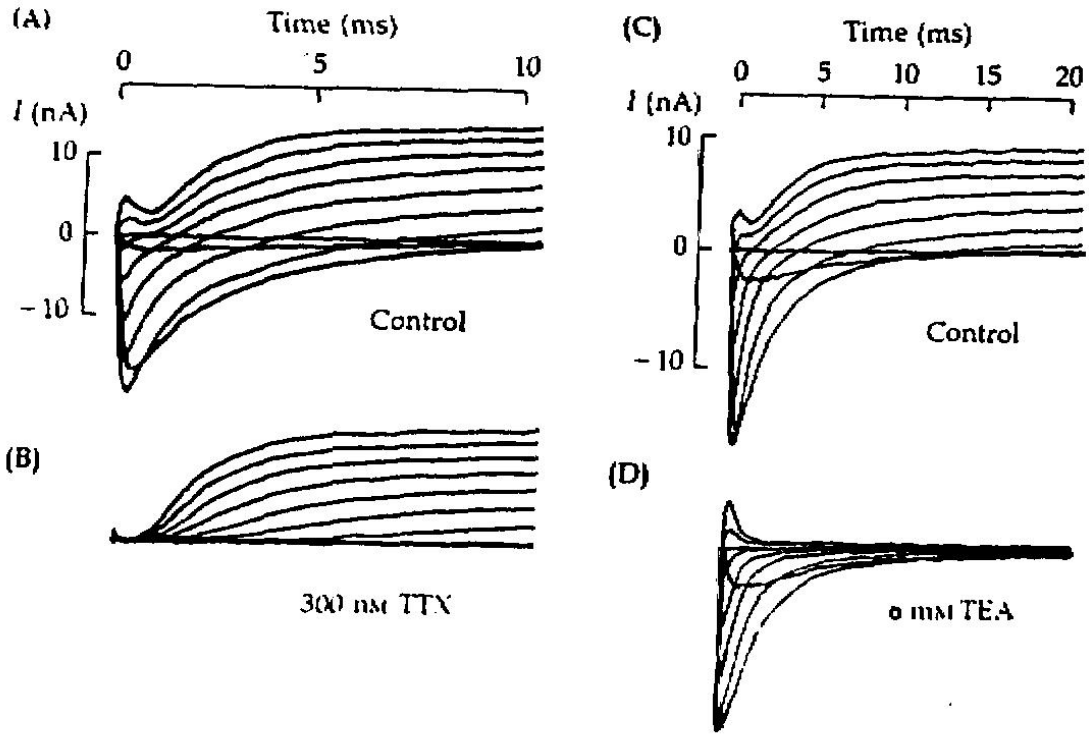

2 SPECIFIC BLOCK OF IONIC CHANNELS

Pharmacological dissection of I_{Na} and I_K. A node of Ranvier under voltage clamp is held at −95 mV, hyperpolarized for 40 ms to −120 mV, and then depolarized to various potentials ranging from −60 to +60 mV in 15-mV steps. Leakage and capacity currents are subtracted by a computer. (A) Normal I_{Na} and I_K in Ringer's solution. (B) Same node after external addition of 300 nM TTX. Only I_K remains. T = 13°C. [Adapted from Hille, 1966.] (C) Control measurements in another node. (D) Same node after external addition of 6 mM TEA. Only I_{Na} remains. T = 11°C. [Adapted from Hille, 1967a.]

shellfish poison," remind us that contaminated shellfish, including the Alaskan butter clam, *Saxidomus*, can be dangerous to eat. Cooking does not destroy the toxin, and eating even a single shellfish can be fatal. Fortunately, public health authorities monitor the commercial shellfish harvest continually. Many interesting, early reports on STX and TTX are described in Kao's (1966) excellent review. Newer work is considered later in this book (Chapter 15). For now, the important result is that STX and TTX block I_{Na} selectively, completely, and reversibly in axons.

A third important blocking agent with actions complementary to those of TTX and STX is the tetraethylammonium ion (TEA). It prolongs the falling phase of action potentials by selectively blocking I_K but not I_{Na}. The first voltage-clamp experiments using TEA were done with ganglion cells of the mollusc *Onchidium verruculatum* (Hagiwara and Saito, 1959), the squid giant axon (Tasaki and Hagiwara, 1957; Armstrong and Binstock, 1965), and frog nodes of Ranvier (Koppenhöfer, 1967; Hille, 1967a). Figure 2D shows the block of I_K by 6 mM TEA applied outside a node of Ranvier. I_K is gone and I_{Na} is not changed. The block may be quickly reversed by a rinse with Ringer's solution. Again the drug

separates I_{Na} from I_K, giving results equivalent to the ionic substitution method.

The selectivity and complementarity of the block with TTX or STX on the one hand, and with TEA on the other, provided the most important arguments for two separate ionic pathways for I_{Na} and I_K in the membrane. No drug blocks leakage currents; they must use other ionic pathways.

By the late 1960s the names "Na channel" and "K channel" began to be used consistently for these ionic pathways. These names had already appeared, albeit very infrequently, in the earlier literature (Hodgkin and Keynes, 1955a,b, 1957; Lüttgau, 1958a, 1961; Katz, 1962; Adrian, 1962; Nakajima et al., 1962; Hodgkin, 1964; Narahashi et al., 1964; Armstrong and Binstock, 1965; Chandler and Meves, 1965; Woodbury, 1965). Indeed, as Chapter 11 describes in detail, the words "channel" or "canal" also appear in still older literature, where they denote in a generic sense the aqueous space available for diffusion in a pore (e.g., Brücke, 1843; Ludwig, 1852; Michaelis, 1925).[2] The acceptance of these ideas initiated serious thinking about the structure, pharmacology, genetics, development, evolution, and so on, of individual ionic channels from a molecular viewpoint. Now that we can record from single channels—and even purify them chemically, and sequence and modify their genes—there remains no question of their molecular individuality.

As we shall see later, TTX, STX, and TEA are not the only blocking agents for Na and K channels. The list of useful blockers for K channels includes the inorganic cations Cs^+ and Ba^{2+}, and the organic cations 4-aminopyridine, TEA, and many related small molecules with quaternary or protonated nitrogen atoms. Particularly valuable clinical blocking agents of Na channels include the local anesthetics. Sigmund Freud and Karl Koller introduced cocaine as a local anesthetic more than 100 years ago. Since then, pharmaceutical chemists have developed a large number of more practical local anesthetic compounds, starting with procaine (Figure 1). Chapter 15 argues that the channel-blocking agents TEA, Cs^+, Ba^{2+}, and local anesthetics act by physically entering the pore and plugging the channel. Chapter 17 discusses another useful class of agents that modify the gating of channels, often holding them open for longer than usual.

Drugs and toxins act at receptors

A toxin like TTX could not alter a physiological function without having molecular interactions with one or several tissue components. Pharmacologists call these sites of interaction RECEPTORS. The power of pharmacology lies in the intellectual leap from action to receptor, which stimulates thinking about molecules and molecular interactions. The receptor is a molecule.

The simplest approach to receptors supposes that the toxin binds reversibly to a single class of sites and that binding of a toxin molecule to one receptor site blocks a fixed fraction of the function without influencing the binding of the

[2] In the European languages, except English, no distinction is made between canal and channel, and a single word pronounced *kanal* is used, for example, for the canals of Venice, television channels, and ionic channels.

other toxin molecules to the other receptors. Like any reversible bimolecular reaction, the binding of toxin (T) to receptor (R) could then be characterized by an equilibrium dissociation constant K_d (units: moles per liter), defined in terms of the forward and backward rate constants of the reaction k_1 (s^{-1} M^{-1}) and k_{-1} (s^{-1}),

$$T + R \underset{k_{-1}}{\overset{k_1}{\rightleftharpoons}} TR \qquad K_d = \frac{k_{-1}}{k_1} = \frac{[T]\,[R]}{[TR]} \tag{3-1}$$

where the brackets denote equilibrium concentrations. At equilibrium the fractional occupancy y of receptors is a saturation function of [T] sometimes called the LANGMUIR ADSORPTION ISOTHERM:

$$y = \frac{[TR]}{[TR] + [R]} = \frac{[T]}{[T] + K_d} = \frac{1}{1 + K_d/[T]} \tag{3-2}$$

The equations are identical to those for titration of an acid with a base and similar to those for the Michaelis–Menten theory of enzyme kinetics. Half-maximal occupancy occurs when [T], the concentration of free toxin, is numerically equal to K_d. We can also write an equation for the fraction of free receptors, $1 - y$:

$$1 - y = \frac{K_d}{[T] + K_d} = \frac{1}{1 + [T]/K_d} \tag{3-3}$$

These ideas are illustrated by dose-response studies of STX blocking I_{Na} in a frog node of Ranvier (Figure 3). Relative amplitudes of I_{Na} at different extracellular STX concentrations are plotted as filled circles together with a theoretical curve

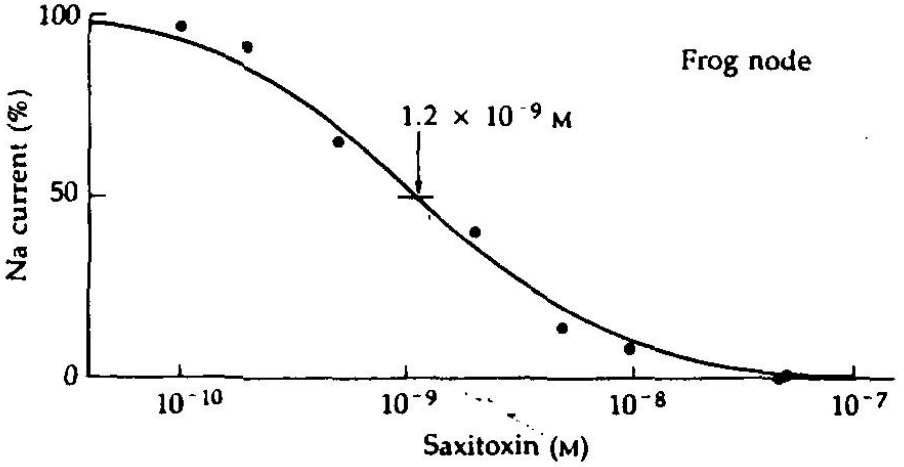

3 SAXITOXIN DOSE-RESPONSE RELATIONSHIP

The relative peak I_{Na} is measured in a node of Ranvier under voltage clamp while solutions containing different concentrations of added STX are placed in the bath. All values are normalized with respect to drug-free Ringer's solution. The solid line is the expected dose-response curve if one STX molecule must bind reversibly to a channel with a dissociation constant K_d = 1.2 nM STX in order to block the current (see Equation 3-3). T = 4°C. [From Hille, 1968a.]

drawn from Equation 3-3 with K_d = 1.2 nM. Such results support the conclusion that Na channels are blocked in a one-to-one manner when STX binds to a receptor on the extracellular side of the membrane. When TTX or STX is applied to the *intracellular* side, I_{Na} is not blocked.

Toxin binding can be used to determine the density of specific toxin receptors in the tissue. This would be easy if, when a solution of toxin is applied, all the uptake followed Equation 3-2. The toxin concentration could be raised well into the saturating range, and the total bound toxin measured at once. Unfortunately, extra toxin molecules are always taken up either by weak binding sites or simply in the imbibed solution that must occupy the extracellular space of the test tissue. Therefore, there are two components to the measured uptake U, a saturable component representing binding to specific receptor sites and a linear component representing uptake in aqueous spaces of the tissue and "nonsaturable binding." If there are B_{max} specific binding sites, the total radioactivity taken up is

$$U = \frac{B_{max}}{1 + K_d/[T]} + a[T] \qquad (3\text{-}4)$$

In practice, the equilibrium uptake is determined at several concentrations of toxin so that Equation 3-4 can be fitted to the results, often with one very high value of [T] to determine the coefficient a. The useful results of the experiment are B_{max}, the number of binding sites, and K_d, the dissociation constant of the drug-receptor complex. If the toxin can be made radioactive, then binding can be measured with a radiation counter. This has been done with [^{3}H]TTX, [^{3}H]STX, and many other molecules. With labeled molecules, it is essential to know how much radioactivity is associated with each mole of the toxin (the specific radioactivity) and to determine how much radioactivity is associated with molecules other than the toxin (radiochemical impurities).

Figure 4 shows a binding experiment with rabbit vagus nerve exposed to [^{3}H]STX. As the STX concentration is increased from 2 nM to 85 nM, equilibrium uptake (filled circles) rises, first rapidly and then slowly, along a curve such as that described by Equation 3-4. The addition of 10 μM unlabeled TTX, to saturate the STX-TTX receptors, reduces the uptake of [^{3}H]STX (open circles) to low values, representing the nonspecific component. Subtraction of the nonspecific component from the total uptake leaves the saturable binding, which is half maximal at K_d = 1.8 nM STX and saturates when 110 nM of STX is bound per kilogram of wet vagus nerve tissue. The vagus was chosen because it contains many small, unmyelinated axons and hence a large surface area of axon membrane—about 6000 cm^2 (g wet)$^{-1}$. Dividing specific binding by membrane area yields an average STX-receptor density of 110 sites per square micrometer on the axon membranes of the vagus, assuming that all the sites are on axons (Ritchie et al., 1976). We now know that the TTX-STX receptor is a single site on the Na channel (Chapters 15 and 16), so this experiment tells us how many Na channels there are in the membrane. Surface densities of 100 to 400 channels/μm^2 are typical of unmyelinated axons and vertebrate skeletal muscles (Chapter 12).

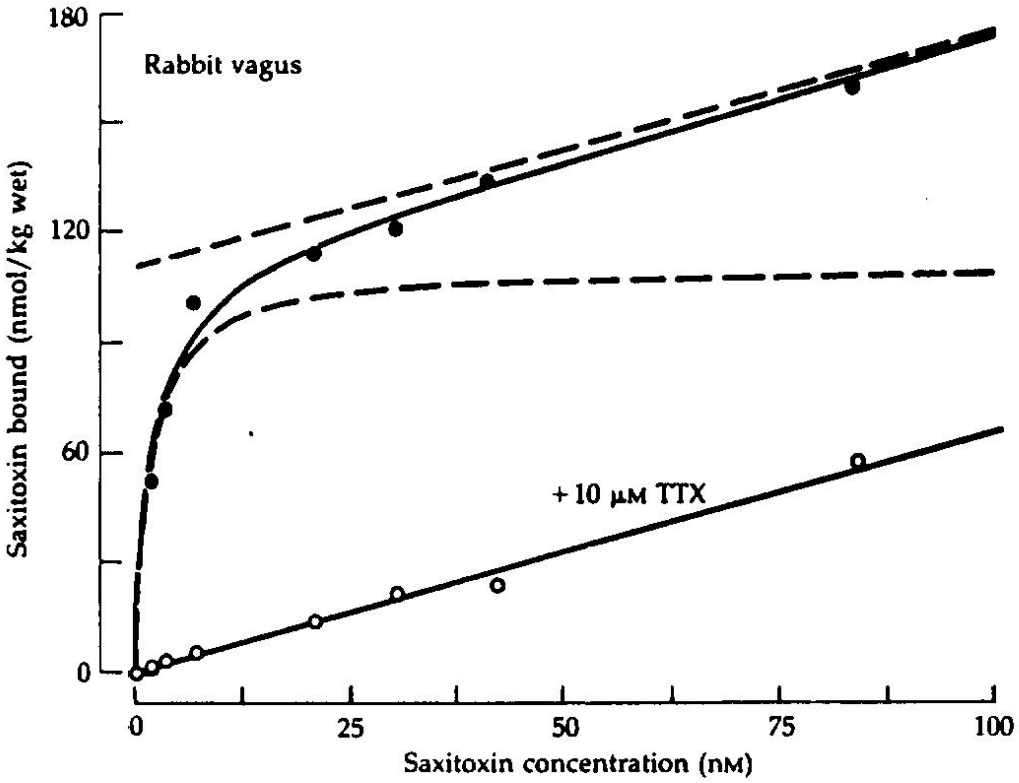

4 COUNTING Na CHANNELS WITH SAXITOXIN

Binding of labeled STX to rabbit vagus nerve (mostly unmyelinated fibers) is measured as a function of STX concentration both with (open circles) and without (filled circles) an addition of a saturating amount of unlabeled TTX to block specific binding. Nerves were incubated with label for 8 hours. The upper smooth curve is Equation 3-4 fitted to the observations. The slope a of the nonspecific binding is defined by the measurements in TTX (lower solid line). The lower dashed line is the derived saturable binding and is drawn according to Equation 3-2. The fitted number of sites is B_{max} = 110 nmol/(kg wet); the dissociation constant is K_d = 1.8 nM STX. T = 3°C. [From Ritchie et al., 1976.]

What does a channel look like?

We are now learning a great deal about the chemical structure of channels because of rapid advances in molecular biology and protein chemistry. Questions of structure are considered in detail starting in Chapter 9, but to provide a framework for thinking about biophysical studies we have a brief preview here.

In the 1970s the first membrane proteins were isolated by solubilizing them with detergents and purifying them on the basis of their ability to bind specific toxins with high affinity. The Na channel was purified this way using TTX as the specific marker. It turned out to be a large, richly glycosylated protein. Later, cDNAs coding for the major subunit of several Na channels were cloned, so we know complete amino acid sequences of this protein. The many runs of hydrophobic amino acids show that the peptide chain crosses the membrane at least 20 times, and the long hydrophilic loops in between show that the channel has significant extracellular and intracellular domains too. Nevertheless, as se-

quences do not specify 3-dimensional structure, we still rely heavily on biophysical work to suggest structural hypotheses.

A hypothetical view of a voltage-gated channel is shown in Figure 5. The channel is shown as a transmembrane protein sitting in the lipid bilayer of the membrane, but anchored to other membrane proteins or to elements of the intracellular cytoskeleton. The macromolecule is known to be large, consisting of 1,800–4,000 amino acids arranged in one or several polypeptide chains with some hundreds of sugar residues covalently linked as oligosaccharide chains to amino acids on the outer face. When open, the channel forms a water-filled pore extending fully across the membrane. The pore is much wider than an ion over most of its length and may narrow to atomic dimensions only in a short stretch,

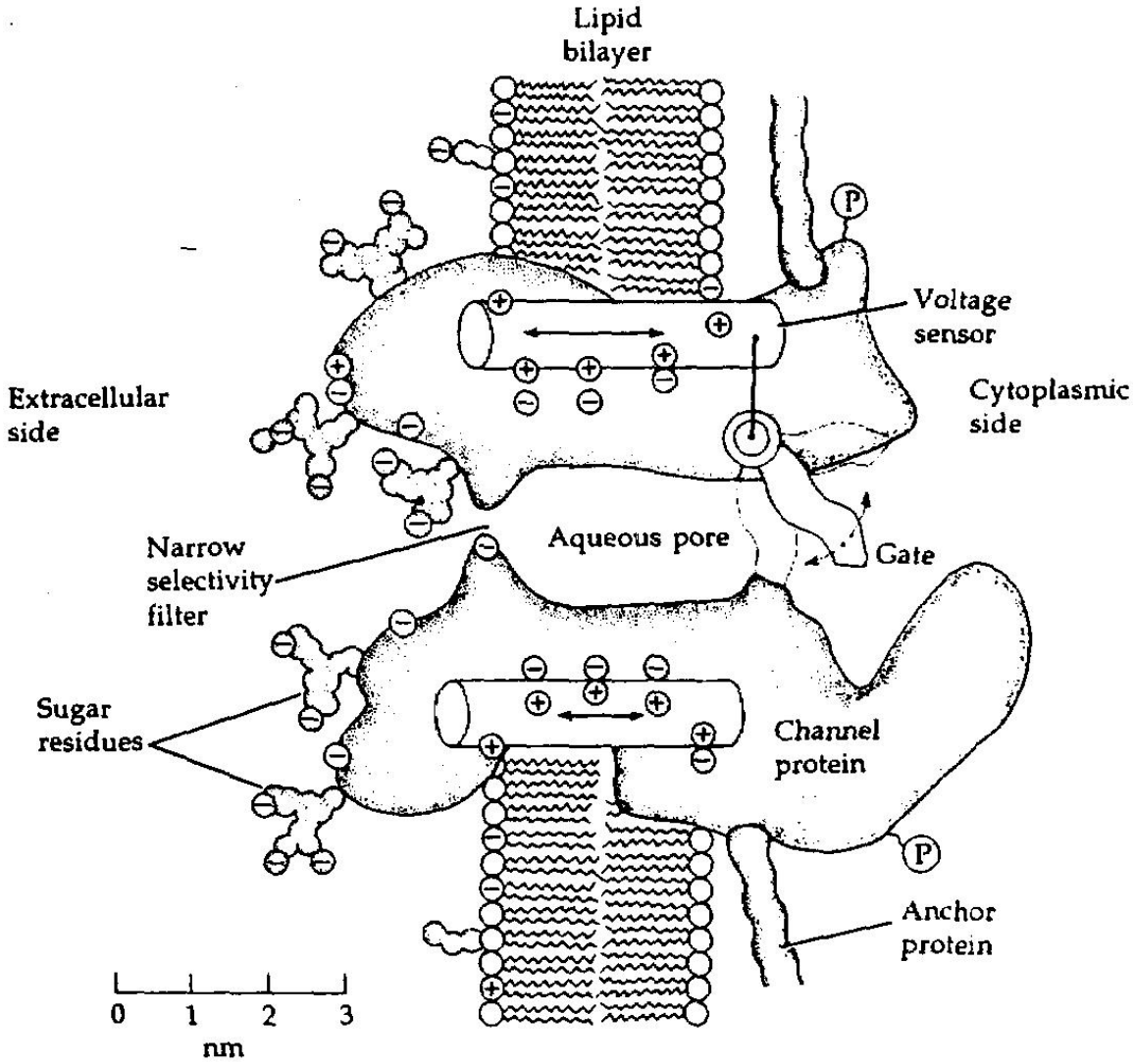

5 WORKING HYPOTHESIS FOR A CHANNEL

The channel is drawn as a transmembrane macromolecule with a hole through the center. The external surface of the molecule is glycosylated. The functional regions—selectivity filter, gate, and sensor—are deduced from voltage-clamp experiments and are only beginning to be charted by structural studies. We have yet to learn how they actually look.

the selectivity filter, where the ionic selectivity is established. Hydrophilic amino acids might line the pore wall and hydrophobic amino acids would interface with the lipid bilayer. Gating requires a conformational change of the pore that moves a gate into and out of an occluding position. The probabilities of opening and closing are controlled by a sensor. In the case of a voltage-gated channel, the sensor has to include many charged groups that move in the membrane electric field during gating (Chapter 2). It should be emphasized again that the drawing of the pore and gate in Figure 5 is a working hypothesis inspired by functional studies. We now need to find more direct structural methods to reveal the geometry of channels.

The molecular nature of channels is also revealed by the unitary current steps seen with the patch-clamp recording method. Sample current records for Na channels in Figure 6A and K channels in Figure 7A illustrate one of the major findings. When a channel opens, the ionic current appears abruptly, and when it closes, the current shuts off abruptly. These traces are heavily filtered to allow the small channel currents to stand out better above the inevitable background noise. This does introduce a rounding of the rise and fall. However, when the best available time resolution is used, individual channels appear to pop open and closed suddenly without any evidence of gradualness in the transition. At the single-channel level, the gating transitions are stochastic; they can be predicted only in terms of probabilities. Each trial with the same depolarizing step shows a new pattern of openings. Nevertheless, as Hodgkin and Huxley showed, gating does follow rules. In Figure 6, brief openings of Na channels are induced by repeated depolarizing steps from -80 mV to -40 mV. The openings appear after a short delay and cluster early in the sweep. When many records like this are averaged together, they give a smoother transient time course of opening and closing, resembling the classical activation–inactivation sequence for macroscopic I_{Na} (Figure 6B). The results with K channels show much longer openings beginning later in the depolarization, and again the ensemble average is like the macroscopic I_K (Figure 7). As we know, the HH model describes the time courses neatly in terms of the time- and voltage-dependent parameters m, h, and n. Qualitatively, the HH model predicts brief open times for single Na channels and long ones for K channels, in agreement with Figures 6 and 7. However, at least for Na channels, the detailed predictions of number of openings, latency to first opening, and duration of each opening often do not agree with the observations (Chapter 18). Therefore we must regard the macroscopic model as a convenient empirical description of averaged time courses that may contain important mechanistic clues but that does not correctly include all the observable details of the underlying molecular steps. This conclusion probably extends to all the HH-like models derived solely from macroscopic ionic current measurements, whether for Na channels, K channels, or Ca channels.

Armed with some pharmacology, a molecular picture of ionic channels, and a caveat concerning kinetic models, we can now return to the biophysical description of various cells.

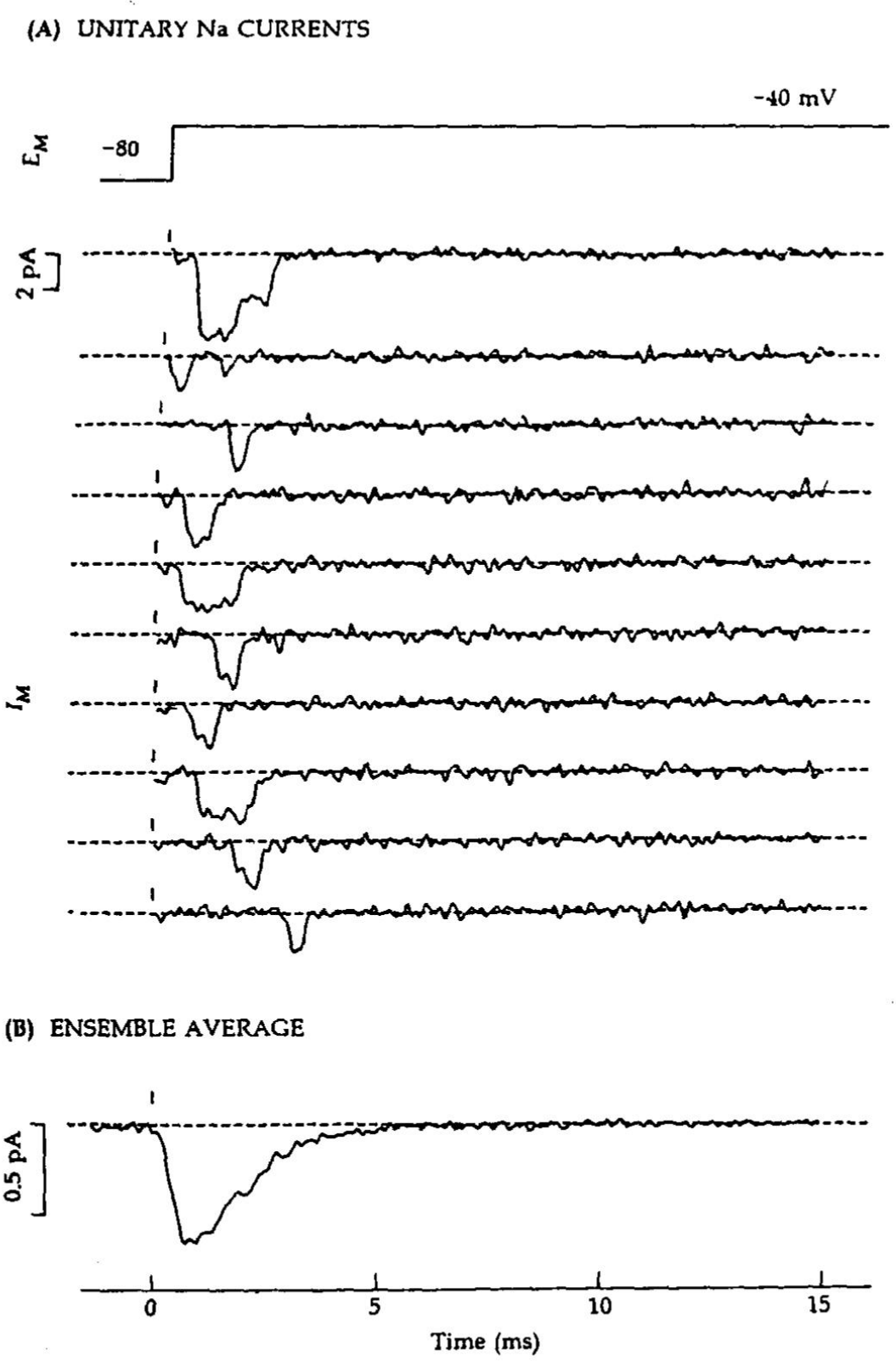

6 GATING IN SINGLE Na CHANNELS

Patch-clamp recording of unitary Na currents in a toe muscle of adult mouse during a voltage step from −80 to −40 mV. Cell-attached recording from a Cs-depolarized fiber. (A) Ten consecutive trials filtered at 3-kHz bandwidth. Two channel openings are superimposed in the first record but not in any of the others. This patch may contain >10 Na channels. Dashed line indicates the current level when Na channels are closed. (B) The ensemble mean of 352 repeats of the same protocol. T = 15°C. [Kindly provided by J.B. Patlak; see Patlak and Ortiz, 1986.]

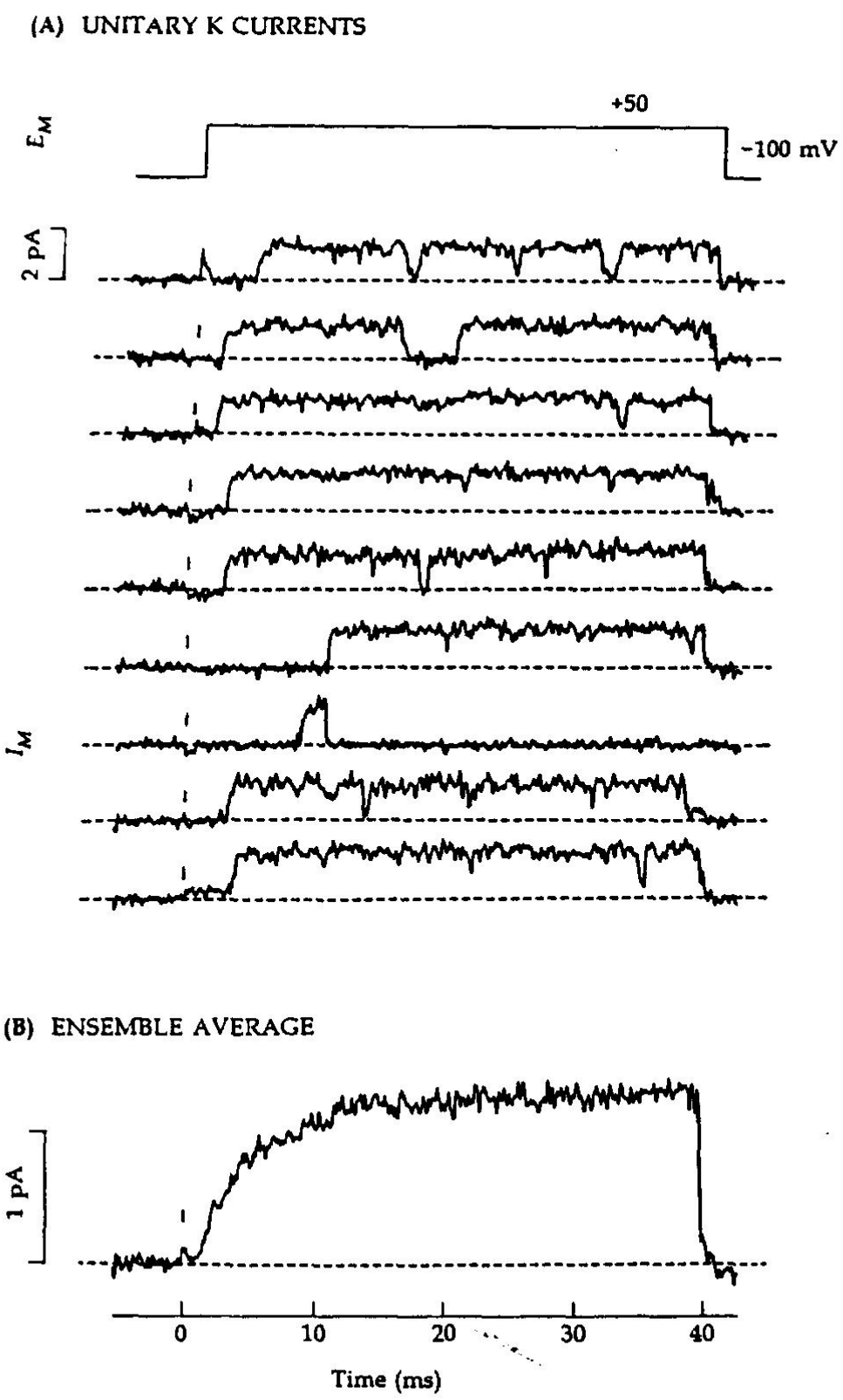

7 GATING IN SINGLE K CHANNELS

Patch-clamp recording of unitary K currents in a squid giant axon during voltage steps from −100 to +50 mV. To avoid the overlying Schwann cells, the axon was cut open and the patch electrode sealed against the cytoplasmic face of the membrane. (A) Nine consecutive trials showing channels of 20-pS conductance filtered at 2-kHz bandwidth. (B) Ensemble mean of 40 repeats. T = 20°C. [Kindly provided by F. Bezanilla and C.K. Augustine; see Llano et al., 1988.]

The Hodgkin–Huxley program continues

The work of Hodgkin and Huxley was so new, so thorough, and so technical that other electrophysiologists were unprepared in 1952 to pick up the story and extend it. Only after a period of 5 to 10 years were voltage-clamp techniques developed in other laboratories as the new biophysics caught on, and eventually new questions were asked broadly along two lines. The more mechanistic inquiries sought to find out how ionic permeability changes work, ultimately aiming at a molecular understanding of excitability. This mechanistic approach, a major subject of this book, is considered in earnest starting in Chapter 10. The other approach was a more biological one: How are different excitable cells of different organisms adapted to their special tasks? Do they all use Na and K channels or is there a diversity of mechanisms corresponding to the diversity of cell functions or of animal taxa? We begin with such questions here, introducing new channels and approaches in the next six chapters as a descriptive background for deeper study of mechanism.

The natural tendency was to assume that all electrically excitable cells are similar to the squid giant axon. Where their action potentials had clearly different shapes, as in the prolonged plateau of cardiac action potentials, it was assumed that small modifications of the time and voltage dependence of the kinetic parameters of the Na and K channels might suffice to explain the new shape (e.g., Noble, 1966). These assumptions often proved wrong. In fact, other excitable membranes have a variety of channels not seen in the squid axon work of Hodgkin, Huxley, and Katz. Early on, when, for example, Ca channels were first found in crab muscle (Fatt and Ginsborg, 1958) and a new kind of potassium channel was found in frog muscle (Katz, 1949), the new channels were commonly regarded as exceptional cases, perhaps restricted in significance. Again this assumption proved wrong. These channels and many others are found in any animal with a nervous system. To see most of the diversity of channels, it is unnecessary to look at different organisms. It suffices to look at the different excitable cells of one organism.

The investigation of different cells continues today. The procedure is to repeat the Hodgkin–Huxley program: Develop a voltage clamp for the new cell to measure current densities in reasonably isopotential membrane areas; change ions and add appropriate inhibitory drugs; separate currents; make a kinetic model; predict responses.

Although the approach is conceptually clear, each new cell presents new practical challenges. Few have been clamped as well as the squid giant axon and few yield as simple and unambiguous results. Most cells have more channel types than Hodgkin and Huxley found in the squid giant axon, and the kinetic dissection of the total ionic current is correspondingly more subtle. The pharmacology of the channels may not be the same as in axons. Moreover, ionic concentration changes have direct effects on the gating of some channels, rather than just affecting the availability of permeant ions. In cells with a high surface-to-volume ratio, changing the external ion concentration may also quickly cause

a change in internal ion concentrations. Some channels serve their functions on membrane infoldings or buried in clefts where neither the external potential nor the external ionic concentrations stay constant during the flow of ionic current. Such important practical considerations require biophysical ingenuity to circumvent. They are discussed extensively in the original literature, but like other methodological questions, are mentioned only in passing here.

Axons have similar channels

Axons are the highly specialized conducting processes of neurons. Their role in electrical signaling seems to be only to speed pulse-like signals, the action potential, from one point to another. The action potentials of axons are usually brief and therefore can follow one another in rapid succession. The action potential code of axons is all-or-none and carries no information in the amplitude or duration of each pulse. Only the time and frequency of the impulse is important. In this sense the signaling job of an axon is a simple one not calling for sophisticated modulation and regulation. The axon only follows. It does not synthesize. George Bishop (1965) said: "The axon doesn't think. It only ax."

Large axons from four phyla have been studied extensively with the voltage clamp. From the molluscs, there is of course the squid giant axon. The arthropods are represented by the paired ventral or circumesophageal giant fibers of lobster, crayfish, and cockroach (Julian et al., 1962; Shrager, 1974; Pichon and Boistel, 1967). Annelids are represented by the medial giant axon of the marine worm *Myxicola* (Goldman and Schauf, 1973). Finally, the vertebrates are represented by the largest myelinated nerve fibers of amphibians, birds, and mammals (Dodge and Frankenhaeuser, 1959; Frankenhaeuser, 1960a, 1963; Chiu et al., 1979; see also references in Stämpfli and Hille, 1976). Invertebrate nerve fibers with diameters less than 50 μm and vertebrate nerve fibers with diameters less than 8 μm have never been voltage clamped.

We have already seen that frog myelinated nerve fibers have Na and K currents with kinetics closely resembling those of squid giant axons (Figures 14 and 15 of Chapter 2, and Figures 2 and 3 of this chapter). Indeed, so do all axons that have been studied. In each case, I_{Na} activates with kinetics that can be approximated by the empirical m^3h formalism or by close variants such as m^2h, and I_K activates with a delay that can be approximated by the n^4 formalism or n^2, n^3, or n^5. The voltage dependence of membrane permeability changes is steep and qualitatively the same in axons of molluscs, annelids, arthropods, and vertebrates and, when the temperature is the same, the rates of the permeability changes are also similar. The Na channels of these axons are blocked by nanomolar concentrations of TTX applied externally, and the K channels, by millimolar concentrations of TEA applied internally. However TEA does not block K channels from the outside in all of these axons. Neglecting such small differences as do exist, we can conclude that axonal Na and K channels were already well designed and stable in the common ancestor of these phyla, some 500 million years ago (Chapter 20). Apparently all axons use the two major

channel types first described in the squid giant axon. The simplicity of the excitability mechanism of axons is in accord with the simplicity of their task: to propagate every impulse unconditionally.

The classical neurophysiological literature shows that large axons conduct impulses at higher speed than small ones. Large axons also need smaller electrical stimuli to be excited by *extracellular* stimulating electrodes. These differences, however, do not require differences in ionic channels. They can be fully understood from the differences in geometry, that is, by cable theory (Rushton, 1951; Hodgkin, 1954; Jack et al., 1983).

There is a diversity of K channels

Voltage-sensitive ionic permeabilities are found in virtually all eukaryotic cells, and since some membranes have far more complicated electrical responses than those of axons, it is not surprising that they also have more kinds of channels playing more roles than in axons.

The most impressive diversification has occurred among voltage-dependent K channels. Most open only after the membrane is depolarized, but some only after it is hyperpolarized. Some open rapidly and some, slowly. Some are strongly modulated by neurotransmitters or intracellular messengers. Although K^+ ions are always the major current carrier, the responses and the pharmacology differ enough to require that fundamentally different channels are involved. Each excitable membrane uses a different mix of these several K channels to fulfill its need. The K channel of axons was given the name "delayed rectifier" because it changes the membrane conductance with a delay after a voltage step (Hodgkin et al., 1949). This name is still used to denote axon-like K channels, even though almost all of the other known kinds of K channels also change membrane conductance with a delay. The distinguishing properties and nomenclature of other K channels are described in Chapter 5. With them, cells can regulate pacemaker potentials, generate spontaneous trains and bursts of action potentials, make long plateaus on action potentials, or regulate the overall excitability of the cell.

Delayed rectifier K channels of axons vary in their pharmacology (Stanfield, 1983). Those in the frog node of Ranvier can be blocked by the membrane-impermeant TEA ion either from the outside or from the inside (Koppenhöfer and Vogel, 1969; Armstrong and Hille, 1972). The external receptor requires only 0.4 mM TEA to block half the channels (Hille, 1967a). On the other hand, the external receptor of *Myxicola* giant axons requires 24 mM TEA to block half the channels, and even 250 mM external TEA has no effect on squid giant axons (Wong and Binstock, 1980; Tasaki and Hagiwara, 1957). Whereas the external TEA receptors are clearly different, the internal TEA receptors of all axons seem similar.

There are equally pronounced differences between cells of the same organism. For example, delayed rectifier K channels of frog heart are hardly affected by 20 mM external TEA, those of frog skeletal muscle require 8 mM TEA for half blockage, and only 0.4 mM TEA is needed at the node (Stanfield, 1970a, 1983). The gating kinetics of these channels differ as well. Thus, in frog heart, which makes action potentials almost 1000 times longer than those of axons, the activation kinetics of delayed rectifier K channels are 1000 times slower than in frog nodes of Ranvier (Figure 9). We now know that I_K of many cells not only activates with depolarization, but it also inactivates (Nakajima et al., 1962; Ehrenstein and Gilbert, 1966), a phenomenon not reported in the original work of Hodgkin, Huxley, and Katz (1952) because it requires much longer depolarizations than they used. In frog skeletal muscle, I_K inactivates exponentially and nearly completely with long, large depolarization (Nakajima et al., 1962; Adrian et al., 1970a). The time constant of the decay is 600 ms at 0 mV and 19°C, and the midpoint of the K-channel inactivation curve is near -40 mV (Figure 10). In frog myelinated nerve, I_K also inactivates, but nonexponentially, more slowly, and less completely than in muscle (Figure 11). Near 0 mV, the decay proceeds in two phases, with time constants of 600 ms and 12 s at 21°C, and about 20% of the current does not inactivate (Schwarz and Vogel, 1971; Dubois, 1981).

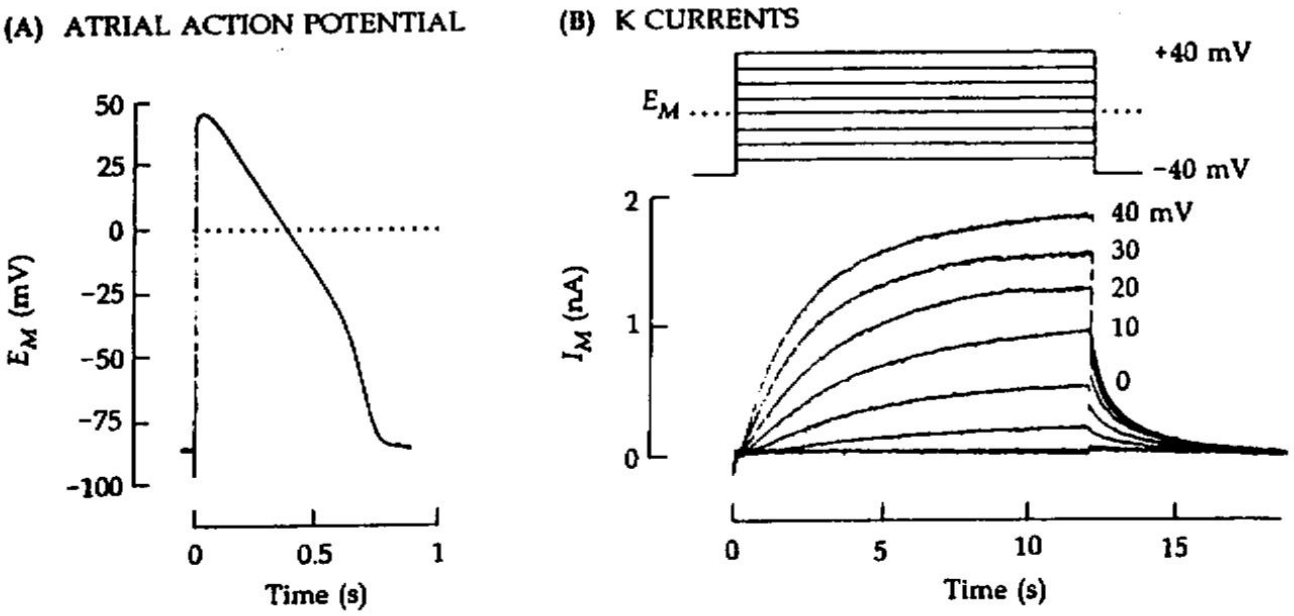

9 SLOW ACTIVATION OF I_K IN FROG HEART

(A) Action potential of an isolated bullfrog atrial muscle cell stimulated by a short shock. (B) Ionic currents evoked by depolarizing voltage steps under voltage-clamp conditions. The outward currents are primarily I_K in slowly gated/delayed-rectifier K channels. Note that the time scale is in seconds and compare with Figure 2B. T = 23°C. [From Giles et al., 1989.]

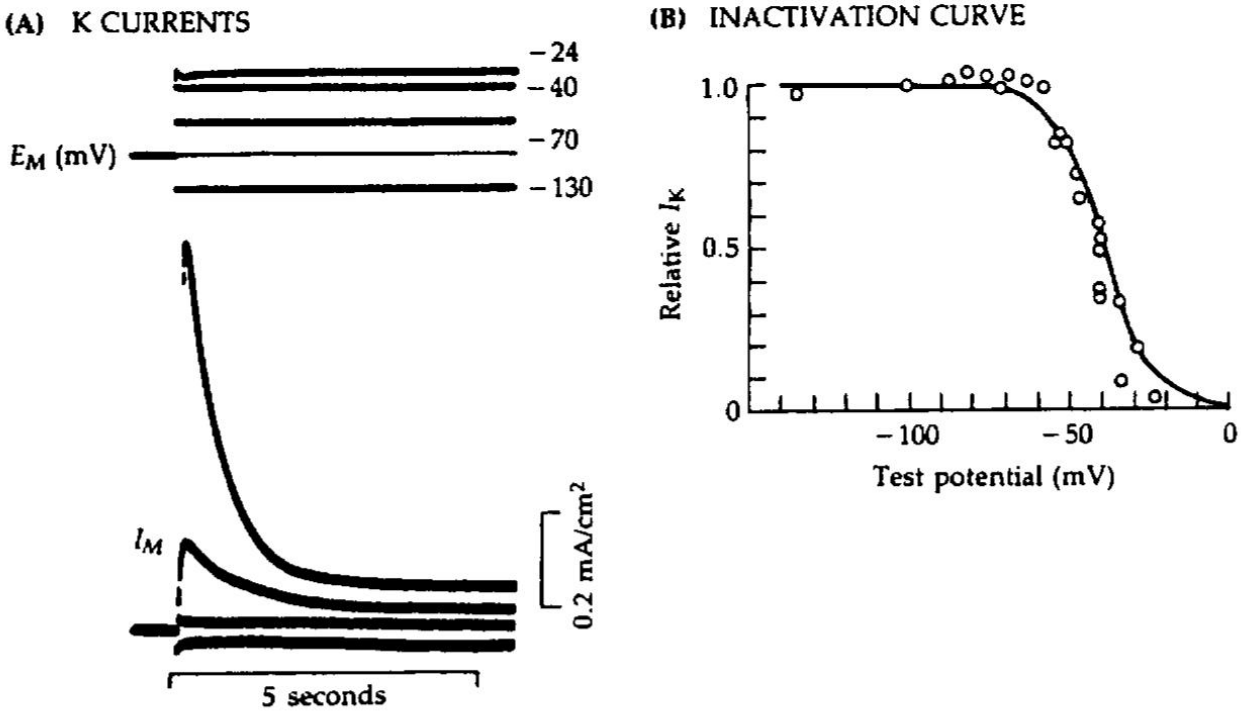

10 INACTIVATION OF I_K IN FROG MUSCLE

A frog sartorius muscle fiber treated with TTX to block Na channels is voltage clamped by a method using three intracellular microelectrodes. (A) K channels activate quickly during a depolarization but then inactivate almost completely within a couple of seconds. T = 19°C. (B) The steady-state inactivation curve for muscle K channels is steep and shows 50% inactivation at −40 mV. [From Adrian et al., 1970a.]

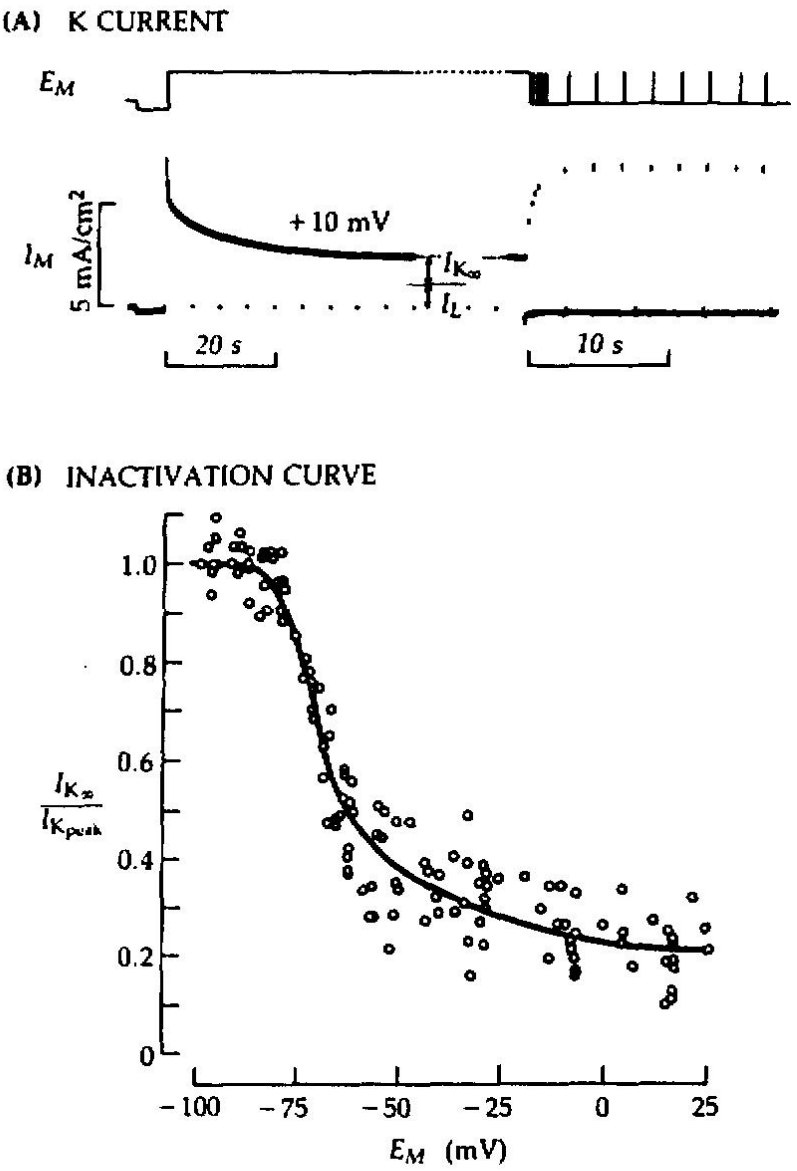

11 INACTIVATION OF I_K IN FROG NERVE

A frog node of Ranvier bathed in Ringer's solution is voltage clamped by the Vaseline gap method using a test pulse lasting tens of seconds. (A) K channels activate quickly during the depolarization to +10 mV and then inactivate partially in 10 to 30 s. The inactivation develops in fast and slow phases. It is removed within a few seconds at the resting potential, as is indicated by the growing peak I_K responses to the subsequent brief test pulses. (B) The steady-state inactivation curve for K channels of the node. Around the resting potential the curve is steeply voltage dependent, but for depolarized potentials the voltage dependence is weak and inactivation never removes the last 20% of the current. T = 21°C. [From Schwarz and Vogel, 1971.]

The microheterogeneity of K channels extends to the single-cell level. A closer analysis of gating kinetics and pharmacology shows more than one component of delayed K currents in a single node of Ranvier (Dubois, 1981, 1983; Benoit and Dubois, 1986). Dubois distinguishes three (Figure 12): Component f_1 activates rapidly, inactivates very slowly, and is selectively blocked by

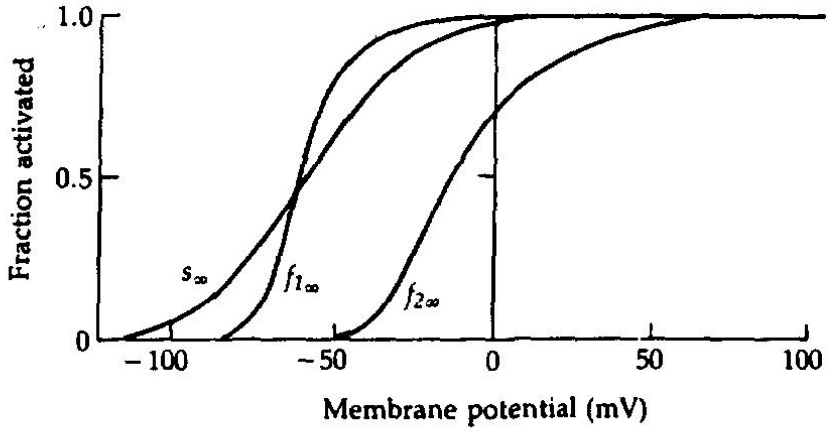

12 SEVERAL COMPONENTS OF g_K IN ONE AXON

Steady-state voltage dependence of three components of delayed rectification in frog nodes of Ranvier. The components differ in kinetics and drug sensitivity. The activation curves, s_∞ for slow K channels and $f_{1\infty}$ and $f_{2\infty}$ for two types of fast channels, show the fraction of each channel type open. [From Dubois, 1983.]

peptide toxins from mamba snakes (genus *Dendroaspis*). Component f_2 activates rapidly, inactivates slowly, and is selectively blocked by the hot pepper ingredient, capsaicin. Component s activates slowly (hundreds of milliseconds) and does not inactivate in 3 min. It also is insensitive to 1 mM 4-aminopyridine, which blocks components f_1 and f_2 fully. The ratio of fast to slow subtypes is higher in the internode than at the node (Röper and Schwarz, 1989). Such results are typical of experimental discoveries today. The finer the method of analysis, the more apparent subtypes of channels are discovered. Even the "simple" axon has subtypes of delayed rectifier K channels—for reasons that we have yet to fully understand. In the node, the existence of multiple subtypes clarifies the complex kinetics of inactivation of the total I_K (Figure 11A). Patch-clamp recordings have been made on myelinated axons whose nodal gap has widened after treatment with proteolytic enzymes (Jonas et al., 1989). The three sizes of unitary K currents that were found probably correspond to the three macroscopic I_K components of Dubois.

These phenomenological differences suggest that frog nerve, heart, and skeletal muscle have different delayed rectifier channels, probably encoded by different genes. We are beginning to learn that much as enzymes have isozymes coded by different genes, channels have tissue-specific and developmentally regulated isoforms, often called subtypes. Indeed in the first four years of cloning, sixteen different genes for K channels have been identified in the rat genome (Chapter 9), and the rate of discovery is not slowing. Nevertheless, one cannot be sure from physiological experiments alone that functional differences mean that a different *gene* is being expressed. In later chapters we will encounter examples of profound functional differences arising from changes of channel protein phosphorylation, changes of concentration of small molecules such as Ca^{2+} ions, addition of a toxin, alternative splicing of the RNA transcript from a single gene, or exposure of the membrane to amino-acid-modifying reagents.

Na channels are less diverse

Less functional diversification has been noticed among Na channels in excitable cells.[4] Nevertheless, they are clearly not all the same (Barchi, 1988; Trimmer and Agnew, 1989; Neumcke, 1990). There are appreciable kinetic differences between fast TTX-sensitive Na channels of innervated vertebrate skeletal muscle and the slower TTX-insensitive channels of the same muscles after denervation (Pappone, 1980; Weiss and Horn, 1986) or between the fast Na channels of vertebrate central neurons and the slower ones of glia (Barres et al., 1989).

In axons, Na channels have one primary function: to generate the rapid regenerative upstroke of an action potential. In other membranes, they can also contribute to pacemaker and subthreshold potentials that underlie decisions to fire or not to fire. Not all excitable cells use Na channels, but where they do exist (e.g., axons, neuron cell bodies, vertebrate skeletal and cardiac muscles, and many endocrine glands), one is impressed more with the similarity of function than with the differences. Figure 13 compares the time courses of I_{Na} in nerve and muscle cells from four different phyla. They all show brisk activation and inactivation, qualitatively as described by the HH model for squid giant axons. After correction for temperature, their activation and inactivation time constants would not differ by more than twofold, except that the midpoint of activation and inactivation curves may vary by 10 to 20 mV in different membranes. In general, Na channels inactivate nearly completely (>95%) with depolarizations to 0 mV and beyond, as in the HH model. Ironically, the one axon deviating in a major way is the squid giant axon itself (Figure 13F), a fact not appreciated until methods of pharmacological block, internal perfusion, and computer recording were used. In this axon, a significant sodium conductance remains even during 1-s depolarizations to +80 mV (Chandler and Meves, 1970a,b; Bezanilla and Armstrong, 1977; Shoukimas and French, 1980). Several reports suggest that central neurons and axons may also have separate, minor populations of TTX-sensitive Na channels specialized to operate in the subthreshold range of membrane potentials (Llinás, 1988; Gilly and Armstrong, 1984). Such channels could play a significant regulatory role in spike initiation.

The ionic selectivity of Na channels is relatively invariant. It has been compared in the giant axons of squid and *Myxicola*, in frog nodes of Ranvier, and in frog and mammalian twitch muscle (see Chapter 13). Biionic potential measurements and Equation 1-13 give a selectivity sequence for small metal ions: $Na^+ \approx Li^+ > Tl^+ > K^+ > Rb^+ > Cs^+$. Small nonmethylated organic cations such as hydroxylammonium, hydrazinium, ammonium, and guanidinium are also appreciably permeant in Na channels, suggesting a minimum pore size of 3 Å × 5 Å (0.3 × 0.5 nm) for the selectivity filter of the channel (Hille, 1971). Methylated organic cations such as methylammonium are not permeant.

Despite major functional similarities of Na channels across the animal kingdom, when nonphysiological properties are considered, differences can be detected from tissue to tissue in one organism. Monoclonal antibodies have been

[4] Here we are not speaking of the "light-sensitive Na channel" of vertebrate eyes or the "amiloride-sensitive Na channel" of epithelia or other such electrically inexcitable, Na-preferring channels that are only remotely related to the TTX-sensitive Na channel described by the HH model.

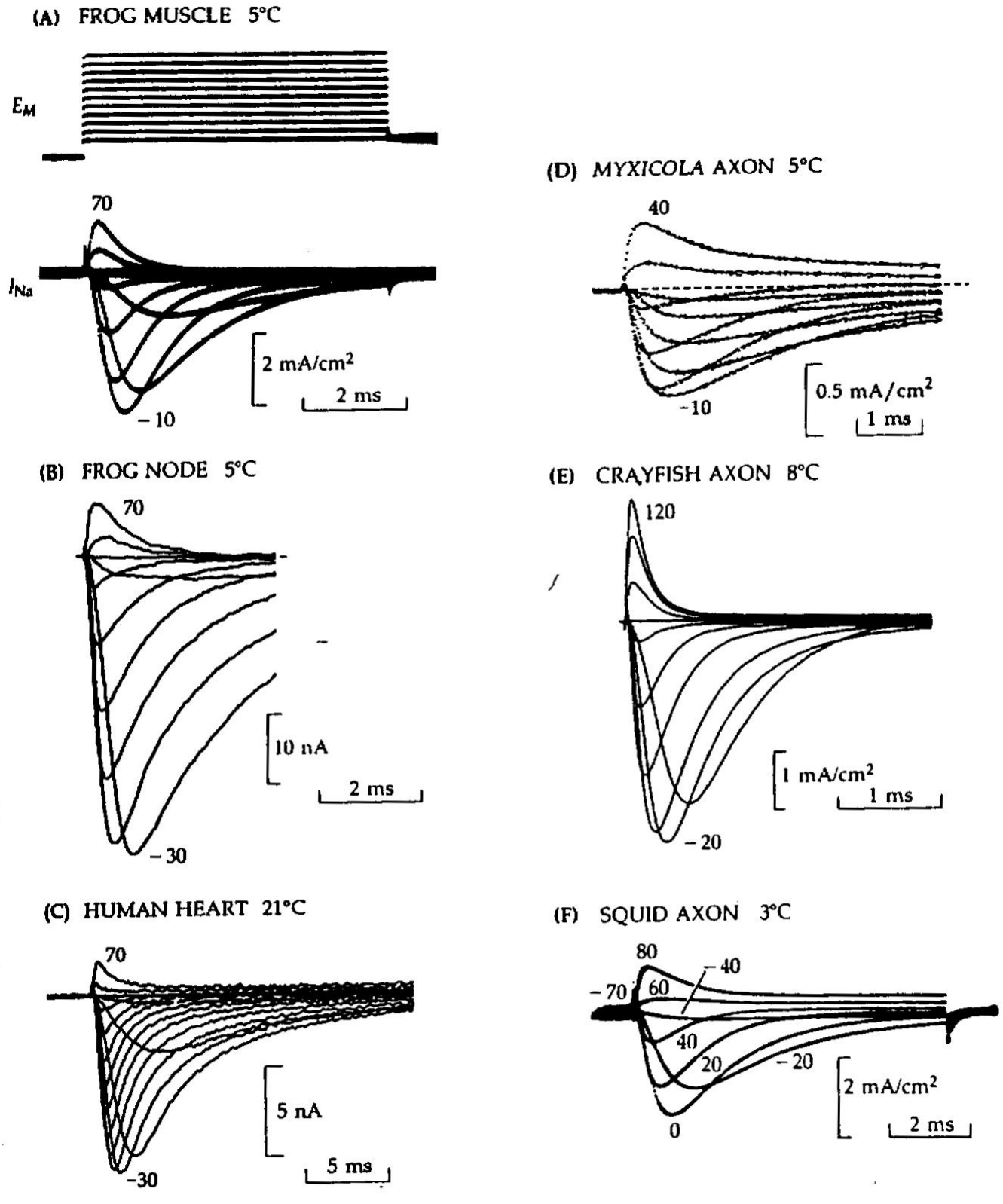

13 SIMILARITY OF I_{Na} IN MANY CELLS

Families of sodium currents recorded under voltage clamp in a variety of excitable cells. Potassium currents are blocked by Cs, TEA, or 4-aminopyridine and linear leakage currents are subtracted. The membranes are (A) frog semitendinosis skeletal muscle fiber; (B) frog sciatic node of Ranvier; (C) dissociated human atrial cells; giant axons of (D) *Myxicola* ventral cord; (E) crayfish ventral cord; and (F) squid mantle. [From Hille and Campbell, 1976; Hille, 1972; C.H. Follmer and J.Z. Yeh, unpublished; L. Goldman, unpublished; Lo and Shrager, 1981; Armstrong et al., 1973.]

made against mammalian Na channels. Different antibodies can distinguish Na channels on central axons from those on peripheral axons, channels on nerve from those on muscle, or even channels in the transverse tubular system of a muscle fiber from those on the rest of the plasma membrane of the same fiber (Barchi, 1988).

The pharmacology of Na channels shows major similarities yet obvious differences. Catterall (1980) distinguishes several primary sites of neurotoxin action on Na channels. One is the external tetrodotoxin-saxitoxin receptor, which we have discussed. The others are external receptors for polypeptide neurotoxins that depress inactivation or shift activation of Na channels and hydrophobic receptors for lipid-soluble neurotoxins that open Na channels (see Chapter 17). We could also add the receptor for local anesthetics that block channels from the cytoplasmic side. These sites are diagnostic for Na channels in all higher animal phyla, but there are differences. The TTX receptor site shows significant variability. For example, vertebrate cardiac Na channels are much less sensitive to TTX than are vertebrate skeletal muscle or nerve Na channels. Binding and blocking experiments (Figure 3) give inhibitory dissociation constants of 0.5 to 10 nM for TTX and STX acting on axons and skeletal muscle of fish, amphibians, and mammals (Ritchie and Rogart, 1977c) and values as high as 1.0 to 6.0 μM for Purkinje fibers and ventricular fibers of mammalian heart (Cohen et al., 1981; Brown, Lee, et al., 1981). In addition, some fraction of the Na channels of embryonic neurons and skeletal muscle are TTX and STX resistant during development (Spitzer, 1979; Weiss and Horn, 1986; Gonoi et al., 1989). Finally, the Na channels of those puffer fish and salamanders that make TTX for self-defense are also highly resistant to the toxin (Chapter 20).

Once again these small differences suggest that Na channels have multiple subtypes. This conclusion is confirmed by the cloning of (so far) six Na channel transcripts from rodents, four from brain, one from skeletal muscle, and one from heart (Chapter 9). The functional advantages of each subtype remain to be determined.

Recapitulation

Pharmacological experiments with selective blocking agents convinced biophysicists that there are discrete and separate Na and K channels. These channels are present in axons of all animals. In myelinated nerve they assume a very nonhomogeneous distribution, with high concentrations of Na channels at nodes of Ranvier.

There is microheterogeneity among the K channels of a single axon, but to find more striking diversity one can look at nonaxonal membranes. They show a variety of clearly different K channels. As the next five chapters document, these nonaxonal membranes also express Ca channels, Cl channels, and a vast variety of transmitter-sensitive and sensory transduction channels.

The adaptive radiation of channels shows that, like enzymes, ionic channels are more diverse than the physiological "substrates" (Na^+, K^+, Ca^{2+}, and Cl^-)

they handle. There coexist multiple forms with different function and regulation. Comparisons from one tissue to another are confounded by the usual taxonomic problems of separation, identification, and nomenclature. Thus far the criteria for distinguishing one channel from another have been primarily their functional properties, but ultimately must be their genetic coding and molecular structure.